Engineered Adeno-Associated Viral Vectors for Gene Therapy in the Retina

By

Leah Caroline Thomas Byrne

A dissertation submitted in partial satisfaction of the

requirements for the degree of

Doctor of Philosophy

In

Neuroscience

in the

Graduate Division

of the

University of California, Berkeley

Committee in charge:

Professor John G. Flannery, Chair
Professor David Schaffer
Professor Lu Chen
Professor Laurent Coscoy

Fall 2011

Abstract

Engineered Adeno-Associated Viral Vectors for Gene Therapy in the Retina

by

Leah Caroline Thomas Byrne

Doctor of Philosophy in Neuroscience

University of California Berkeley

Professor John Flannery, Chair

Inherited retinal degenerations are genetically heterogeneous conditions affecting roughly 1:3000 people and are characterized by the loss of photoreceptors. Progressive retinal degenerative disease is the leading cause of vision loss in industrialized countries, and is the result of a wide range of mutations, mostly in rod-specific transcripts. Over 140 disease-causing genes have been identified to date. As the genetic mechanisms underlying inherited forms of retinal degeneration are identified, gene therapy is becoming a promising approach for the treatment of many inherited blinding diseases.

Indeed, the recent success of three clinical trials using adeno-associated virus (AAV) to deliver a normal copy of the RPE65 gene to the retinas of Leber congenital amaurosis (LCA) patients illustrates the potential of gene therapy in the retina. AAV has been shown safe and effective especially in a younger cohort of patients. Some important obstacles remain, however, for AAV-mediated gene therapy to become widely applicable across the range of existing retinal degenerative diseases. It will be essential to carefully evaluate the method used to deliver therapeutic genetic material to the retina, as this will determine the success of the treatment.

The serotype of vector used, the promoter chosen to drive expression and the method of injection are important components of the gene delivery system. A wide variety of AAV serotypes exist with different tropisms for cell populations in the retina, potentially allowing treatments to be targeted to specific cell types. The retinal cell types AAV can infect differs, however, depending on whether the vector is delivered into the vitreous cavity or the subretinal space. Subretinal injections, which were used in the LCA trials, result in the creation of a retinal detachment and localized injury to the retina while delivering high concentrations of transgene to only a limited area. An intravitreal approach has the potential to transduce panretinally and is less invasive, and therefore preferable, but naturally occurring serotypes of AAV transduce photoreceptors poorly from the vitreous, as a result of structural barriers that exist on the inner surface of the retina.

Recent advances in the understanding of AAV and the production of viral vectors have shown the flexibility of this virus, indicating that its function can be altered and tailored to the requirements of retinal gene therapy. A directed evolution approach has been used to select, out of a highly diverse library of AAV capsid variants, a novel variant with improved tropism for Müller glia. And in a parallel approach, residues on the capsid surface have been mutated to avoid ubiquitination and altering the nuclear trafficking of the virus.

This dissertation examines the use of engineered viral vectors for gene therapy in the retina. The creation of a novel variant of AAV, called 7m8, which is characterized by increased transduction of photoreceptors from the vitreous, is described below. 7m8 was derived from an AAV2 peptide insertion library and contains a 7mer motif. Injected intravitreally, 7m8 transduces cells throughout the retina, including photoreceptors in the outer retina, significantly more efficiently compared to the parental serotype. Expression was restricted to photoreceptors using a rhodopsin promoter. This virus, as well as the previously described Müller-specific variant ShH10, was used to deliver a wild-type copy of the retinoschisin gene to mice lacking this protein. Retinoschisin is secreted from photoreceptors, and retinas deficient in this protein are severely structurally impaired. Subretinal injections, which are damaging in nature, are therefore suboptimal because they are likely to cause additional injury. We show that 7m8 is able to efficiently target photoreceptors via intravitreal injection in this mouse model, leading to high levels of retinoschisin protein production, as well as structural and functional rescue. This rescue is longer lasting than that seen using ShH10, indicating the importance of targeting photoreceptors in this disease model.

AAV9 has been shown to transduce the murine retina when injected intravenously through the tail vein. We used two surface tyrosine-to-phenylalanine mutations to improve the retinal expression of AAV9, and demonstrated that these mutations lead to higher infectivity of all retinal layers, most dramatically in photoreceptors and the inner nuclear layer, but also including the retinal pigment epithelium and ganglion cells. This novel vector was then used to explore the bifunctionality of the *Nxnl1* gene, which encodes two isoforms of the rod-derived cone viability factor (RdCVF). The short form of RdCVF is secreted and has been shown to support cone survival, while the long isoform is retained intracellularly and has been implicated in redox signaling. AAV92YF and 7m8 were used to express the two isoforms of RdCVF in the *rd10* mouse model of retinitis pigmentosa. RdCVF rescued cone survival when injected intravenously or intravitreally, but had little effect on rod survival. Early expression of RdCVFL in dark-reared *rd10* mice delayed rod, and subsequently cone death.

For my parents,
Stephanie and Joseph Byrne

Acknowledgments

First and foremost, I'd like to thank Professor John Flannery, for his outstanding mentorship. I've had an incredibly rewarding experience learning from him and working in the Flannery Lab. He has always provided support, encouragement, criticism and guidance. The atmosphere he fosters in his lab is one of positivity, collaboration and teamwork, and I am truly appreciative of the opportunities he's made possible for me. His encouragement of my ideas, including traveling to Paris for the Bourse Chateaubriand, has made this work and the success of my graduate career possible. I am truly lucky to have had such outstanding PI, and hope to be able to follow in his footsteps as an outstanding scientist and mentor in the future.

I'd also like to thank my colleagues in the Flannery Lab. Deniz Dalkara has been a supportive friend and colleague whose opinion on all scientific matters I value and trust. Her collaboration has been an integral part of my work in the Flannery Lab and this dissertation. Meike Visel has been my teacher for many of the protocols used in these experiments. She also has been an invaluable colleague and collaborator, and this work would not have been possible without her. Trevor Lee contributed to many aspects of this work from Matlab programming to ocular injections. His expertise in many technical aspects of these experiments was incredibly helpful, and it has always been a pleasure to be a member of the same team as him. Natalie Hoffmann was also a contributor to much of the work done for this dissertation. I've also learned from her integrity and work ethic. I'd also like to thank Fakhra Khalid, my undergrad intern, whose cheerfulness and determination, as well as her never-ending helpfulness make working with her an absolute pleasure. Jas Mann, our reliable and efficient undergrad, has also put in many hours of maxiprepping and has been a huge help to me.

I'd also like to thank previous members of the Flannery Lab including Ken Greenberg, my grad student mentor during my rotation in the Flannery Lab, as well as Scott Geller, Karen Guerin, Ryan Klimczak, and Kate Kolstad.

In addition I thank my collaborators from Paris, Thierry Léveillard, Emmanuelle Clérin, José Sahel, and Irene Lee-Rivera.

And lastly, I would like to thank Miguel Betegón Ramiro, who has been my most important source of support during my entire graduate career, through rotations, my qualifying exam, teaching, presentations, long nights, weekends in the lab, and this dissertation. He has listened to, read or edited most of what I've presented, as well as wrote the code used for cone counting experiments and solved countless computer issues. Above all, the moral support he has provided has been invaluable.

Table of Contents

Abstract

Dedication - i

Acknowledgements - ii

Table of Contents - iii

Figure and Table Legend - v

Chapter 1: Introduction - 1

Chapter 2: In vivo directed evolution of AAV yields a photoreceptor permissive viral variant capable of transduction from the vitreous

Title page - 10

Abstract - 11

Introduction - 11

Results - 12

Discussion - 21

Materials and Methods - 22

Chapter 3: Engineered AAV variant-mediated delivery of retinoschisin via intravitreal injection in the retinoschisin-deficient mouse

Title page - 25

Abstract - 26

Introduction - 26

Results - 30

Discussion - 37

Materials and Methods - 39

Chapter 4: Enhanced gene delivery to the retina through systemic administration of tyrosine mutated AAV9

Title page - 42

Abstract- 43

Introduction - 43

Results - 46

Discussion - 54

Materials and Methods - 55

Chapter 5: Engineered AAV-mediated expression of two isoforms of rod-derived cone viability factor delays retinal degeneration in the *rd10* mouse

Title page - 58

Abstract - 59

Introduction - 59

Results - 60

Discussion - 67

Materials and Methods - 69

Chapter 6: Conclusions - 72

References - 74

Figure and Table Legend

Chapter 1: Introduction

Figure 1 - 1

Figure 2 - 4

Figure 3 - 5

Table 1 - 6

Figure 4 - 9

Chapter 2: In vivo directed evolution of AAV yields a photoreceptor permissive viral variant capable of transduction from the vitreous

Figure 1 - 13

Table 1 - 14

Figure 2 - 15

Figure 3 - 16

Figure 4 - 17

Figure 5 - 18

Figure 6 - 20

Chapter 3: Engineered AAV variant-mediated delivery of retinoschisin via intravitreal injection in the retinoschisin-deficient mouse

Figure 1 - 29

Figure 2 - 31

Figure 3 - 33

Figure 4 - 34

Figure 5 - 35

Figure 6 - 36

Figure 7 - 37

Chapter 4: Enhanced gene delivery to the retina through systemic administration of tyrosine mutated AAV9

Figure 1 - 45

Figure 2 - 47

Figure 3 - 48

Figure 4 - 50

Figure 5 - 52

Figure 6 - 53

Supplemental Figure 1 - 57

Supplemental Figure 2 - 57

Chapter 5: Engineered AAV-mediated expression of two isoforms of rod-derived cone viability factor delays retinal degeneration in the *rd10* mouse

Figure 1 - 61

Figure 2 - 62

Figure 3 - 63

Figure 4 - 64

Figure 5 - 66

Figure 6 - 67

Chapter 1

Introduction

The retina

The retina is a highly organized piece of neural tissue about half a millimeter thick lining the back of the eye, and is responsible for mediating vision, arguably the most important of the senses. The retina contains photosensitive cells called photoreceptors that detect light and transmit electrical signals containing information about the visual field to bipolar and horizontal cells, which in turn send impulses to ganglion cells. Bipolar, horizontal and amacrine cells perform the first stages of image processing, while the output of the retina is carried by the axons of ganglion cells to targets in the brain.

Three layers in the retina contain the cell bodies of all the retinal neurons: The outer nuclear layer (ONL) is located furthest from the vitreoretinal interface and contains the soma of rod and cone photoreceptors. The perikarya of bipolar, horizontal and amacrine cells, as well as the primary glial cell type in the retina, Müller cells, lie in the inner nuclear layer. Ganglion cells and displaced amacrine cells are located in the ganglion cell layer. Plexiform layers between layers of cell bodies contain the synapses linking neurons together via vertical and horizontal connections (Figure 1).

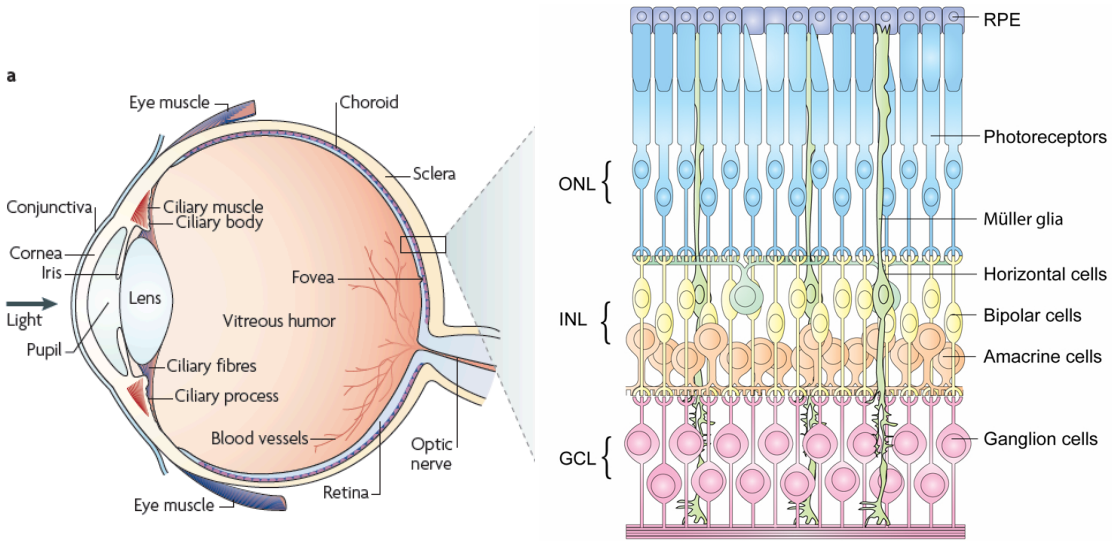

Figure 1. Organization of the retina.

Photoreceptor cell bodies lie in the ONL, while Müller glia, amacrine cells, horizontal cells and bipolar cell bodies lie in the INL. Ganglion cell bodies lie closest to the center of the eye in the ganglion cell layer.

Photoreceptors are counter-intuitively located at the back of the retina, furthest from the source of light, and therefore photons must travel through the transparent cells of the retina to reach them. Photoreceptors interact closely with the underlying retinal pigment epithelium (RPE), which provides nutritional and functional support. Some of the important functions of the RPE include phagocytosing outer segments that are continually shed, recycling of photopigments involved in the phototransduction cascade, and constituting part of the blood-retina barrier. These pigment-filled cells also absorb excess photons, preventing glare, and protect photoreceptors from exposure to high intensity light.

All vertebrates use two types of photoreceptors: rods and cones. Rods are specialized for scotopic, or dim light vision, while cones mediate high acuity, photopic vision in bright light and are color sensitive. Multiple types of cones can be distinguished based on their sensitivity to varying wavelengths of light. Human retinas contain three types of cones that are sensitive to blue, green and red light, while the rodent retina lacks red-sensitive cones. In the human retina the fovea is densely packed with cones, and rods dominate the peripheral retina.

The outer segments of photoreceptors contain discs of bilipid membrane into which are inserted photosensitive molecules called rhodopsin. Molecules of rhodopsin are composed of 11-cis retinal covalently bound to a seven-transmembrane spanning opsin moiety. Every outer segment contains hundreds of discs, each of which holds thousands of rhodopsin molecules. In response to absorbing a photon of light, retinal photoisomerizes to an all trans form, changing the conformation of the rhodopsin molecule and activating a G-protein called transducin. This G-protein is coupled to a cascade of events, the end result of which is to remove cyclic-GMP from the intracellular environment, closing cGMP-gated channels and hyperpolarizing the photoreceptor. There is then a decrease in the release of glutamate into the photoreceptor synapse, and a reduction in the dark current.

The downstream effects of this reduction in the release of glutamate are dependent upon the type of receptor found on the target of the photoreceptors, the bipolar cells. One type of bipolar cell, the OFF bipolar cell, depolarizes in response to an increase in the amount of glutamate released into the synaptic cleft and is therefore suited to detect light on a dark background. OFF bipolar cells express an ionotropic glutamate receptor that is part of a single complex containing an ion channel. ON bipolar cells, in contrast, depolarize in response to an increase in light, for detection of light stimuli on a dark background, and express metabotropic glutamate receptors. These receptors are coupled to ion channels through a second messenger pathway, which allows a reversal of the sign of the synapse. Bipolar cells then in turn release glutamate and influence their targets, the amacrine and ganglion cells.

Bipolar cells are also directly and indirectly influenced by horizontal cells. Horizontal cells receive input from large numbers of photoreceptors over a wide receptive field, and then in turn couple to each other and to photoreceptors via gap junctions, or through synapses to bipolar cells. As a result of this input, bipolar cells have an increased receptive field that has an added center-surround organizational feature. That is, stimuli that activate the center of the receptive field elicit large depolarizing responses while stimuli in the surround hyperpolarize the cell.

Bipolar cells with center-surround receptive fields then synapse with amacrine cells, another cell type with horizontal connections, or ganglion cells, the output cells of the retina. Amacrine cells play an important role in the rod pathway, and further act to integrate and modulate information flowing through the photoreceptor-bipolar-ganglion cell pathway.

Ganglion cells are the final conduit of information from the retina to the brain. Ganglion cells are also characterized by either on ON or OFF center-surround receptive field and can be subdivided into at least 18 types. There are two main categories of ganglion cells: parvocellular P cells, and magnocellular M cells. The first have smaller receptive fields and are sensitive to changes in color. The second have large receptive fields, are insensitive to color changes and transmit signals with a quicker conduction velocity. Another, more recently identified type of ganglion cell has been shown to express a photopigment called melanopsin and to be sensitive to light [1,2]. These intrinsically photosensitive retinal ganglion cells project to the suprachiasmatic nucleus of the hypothalamus to play a role in aligning circadian rhythm, as well as the olivary pretectal nucleus to mediate the pupillary light reflex.

The axons of ganglion cells carry neural impulses coding the totality of processed information from the retina to its central targets. In primates, the main efferent pathway from the retina projects to the lateral geniculate nucleus, which in turn projects to primary visual cortex, where processing of conscious vision begins. In addition, RGC's innervate regions of the brain involved in visual functions below the level of consciousness including the SCN, the superior colliculus, and the preoptic area.

Inherited forms of retinal degeneration

As humans, our sense of vision is integral to our daily lives, from navigation through the environment to communication and recreation. Loss of sight can therefore be devastating. In some cases, vision loss can be an inherited condition resulting from mutations in genes important to the function of the retina. Inherited retinal dystrophies are marked by the degeneration of RPE and photoreceptors, and are the result of a wide spectrum of mutations affecting a variety of molecular pathways important for the visual cycle and the structure of the retina. They are characterized by autosomal dominant, recessive and X-linked patterns of inheritance. Millions of people worldwide are affected by inherited forms of progressive retinal degeneration, with a wide range in the final outcome of the clinical phenotype. In recent years studies identifying the genetic mutations underlying a variety of retinal degenerative diseases have greatly increased our understanding of the molecular mechanisms involved. Over 240 genes have been identified as linked to retinal degenerative diseases, and the vast majority of inherited forms of retinal degeneration are caused by mutations in photoreceptor-specific transcripts (http://www.sph.uth.tmc.edu/retnet/disease.htm).

Retinitis pigmentosa (RP), one of the most common forms of inherited retinal degeneration, affects 1/4000 people and is characterized by the death of rods and consequently the loss of peripheral and dim-light vision, followed by formation of pigment filled bone spicules and eventually, in a second wave of degeneration, the loss of cone photoreceptors (Figure 2). RP is a heterogeneous group of retinal dystrophies encompassing a wide variety of mutations in photoreceptor and RPE transcripts, 42 of which have been identified (http://www.sph.uth.tmc.edu/retnet/disease.htm). RP can be passed down through autosomal recessive, autosomal dominant, or X-linked patterns of inheritance. It is often diagnosed in young adults or adolescents and is a progressive disorder with no cure available. The most widely prescribed treatments are low vision aids along with a vitamin A enriched diet and docosahexaenoic acid. The final outcome of the disease varies widely, from impaired vision to total blindness.

Figure 2. Illustration of the primary and secondary stages of retinal degeneration in retinitis pigmentosa. A primary loss of peripheral vision caused by loss of rods is followed by secondary loss of central and color vision as a result of cone loss.

Leber congenital amaurosis (LCA) is a leading cause of congenital blindness affecting 1/30,000 people worldwide [3]. The underlying genetic mutation has been identified in about 70 percent of cases [4]. 14 genes have been identified as related to LCA, with mutations in CEP290 accounting for 15%, GUCY2D 12%, and CRB1 10% of cases. It is most often passed down as a recessive condition, and is often diagnosed in infancy as a result of a more severe blindness phenotype. There are no effective treatments for LCA, although the disease is a target of a variety of areas of research, and a number of rodent, avian and canine animal models exist.

The leading cause of blindness in North America is age-related macular degeneration (AMD), with about 10 million people in the US alone at risk. AMD is characterized by a progressive loss of central vision that often appears as a blurring or distortion of the image. Two types of AMD exist: dry and wet AMD. The dry form of AMD is the most common and is associated with the formation of fatty protein deposits called drusen, which are still poorly understood. The progression of the wet form of AMD can be slow, and total vision loss is rare. Wet AMD makes about 10% of cases of AMD and is associated with neovascularization and leakage of blood into the retina. The vision loss associated with wet AMD is often more severe than in dry AMD, however, treatment with an anti-angiogenic drug called Lucentis, a vascular endothelial growth factor A (VEGF-A) antagonist, has proven to be an effective treatment. About half of the cases of AMD appear to have a genetic component, making this one of the most pervasive forms of inherited retinal degenerative disease[5-7].

Beyond these most frequent forms, numerous other retinal degenerations exist, including Stargardt Disease, Best Disease, and X-linked Retinoschisis, as well as syndromic conditions such as Joubert syndrome, Usher Syndrome, and Bardet-Biedl Syndrome in which retinal degeneration is one of many symptoms.

Gene therapy in the retina

As the genetic causes underlying the variety of retinal degenerative disorders are elucidated, one of the most promising areas of research for treating inherited retinal degeneration is the field of gene therapy, whereby a therapeutic gene is transferred to the retina using a viral or nonviral vector. The retina is a complex structure with each cell type interacting with many others, and therefore a single mutation can cause a cascade of defects, as malfunction in a single pathway can affect a whole cell type, which in turn can lead to complicated symptoms throughout the retina. Under these circumstances it may be a more efficient and effective approach to correct the underlying cause of the disorder rather than the myriad of symptoms. In addition, the retina constitutes an attractive target for gene therapy studies due to its accessibility, and the ease with which the eye can be imaged. The retina is contained within a pseudo-immune privileged compartment, separated from the general vascular circulation by the blood-retina barrier, which makes it possible to deliver viral vectors or other reagents in isolation from the rest of the organism.

A multitude of animal models of retinal degenerative diseases exist for many of the most prevalent forms of retinal degeneration, including some with the same mutations found in humans. In many studies one eye is left untreated, acting as an internal control. A number of noninvasive techniques are available for imaging the retina, such as optical coherence tomography (which uses interferometry to create three-dimensional reconstructions of the retina), and white light and fluorescent fundus imaging, as well as functional tests that allow researchers to monitor the recovery of retinal function, such as the electroretinogram, a recording of a field potential response from the retina in response to a flash of light.

The ERG results in a characteristic waveform with a downward A-wave that is indicative of photoreceptor function, followed by a positive B-wave that results from cells in the inner retina including ON-bipolar cells (Figure 3). Changes in the amplitude and waveform of the ERG allow an analysis of the function of subsets of cells in the retina and overall retinal function, and can be repeated throughout the progression of a disease to obtain a time course of rescue.

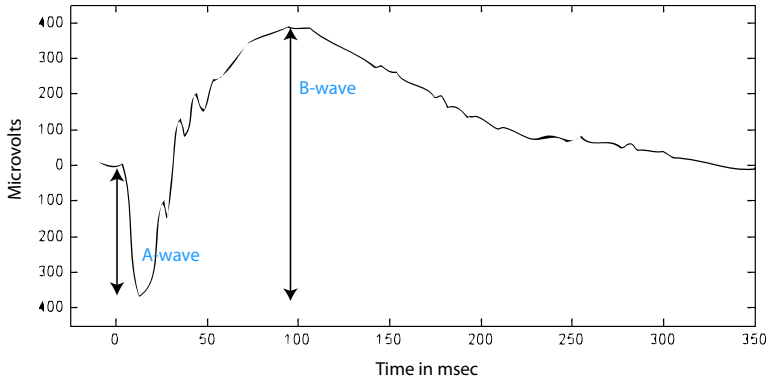

Figure 3. Characteristic electroretinogram recording from a WT mouse.

The electronegative A-wave is followed by a positive B-wave. The A-wave results from photoreceptor hyperpolarization while the B-wave is indicative of function in the inner retina, including bipolar cells.

Gene therapy approaches encompass not only gene replacement strategies, which are possible only in conditions where the exact genetic mutation has been identified, but also trophic factor therapies, which promote cell survival through expression of anti-apoptotic proteins. Gene silencing and knockdown strategies using RNA interference may be effective in treating dominant forms of retinal degeneration, either alone or in combination with gene replacement. Combinations of trophic factor and gene replacement strategies have also been tested in animal models.

Rodent, canine, avian and non-human primate models have been used to investigate gene therapies for RP, LCA, Stargardt disease, XLRS, and many other diseases with great promise (Table 1), including the notable success of studies in the Briard dog, a canine model of LCA with a mutation in the gene encoding the protein RPE65, which plays an important role in vitamin A metabolism and recycling of the visual pigment. In these experiments, subretinal injections were used to deliver a viral vector carrying the gene for RPE65 to the retina of dogs, leading to long-term and stable recovery of vision [8].

Gene	Vector	Delivery	Model	Outcome
Retinitis pigmentosa				
Prph2	AAV-Rho-Prph2	subretinal	$Prph2^{Rd2/Rd2}$ mouse	Long-term photoreceptor ultrastructure preservation, ERG rescue, improved central superior colliculus signaling, more improvement in younger subjects
Bcl2	Ad-2.5HRP-Bcl2	Subretinal	Rd mouse	Rescued photoreceptors for up to 6 weeks, not as effective as Ad-CMV-BPDE
PEDF	SIV-PEDF	Subretinal	RCS rat	Preserved light sensitivity, prevented photoreceptor loss
FGF-2	AAV-CMV-FGF-2	Subretinal	TgN S334ter-4 transgenic rat	Enhanced photoreceptor survival, did not significantly improve ERG
PEDF and FGF-2	SIV-PEDF and SIV-FGF-2	Subretinal	RCS rat	Synergistic protective effects in photoreceptors over SIV-PEDF or SIV-FGF-2 alone
CNTF	Ad-CMV-CNTF	Intravitreal	Rds mouse	Prevented photoreceptor degeneration, improved ERG response
Leber congenital amaurosis				
GUCY2D	pTYF-EF1alpha-GC1-IRES-EGFP	Embryonic	GUCY1*B chicken	Slowed retinal degeneration, partially restored ERG response
RPE65	rAAV2/5-CBA-hRPE65	Subretinal	Rd12 mouse	Improved rhodopsin levels, corrected ERG for 7 months, early treatment more effective
RPE65	AAV-RPE65	Subretinal	RPE65-/- dog	Partially restored ERG, improved pupillary response, visual function for 3 years, well tolerated
RPE65	rAAV2/4-RPE65	Subretinal	RPE65-/- dog	Restored rod and cone function for 8-11 months, not effective in older dogs
RPE65	AAV-RPE65	Subretinal	Cynomolgus monkey	No systemic toxicity, mild ocular inflammation, no vector sequences in optic nerve or brain
Achromatopsia				
GNAT2	rAAV2/5-PR2.1-Gnat2	Subretinal	GNAT2cpfl3 mouse	Rescued cone mediated ERG response and visual acuity
Stargardt disease				
ABCA4	rAAV2/5-CMV-ABCA4	Subretinal	Abca4-/- mouse	Corrected lipofuscin levels, improved RPE morphology and retinal function
X-linked retinoschisis				
Rs1	AAV-CMV-Rs1h	Intravitreal	Rs1h-/- mouse	Rescued retinal morphology, ERG, restored synaptic connections in photoreceptors
Rs1	rAAV2/8-Rs1h	Intravitreal	Rs1h-/- mouse	Decreased schisis cavities, improved ERG
Rs1	rAAV2/5-opsin-Rs1h	Subretinal	Rs1h-/- mouse	Slowed photoreceptor degeneration, improvements observed during late disease stages
Red-green color blindness				
L-opsin	rAAV2/5-L-opsin	Subretinal	L-opsin-deficient adult squirrel monkey	Restored trichromatic color vision behavior

Table 1. Summarizing the use of a variety of animal models in the use of preclinical studies for viral vector-mediated gene therapy in the retina [9].

These studies laid the foundation for groundbreaking clinical trials in humans, demonstrating the safety and efficacy of viral vector-mediated gene replacement treatments [10-12]. Three separate groups initiated Phase I clinical trials for AAV-mediated gene therapy for LCA2 at the Moorfields Eye Hospital/University College in London, at the Children's Hospital of Philadelphia and at the University of Pennsylvania/University of Florida/National Eye Institute. All three used similar adeno-associated (AAV) serotype 2 vectors packaged with different expression cassettes, administered subretinally in the worse eye. These initial trials demonstrated the safety of the procedure and resulted in some promising functional recovery, as assessed by increased ability to circumnavigate an obstacle course and nystagmus measurements, although there was still no recordable ERG. Recently, fMRI studies of these patients have shown increased activity in visual cortex after presentation of a stimulus to the treated eye, suggesting preservation of visual pathways despite long-term vision loss [13]. In general, younger patients had a more significant response to the treatment, and additional clinical trials are now underway targeting younger patients who may have a greater potential for functional rescue as a result of less advanced cell death and retinal remodeling. Although a limited number of patients have been identified with this particular RPE65 mutation, above all these clinical trials demonstrated the therapeutic potential and safety of gene replacement therapies in humans, paving the way for future studies and clinical trials.

Adeno-associated viral vectors for gene therapy

One essential element of these clinical trials as well as studies in animal models has been the vector used to administer therapeutic genetic material. Viral vectors are ideal candidates to accomplish the safe delivery of genetic material into the nucleus because they have evolved over millions of years to do so. Viruses are small particles containing a DNA or RNA genome protected by a protein shell, which is encoded by the viral genes. The protein shell, or capsid, is embedded with proteins that allow for attachment to receptors on the cell surface, which initiates a process of entry into the cell. Once inside, proteins encoded by the viral genome can be synthesized by the cellular machinery.

A variety of viruses with different properties have been used in gene therapy studies including AAV, adenovirus and lentivirus, as well as others. AAV has become the most widely used viral vector because of its favorable properties for transduction of neuronal cells and the fact that it has been well characterized in its wildtype form. AAV is nonpathogenic, and over 90% of the adult population has already been exposed to the virus [14]. Wildtype AAV integrates at a specific location in the human genome (19q13.3-qter for AAV2) [15], but it has been shown that recombinant AAV used in gene therapy studies is inefficient and is no longer targeted [16].

AAV is a parvovirus about 25 nm in diameter and contains a positive or negative linear single-stranded DNA genome. It is a dependovirus and in order to replicate requires a coinfection with a helper virus such as adenovirus. The AAV genome consists of two palindromic inverted terminal repeats (ITR's) that enclose two open reading frames (ORFs), *rep* and *cap,* which encode for the capsid proteins and proteins required for the viral life cycle. Recombinant AAV is created by removing these two ORFs and replacing them with a promoter of choice followed by a therapeutic gene. Over 100 AAV variants have been isolated from a variety of species [17], with the spectrum of AAV variants having diverse tropisms that are suitable for infecting different tissues and cell types. A number of receptors used by different

AAV serotypes have been identified, although work continues to fully understand the mechanisms of cellular entry and trafficking. In addition, recombinant viruses can be created by combining the genome of one serotype with the capsid of another, or by creating chimeric vectors with capsids that are hybrids of two or more serotypes.

Different vector capsids have been shown to have tropisms for different subsets of cells in the retina. For example, AAV4 has been shown to efficiently transduce RPE cells when injected subretinally, while AAV5 has strong tropism for photoreceptors, also from subretinal injection. AAV2 infects photoreceptors less well, but leads to strong expression in ganglion cells when injected into the vitreous. AAV8 can infect Müller glia when injected subretinally, as well as RPE and photoreceptors.

Due to its limited packaging capacity, however, the application of AAV is currently limited to treatments that require a payload of 4.5 kb or less. As a result, a number of other viral vectors have been used in retinal gene therapy studies. Adenovirus is another nonintegrating vector with a DNA genome that possesses the ability to transduce terminally differentiated cells. It has a large packaging capacity of 36 kb. However, these viruses can elicit an immune response that silences gene expression. This immune response can be diminished by using helper-dependent adenovirus vectors, and a number of serotypes exist that are currently being characterized [18].

Lentivirus, which also has a larger packaging capacity, has also been investigated as a candidate for gene delivery, although it has been shown to have a poor tropism for photoreceptors, which are one of the primary targets for retinal gene therapy. Transduction with lentivirus leads to stable and long-term expression in retinal tissue. Lentiviruses are insertional, however, raising concerns about insertional mutagenesis and oncogenesis. Some of the avenues of lentiviral research, therefore, include the production of non-insertional, self-inactivating, and highly deleted lentiviral vectors for increased safety.

Nonetheless, AAV remains the gold standard for ocular gene therapy, and in addition to the extant range of AAV serotypes a number of recent advances have made the vector even more appealing for use in the retina. In a series of studies, Srivastava [19], Hauswirth [20], and others have shown that mutation of tyrosine residues on the surface of the AAV capsid can significantly increase the transduction capacity of the vector, with multiple tyrosine mutations conferring additional benefit in the retina. These tyrosine mutations expand the tropism and increase expression of AAV serotypes 2, 8 and 9 via intravitreal and subretinal delivery.

In another method, directed evolution has been used successfully to create AAV vectors with novel properties [21,22]. This high-throughput method creates highly diversified libraries of AAV mutants through shuffling AAV capsid genes, error prone PCR or insertional mutagenesis, which are then screened for variants with a novel desired property, such as transduction for glia (Figure 4). Successful variants can be subjected to a further round of diversification for a number of cycles, leading to convergence toward a number of successful novel vectors. As demonstrated below, this strategy has promise for creating novel vectors with highly desirable properties for retinal gene therapy.

This dissertation explores the use of engineered adeno-associated vectors for use in gene therapy treatments for progressive degenerative disease in the retina. The experiments described here illustrate the malleability of AAV and the potential of this vector for specialization and improved retinal transduction. This work emphasizes the importance of a rational approach to creating viral vectors that are ideally suited for gene therapy in the retina and designed for targeting specific retinal cell types through safe, noninvasive routes of administration. These

studies contribute to work that is paving the way for highly efficient, long-lasting and easily administered gene therapy treatments that may provide a cure for a wide range of inherited retinal degenerations, and could be translated to the clinic in the near future. The rapid progress currently being made in the field of gene therapy makes this an exciting and hopeful time for research into treatments for retinal degenerative disease.

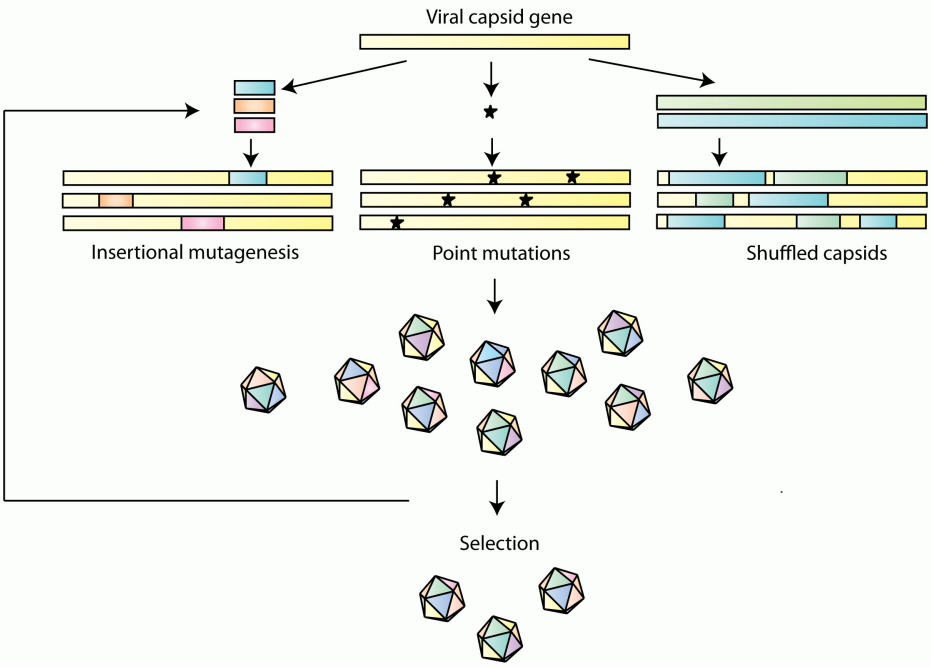

Figure 4. The method of directed evolution.

Through insertional mutagenesis, error prone PCR or genome shuffling, a highly diversified library of vectors are created, which are then screened for variants with a novel desired property. Successful variants are subjected to further rounds of diversification leading to convergence toward a number of successful novel vectors.

Chapter 2

In vivo directed evolution of AAV yields a photoreceptor permissive viral variant capable of transduction from the vitreous[1]

[1]This work was done in collaboration with Deniz Dalkara, Ryan Klimczak, Meike Visel, John G. Flannery and David V. Schaffer.

Abstract

A great majority of retinal degenerations are caused by mutations in photoreceptor or RPE-specific transcripts. Thus far, all gene-based therapies for retinal degenerations have relied on the subretinal delivery of the vector to be able to reach these cells. However, subretinal injections transduce cells in a limited area and pose a substantial risk of tissue trauma during surgery. Non-invasive and widespread retinal gene delivery, which would address these concerns, has thus been a long-sought goal of gene therapy for inherited retinal degenerations. For targeting photoreceptors diseases, an intravitreal delivery route would be desirable in terms of safety, simplicity, and diffusivity of expression. Naturally occurring AAV serotypes are incapable of transducing photoreceptors from the vitreous due to the numerous physiological barriers present in the retina, most significantly the inner limiting membrane and the overlying strata of neuronal and glial cell bodies and processes occluding photoreceptor cell accessibility. Here, we employed an *in vivo* directed evolutionary strategy in a Rho-GFP transgenic line of mice with a panel of three distinct AAV libraries to evolve variants capable of infecting photoreceptors from the vitreous. We successfully isolated a variant from our AAV2 peptide display library, named 7m8, capable of efficient intravitreal photoreceptor transduction. 7m8 was then used to deliver a therapeutic copy of the RS1 gene to photoreceptors in a mouse model of X-linked retinoschisis (XLRS). Significant functional and histological rescue was observed using 7m8, and this rescue was greater than that observed using the parental serotype AAV2.

Introduction

Photoreceptors are the first order neurons of the retina and are responsible for detecting photons and the first stages of processing visual information through phototransduction. The overwhelming majority of inherited retinal diseases result in the loss of these cells, either directly, as in the case of dominant mutations affecting rhodopsin protein folding, or indirectly, as caused by recessive mutations affecting retinal recycling pathways in the retinal pigment epithelium (RPE) [3,23-25]. The convergence of these genetically and mechanistically complex diseases into a common neurodegenerative phenotype makes photoreceptors an attractive gene delivery target for gene replacement, antisense, and/or neurotrophic therapeutic strategies to lessen or even stop photoreceptor cell loss. Viral vectors including lentivirus and adeno-associated virus (AAV) have been used successfully to transduce photoreceptors through subretinal administration for gene-based therapies [26-28]. However, due to the significant advantages of vector transduction via intravitreal injection relative to subretinal injection, namely safety, simplicity, and diffusivity of expression, intravitreal-mediated gene delivery to photoreceptors would be ideal for gene therapeutic purposes. Importantly, in diseases like X-linked retinoschisis (XLRS), in which the retina is severely structurally compromised with islands of surviving neural tissue, an intravitreal injection can be the only relevant surgical route of gene delivery.

Unfortunately, naturally occurring serotypes of AAV are incapable of transducing photoreceptors from the vitreous due to the enormous physical barriers obstructing these cells [29,30]. The inner limiting membrane and the overlying strata of neuronal and glial cell bodies

and processes results in a formidable diffusive obstacle for AAV particles, despite their small size. Most recently, success has been attained in increasing intravitreal photoreceptor gene delivery through mutagenizing tyrosine residues on the AAV capsid surface. Tyrosine residues naturally target AAV particles for proteosome-mediated degradation via an ubiquitin-dependent pathway once they are endocytosed within the cell [20]. This process is initiated by tyrosine phosphorylation by the epidermal growth factor receptor protein tyrosine kinase (EGFR-PTK). Substitution with a phenylalanine residue allows AAV to avoid this pathway, enabling greater efficiency of viral gene delivery to cell nuclei. In this regard, Petrs-Silva et al. achieved intravitreal photoreceptor transduction of murine photoreceptors through the use of a quadruple tyrosine to phenylalanine (AAV2-4YF) vector. These results suggest that AAV2 has the partial ability to reach the ONL from the vitreous and infect photoreceptors.

In this respect, directed evolution of AAV capsid may enable increases in infectivity based on subtle sequence changes that allows virions to better surpass the ILM, evade sequestration within the RGC and INL layers, and / or overcome photoreceptor cellular barriers. Due to the complexity of these physiological barriers, an *in vivo* screening methodology is critical for selecting for permissive variants. The transgenic mouse line bearing a rhodopsin-GFP fusion [31] has enabled this approach as selective expression of GFP in photoreceptor outer segments allows for the isolation of photoreceptors via fluorescence activated cell sorting (FACS). Thus, an evolutionary strategy involving direct vitreal injection of viral libraries followed by photoreceptor cell isolation and PCR rescue may enable the creation of permissive variants for intravitreal photoreceptor transduction.

Here, we describe the results of this selection strategy through the use of three distinct AAV libraries: a novel AAV2 Y444F error prone library, an AAV2 heptamer insertion library, and a shuffled library composed of AAV serotypes 1-9. Importantly, we describe functional and histological rescue of the XLRS disease phenotype by RS1 gene delivery to the photoreceptors in a transgenic mouse model of retinoschisis as a proof of concept for promising photoreceptor targeted gene therapies. The ability of 7m8 to safely and efficiently target the RS1 gene to photoreceptors, the cell type normally producing retinoschisin, has made gene replacement therapy significantly more effective then using AAV2 which provides secretion of the protein from inner retinal cells.

R**esults**

Library selection

Three different libraries with a diversity of approximately $1x10^7$ were used for *in vivo* selection in transgenic rho-GFP mice. Besides the AAV2 7mer insertion and AAV 1-9 shuffled libraries we have employed in previous studies, we created a tyrosine mutated error prone library (AAV2 Y444F EP) in light of the marginal success observed in previous studies for AAV2 Y444F in increasing the infectivity of the virus [19]. The libraries were initially combined in equal ratios and two rounds of selection were performed (Figure 1). One round of evolution consisted of initial library diversification followed by three selection steps. Briefly, in one round of selection, P30 rho-GFP mice were intravitreally injected with 2µL of PBS-dialyzed, iodixanol-purified library with a genomic titer of $1x10^{12}$ vg/mL. One week post-injection, eyes were enucleated and retinas dissociated using a light, papain protease treatment, followed by FACS isolation of photoreceptor populations (Figure 1).

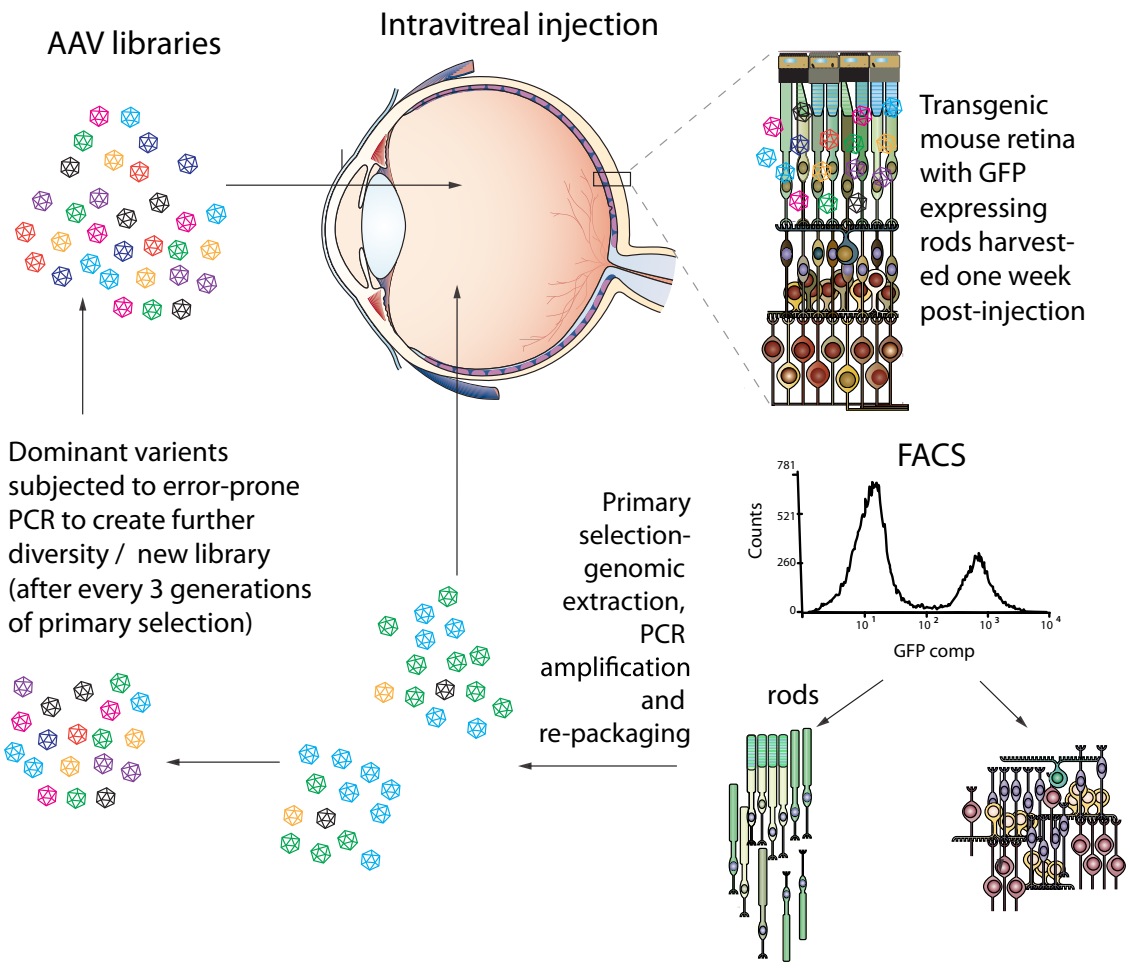

Figure 1. Schematic of in vivo directed evolution process used to generate AAV variants.

An error prone AAV2-Y444F, an AAV1-9 shuffled and a random 7mer insertion library, each with a diversity of 10E7 novel variants were mixed in equal parts (libraries) and injected intravitreally into adult transgenic rho-GFP mice eyes. One week post-injection, eyes were enucleated and retinas dissociated using a light papain protease treatment followed by FACS isolation of photoreceptor populations (representative FACS plot). Successful viral cap genes were then PCR amplified from genomic extractions and further cloned and repackaged. One round of evolution consisted of initial library diversification followed by three selection steps.

Successful virions were then PCR amplified from subsequent genomic extractions and further cloned and repackaged for injection. The expression of a rhodopsin-GFP fusion allows for the segregation of photoreceptor cell populations from retinal dissociate. Following two rounds of evolution, the cap genes of fifty variants were sequenced to determine the most prominent and successful variants to have permissive mutations for intravitreal photoreceptor transduction (Table 1). Remarkably, all isolated clones derived from the AAV2 7mer peptide insertion library. Furthermore, nearly two thirds of them contained the same distinct 7mer motif (~588LGETTRP~). Interestingly, the next most prominent variant (~588NETITRP~) also contained a similar flanking motif consisting of a positively-charged arginine residue in between a polar threonine and a nonpolar proline residue (TRP).

Clone	Percentage of total isolated variants
AAV2~588LALGETTRP	64 %
AAV2~588LANETITRP	12 %
AAV2~588LAKAGQANN	6 %
AAV2~588LAKDPKTTN	4 %

Table 1. Sequencing of isolated variants from directed evolution reveals a high degree of convergence in viral libraries. All variants derived from the AAV2 7mer library, with 64% of variants containing the same 7mer motif (~588LGETTRP~). The rest of the isolated sequences were represented only once within the population and are not included in the table.

In light of the high degree of library convergence from our selection, we made a molecular model of 7m8 based on a prediction of how the 7mer loop would orient itself with respect to the AAV2 capsid. The amino acid residues were inserted into the PDB file 1LP3 (AAV2) at position 588 using Maestro software. This new data file was used in its entirety in the Swiss Model homology mode using default automated settings to build the VP3 monomer (Figure 2B). The monomer was superposed onto the wild type AAV2 VP3 monomer and then http://viperdb.scripps.edu/pdbToViper.php was used to reconstruct the capsid its entity (Figure 2A). Figure 2C shows the predicted loop structure in higher magnification.

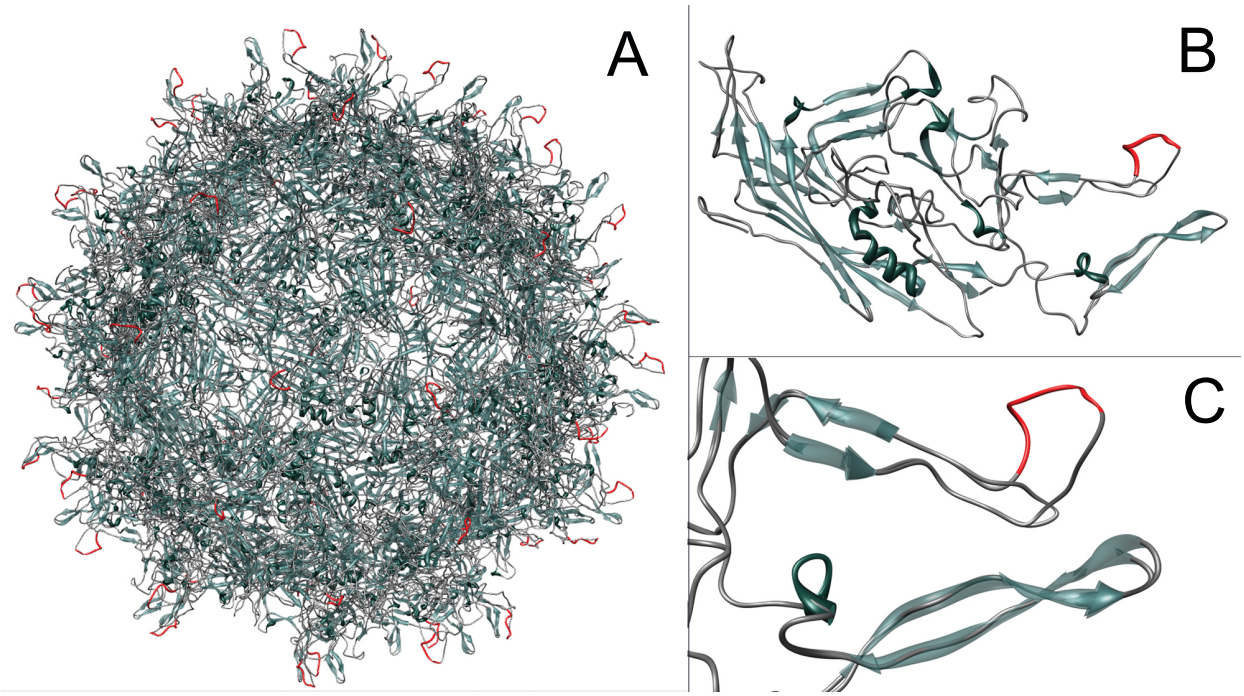

Figure 2. Representative three-dimensional capsid model of AAV2 containing the 7mer motif LALGETTRP (shown in orange) following amino acid 587. The dynamic interactions between the inserted loop and the other surface loops of the capsid likely play a role in the novel receptor binding properties of the virus.

In vivo characterization

A recombinant form of AAV2 ~$_{588}$LGETTRP~ (called 7m8) was cloned and packaged with a scCAG-GFP transgene to visualize its transduction profile. Three weeks following intravitreal injection in adult mice, we observed robust pan-retinal GFP expression in fundus images (Figure 3A). The retinas were extracted at 6 weeks post injection and mounted as retinal flat mounts. The retinal flat-mounts were mounted with the photoreceptor side facing up for imaging. Strong GFP expression was observed throughout the photoreceptors of the retina (Figure 3B). Transverse cryosections showed fluorescence in numerous cell types including RGCs, amacrine cells, and Müller glia throughout the retina (Figure 3D). The substantial difference between the transduction patterns of 7m8 versus its parental serotype AAV2 can be seen in Figure 3C,D. Namely, our positive selection methodology directed virus towards greater infective efficiency, but not specificity, as expression results in all retinal layers when a ubiquitous CAG promoter is used. However, the 7m8 variant (Figure 3D) clearly demonstrates greater levels of intravitreal photoreceptor transduction relative to AAV2 (Figure 3C).

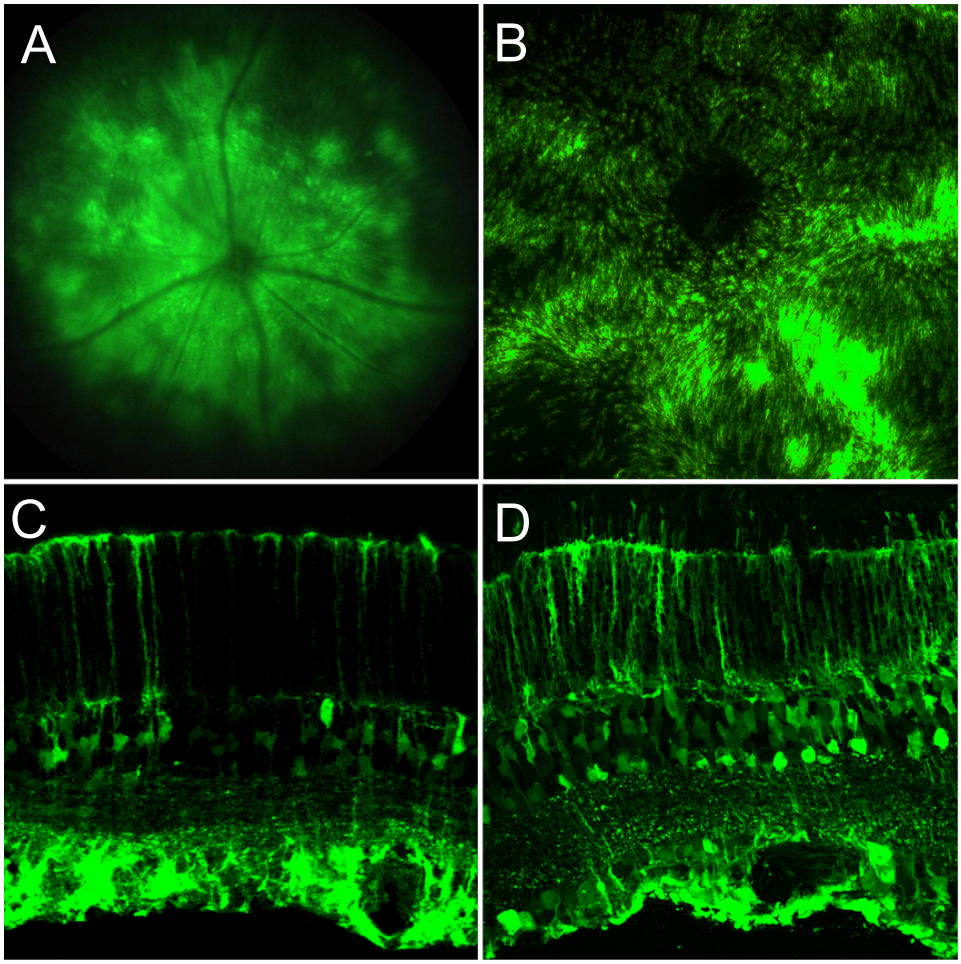

Figure 3. Enhanced outer retinal transduction by novel AAV variant 7m8 compared to AAV2, its parental serotype.

Fundus image of a mouse retina 3 weeks post injection with 7m8-scCAG-GFP, showing pan-retinal gene expression (A). A retinal flat-mount oriented with the ONL facing upwards shows GFP expression in photoreceptor cell bodies and outer segments across the retina (B). 7M8 variant (D) demonstrates greater levels of intravitreal photoreceptor transduction relative to AAV2 (C). Confocal microscopy images of transverse retinal sections were taken six weeks after intravitreal injection of 1μL of 1x1012 vg/mL of 7m8 or AAV2 in adult wild-type mice.

Mechanism

To examine the mechanism of 7m8 transduction, we first assayed its glycan dependencies on a panel of different cell types *in vitro (*Figure 4A). AAV2 and 7m8 transduction efficiencies in CHO cells and pgsA cells, which lack heparin sulfate production, reveal strong heparin dependencies for both viruses with a log drop in infectivity. Conversely, both viruses showed no sialic acid dependence as transduction efficiencies were similar between Pro5 cells and Lec1 cells, which are deficient in sialic acid production. Interestingly, amongst all cell types, 7m8

showed substantial increases in transduction relative to AAV2, with between ten to a hundred fold increase in infectivity. 7m8 demonstrates a sharper elution profile and a lower heparin affinity relative to AAV2, most likely because the inserted 7mer is localized near the AAV2 HSPG binding domain, occluding efficient binding (Figure 4B). We can therefore expect that accumulation around the ILM, an area prominent in HSPGs, is less prominent in 7m8-injected eyes relative to AAV2 and this may account for the better retinal penetration properties of 7m8 in part. In reconciling these observations with our *in vitro* data, 7m8's remarkably high infectivity is most likely a result of efficient binding to another, as yet undefined, cell surface receptor, or the result of greater efficiencies in intracellular viral trafficking and / or nuclear localization.

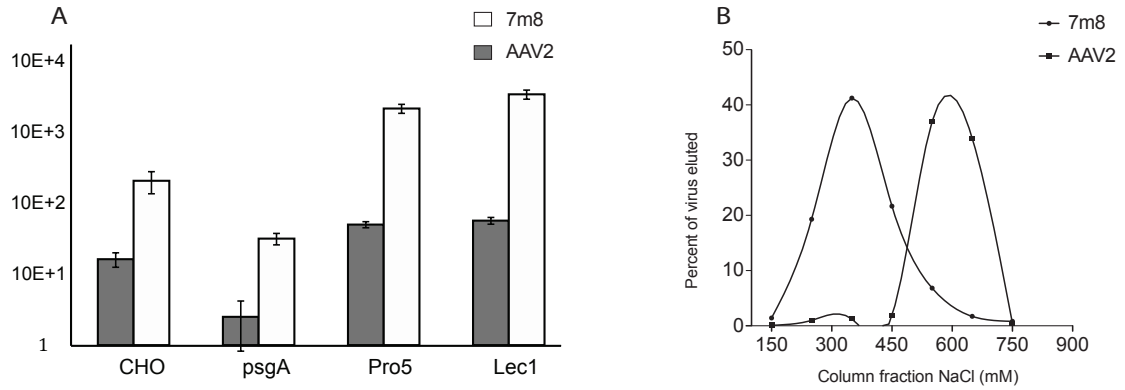

Figure 4. Characterization of 7m8 binding and infection ex vivo.

(A) Ex vivo characterization of 7m8 on relevant cell types. CHO, PgsA, Pro5, and Lec1 cell transduction by AAV2 and 7m8 carrying scCAG-GFP; Y-axis represents the ratio of TU:vg x10^4 in each cell type. CHO/PgsA transduction probes the HSPG dependence, while Pro5/Lec1 transduction examines sialic acid dependence of AAV2 and 7m8. (B) Heparin binding affinity of 7m8 and AAV2. Elution profile from a heparin column for 7m8 and AAV2. Y-axis values represent the fraction of virus eluted, and the X-axis represents the concentration of NaCl in the eluant (mM).

Limiting the expression to photoreceptors

To better characterize the photoreceptor transduction properties of 7m8, we packaged a GFP gene under the control of a mouse rhodopsin promoter and injected the resulting vector into the vitreous cavity of adult wild-type mice. After 3 weeks, pan-retinal GFP expression was detectable in fundus images (data not shown). At 4-6 weeks post injection mice were enucleated and eyes were cryosectioned to reveal the transgene expression patterns across the retina (Figure 5A). Transverse sections show exclusive GFP expression in the photoreceptor layer of the retina. Retinal flat-mounts were also examined, mounted with their photoreceptor side facing up as described above. Strong GFP fluorescence was seen in the outer segments and cell bodies of numerous cells across the retina. Figure 5B shows a confocal image at 20x magnification of the

central retina where the cones have been stained with peanut agglutinin (PNA) showing that the expression pattern is mostly restricted to the rod photoreceptors with the mouse rhodopsin promoter.

We then performed more quantitative analysis of the number of photoreceptor cells transduced in retinas treated with 7m8-rho-GFP in comparison with the AAV2-4YF quadruple mutant that has previously been described to infect photoreceptors from the vitreous. Mouse eyes having received an intravitreal injection of 1x10E10 gc of either 7m8-rho-GFP (n=8) or AAV2-4YF-rho-GFP (n=8) were sacrificed in two separate groups 1 month post injection and 4 retinas were extracted and subjected to papain dissociation. 4 retinas from each group were run through FACS on two separate days. Figure 5C shows the GFP(+) portion of the two samples represented as histograms overlaid to allow comparison. The total number GFP(+) cells were counted for each condition and represented as GFP(+) cells per million cells counted (each dot representing counts from 4 retinas on one particular day). Figure 5D shows GFP(+) cell counts per million cells counted for each condition. In conclusion, 7m8 leads to GFP expression in about twice as many photoreceptors as AAV2-4YF when injected intravitreally.

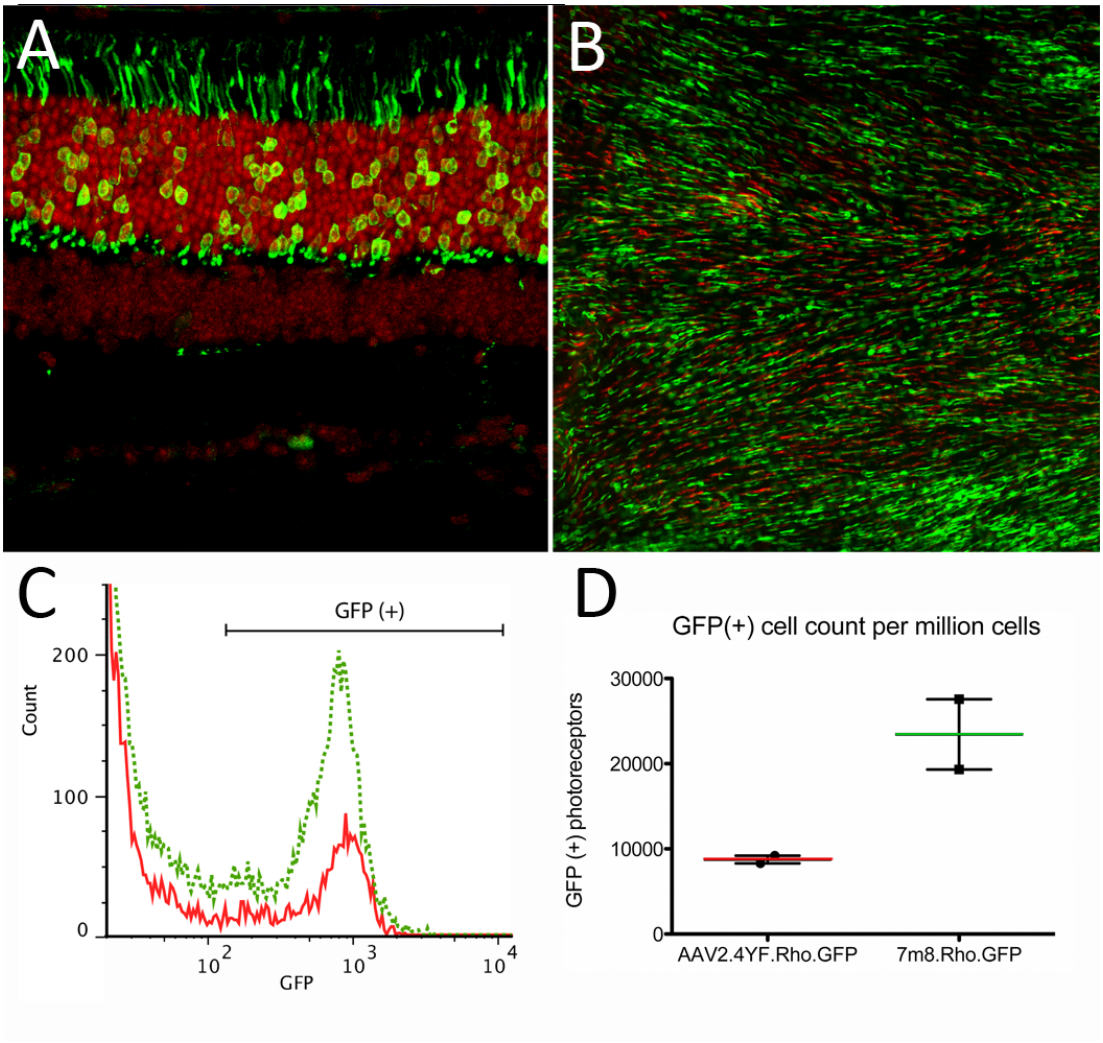

Figure 5. Restricting gene expression to photoreceptor cells through the use of a rhodopsin promoter.

GFP expression was limited to the ONL of the retina by replacing the ubiquitous CAG promoter with a mouse rhodopsin promoter. 7m8-rho-GFP was injected into the eyes of wild-type mice, 15 μm thick cryosections were made at 1 month post injection and anti-GFP immunostaining was performed (A). Retinal flat-mount, ONL side up, stained with peanut agglutinin (PNA) in red (B). Representative FACS histograms of the GFP (+) subpopulation of cells in 7m8 (n=4) shown in green and AAV2-4YF (n=4) in red overlaid for comparison (C). GFP(+) cells per million cells counted for each of the viruses (D). 4 retinas from each group were run through FACS on two separate days. The total number GFP(+) cells were counted for each condition and represented as GFP(+) cells per million cells counted (each dot representing counts from 4 retinas on one particular day with the line representing the average of 8 retinas).

The use of 7m8 in a photoreceptor disease model

Encouraged by the above findings, we proceeded to test the feasibility of a gene replacement therapy using 7m8 in an animal model of photoreceptor disease. X-linked retinoschisis (XLRS) is one of the most common forms of inherited juvenile macular degeneration affecting young males, and is characterized by structural abnormalities including a splitting, or schisis, of the retina and a gradual loss of photoreceptors. XLRS is caused by mutations in the gene encoding the putative cell-adhesion protein retinoschisin, which is secreted from photoreceptors and binds to an as yet unidentified target on the surface of cells in the outer and inner retina. In some patients this structural deficiency leads to permanent retinal detachment and blindness. Since the retinal morphology in this disease is particularly poor, performing invasive subretinal injections is extremely risky, thus making the use of a viral vector targeting the photoreceptors from the vitreous an attractive prospect. We therefore used 7m8 to deliver a healthy copy of the retinoschisin gene to the photoreceptor cells in a mouse model of XLRS. We replaced the GFP gene used above with the RS1 gene under the control of the same rhodopsin promoter and delivered 7m8-rho-RS1 intravitreally in the mouse model of XLRS, lacking *Rs1h*, the mouse homolog of retinoschisin [32]. As a comparison, we injected another cohort of mice with AAV2 carrying the same transgene. 3 months after birth, full-field scotopic electroretinograms were measured to assess retinal function (Figure 6, bottom panels). The amplitude of the full-field scotopic electroretinogram B-wave was measured for 7m8-rho-RS1 (n=3), and AAV2-rho-RS1(n=3). Both 7m8 and its parental serotype AAV2 led to an improvement in B-wave amplitude at P90. The B-wave amplitudes were on average 140% better with 7m8 compared to AAV2. A-wave amplitudes were also improved significantly using 7m8 pointing to the importance of the cell type targeted in the successful rescue of a disease phenotype. This is in agreement with additional data from our group indicating that targeting photoreceptors over Müller cells has been shown to lead to better rescue. High-resolution SD-OCT images of retinas at four months post-injection showed significant reduction in the number of cavities in retinas treated with 7m8, compared to GFP-treated eyes (Figure 6A-F) confirming the ameliorations seen in ERGs. Untreated eyes were characterized by substantial retinal disorganization and large cavities in the inner nuclear layer, which were apparent in retinal cross sections as well as en face images of the inner nuclear layer (Figure 6A,D). In striking contrast

retinas treated with 7m8-rho-RS1 had far fewer cavities, which were barely visible in fundus images and cross sections (Figure 6B,E). Thinning of the outer nuclear layer in treated animals compared to WT indicates that injection at P15 was not sufficient to arrest an early wave of photoreceptor apoptosis, which peaks at P18 in this animal model [33].

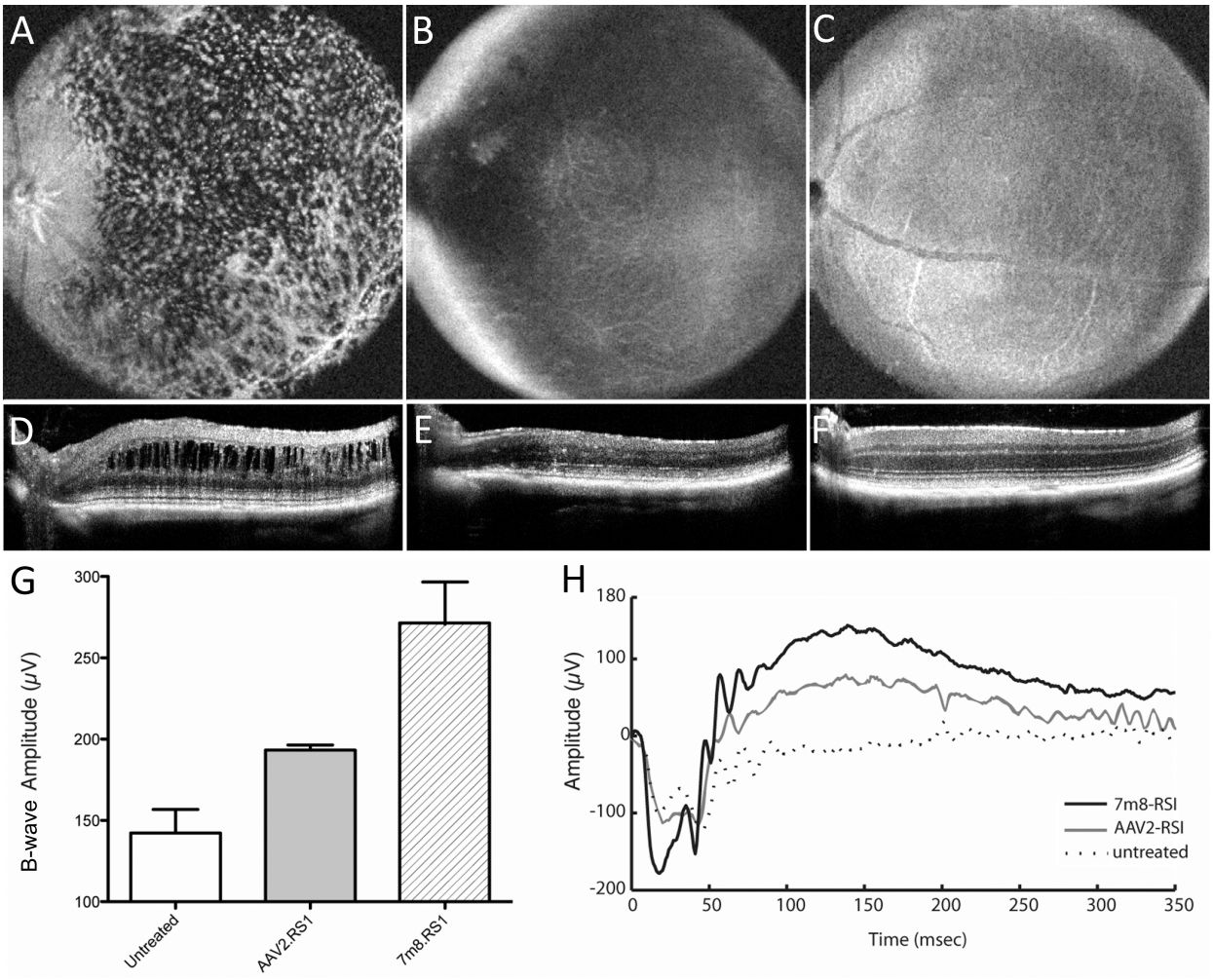

Figure 6. Functional and histological rescue of the XLRS phenotype in transgenic *Rs1h* mutant mice.

Fundus OCT image focusing on the ONL of an untreated RS1 retina at 4.5 months of age (A) compared to age matched 7m8-rho-RS1 treated (B) and wild-type (C) mouse retinas. Transverse views of the fundus images shown above for each of the age matched untreated (D), 7m8-rho-RS1 treated (E) and wild-type (F) mouse retinas. Average ERG B-wave amplitudes from mice treated with AAV2-Rho-RS1 or 7m8-Rho-RS1 at three months post-injection (G) and representative ERG traces corresponding to the averaged B-waves (H).

Discussion

Altogether, our results demonstrate that our *in vivo* selection approach produced a variant capable of overcoming the substantial intravitreal barriers to photoreceptor infection. The striking degree of convergence from our initial starting libraries reflects the tremendous constraints imposed by our positive selection. Variants must not only pass the ILM, but also travel through a tight extracellular matrix network formed between a lattice of retinal cell bodies and processes to reach the ONL. Additionally, they must bind to photoreceptor cell surface receptors and subsequently overcome intracellular barriers to transduction. The predominance of AAV2-based variants from our selection is most likely due to the critical importance of heparin-sulfate in initial binding to the ILM for intravitreal AAV transduction. Our previous studies have shown that amongst natural AAV serotypes in the rodent retina, only those which bind HSPG, such as AAV2, efficiently infect from the vitreous [29]. Thus, within our pool of libraries, variants based on heparin-binding templates held immediate advantage relative to other variants, easily outcompeting them in the first rounds of selection. In future studies, segregating library populations may thus be an effective way to achieve greater variant diversities based on other AAV serotypes with unique tropism profiles. For instance, AAV5's ability to efficiently infect photoreceptors from the subretinal space may make it a promising template for an error prone mutagenesis or peptide insertion library.

In beginning to deduce 7m8's mechanism, the variant's reduced heparin affinity relative to AAV2 may partially explain its unique properties. In first binding to the ILM, the presence of high levels of heparin sulfate in the proteoglycan matrix of the ILM may mediate viral localization at this site, preventing it from being cleared from the vitreous and thus facilitating intravitreal transduction [29]. However, viral HSPG affinities may play a duel role in intravitreal transduction, as too high of an affinity may also encumber efficient viral penetration in the retina, similar to results seen in our previous mechanistic study of our AAV variant ShH10 [22]. Further possibilities for 7m8's increased infectivity, as it appears to not be limited to just photoreceptors, is that its 7mer insert may bind to a common cell surface receptor, or more intriguingly, it may act as a nuclear localization signal within the cell although a protein BLAST search does not reveal any notable sequence matches.

In this study, the successful isolation of a novel AAV variant that transduces photoreceptors from the vitreous serves as an important foundation in the development of new gene therapy strategies for combating a wide array of inherited retinal degenerative diseases. The pan-retinal infective properties of 7m8 coupled with the use of promoters for cell-restrictive expression may make it a valuable vector for targeting other neurons in the retina. For example, gene delivery of synthetic light-sensitive channels, such as LiGluR, or other optogenetic tools such as Channelrhodopsin variants to ON-bipolar cells may allow for the artificial restoration of vision in ONL-depleted retinas. More broadly, further mechanistic dissection of 7m8 and other AAV variants isolated from *in vivo* selections may reveal common motifs that can be exploited to create a new generation of more efficient AAV vectors.

Our results in the rescue of the XLRS phenotype also point to the importance of cell-type-targeting in achieving high levels of properly localized therapeutic gene expression. We observe a 140% better rescue of the ERG B-wave amplitude using 7m8-rho, targeting photoreceptors (the cell type that normally produces the retinoschisis protein), versus AAV2-

CAG that expresses mostly in inner retinal cells including ganglion cells. These results indicate the importance of careful design in the development of gene therapy strategies for optimization.

Viral engineering holds great potential in ameliorating the efficacy of the naturally occurring AAV serotypes currently used in the clinic [10,11]. The high infectivity of the 7m8 capsid (up to 100x AAV2 in certain cell types) also suggests lower doses of this engineered vector can be employed to achieve similar transduction efficiencies as its parental serotype AAV2, lowering the risks of immune response to the capsid, an important consideration for intravitreally delivered AAV vectors [35]. Importantly, AAV variants evolved through directed evolution can be further enhanced using rational mutagenesis approaches. Recently, it has been shown that mutations of the surface-exposed tyrosine residues might allow the vectors to evade phosphorylation and subsequent ubiquitination, preventing proteasome-mediated degradation. It has been documented that tyrosine mutation leads to production of vectors that transduce retinal cells more efficiently at a log lower vector dose [20]. Improved intracellular trafficking to the nucleus may compliment the enhancements afforded at the viral capsid receptor binding afforded by our strategy. In moving forward, we would like to further enhance our 7m8 variant by tyrosine mutagenesis towards the development of AAV vectors that are capable of high-efficiency transduction at even lower doses, important to their use in human gene therapy.

Materials and Methods

Library generation and viral production

Random mutagenesis libraries were generated by subjecting *cap* genes from AAV2 Y444F to error-prone PCR using CAP For and CAP Rev as forward and reverse primers, respectively, as previously described [36]. To generate the Y444F mutation on the AAV2 *cap* gene, as well as all subsequent tyrosine to phenylalanine mutations, a site directed mutagenesis kit was used (QuikChange® Lightning, Agilent Technologies). Peptide display libraries were generated similar to previous reports [37,38]. Briefly, a unique *Avr*II was introduced into pSub2Cap2 between amino acid 587 and 588 by PCR mutagenesis. A random 21 nucleotide insert, 7mer For, was used to synthesize dsDNA inserts, along with the antisense primer 7mer Rev. The resulting dsDNA inserts were cloned into the *Avr*II site of pSub2Cap2 after digestion with *Nhe*I. A previously generated AAV library constructed by DNA shuffling of *cap* genes from AAV1, 2, 4–6, 8, and 9 was also used [39]. The rcAAV libraries and rAAV vectors expressing GFP under a CAG or Rho promoter were packaged as previously described [36,39]. DNase-resistant genomic titers were obtained via quantitative PCR.

Library selection and evolution

The libraries were initially combined and two rounds of evolution were performed. One round of evolution consisted of initial library diversification followed by three selection steps. Briefly, in one round of selection, P30 rho-GFP mice were intravitreally injected with 2µL of PBS-dialyzed, iodixanol-purified library with a genomic titer of approximately $1x10^{12}$ vg/mL. All animal procedures were conducted according to the ARVO Statement for the Use of Animals and the guidelines of the Office of Laboratory Animal Care at the University of California, Berkeley. Before vector administration, mice were anesthetized with ketamine (72 mg/kg) and xylazine (64 mg/kg) by intraperitoneal injection. An ultrafine 30 1/2-gauge disposable needle

was passed through the sclera, at the equator and next to the limbus, into the vitreous cavity. Injection of 2µl was made with direct observation of the needle in the center of the vitreous cavity. One week post-injection, eyes were enucleated and retinas dissociated using a light, papain protease treatment, followed by FACS isolation of photoreceptor populations. Successful virions were then PCR amplified from subsequent genomic extractions and further cloned and repackaged for injection. Following two rounds of evolution, the cap genes of fifty variants were sequenced to determine the most prominent and successful variants to have permissive mutations for intravitreal photoreceptor transduction.

In vivo characterization

P30 wild-type mice were used for characterization after library selection. Intravitreal injections were performed as before. One to three weeks after vector injection, mice were humanely euthanized, the eyes were enucleated, a hole was introduced in the cornea, and tissue was fixed with 10% neutral buffered formalin for 2–3 hours. The cornea and lens were removed. The eyecups were washed in PBS followed by 30% sucrose in the same buffer overnight. Eyes were then embedded in optimal cutting temperature embedding compound (OCT; Miles Diagnostics, Elkhart, IN) and oriented for 10 µm thick transverse retinal sections. Tissue sections were rehydrated in PBS for 5 minutes followed by incubation in a blocking solution of 1% bovine serum albumin, 0.5% Triton X-100, and 2% normal donkey serum in PBS for 2–3 hours. Slides were incubated overnight at 4 °C with commercial rabbit monoclonal antibody raised against GFP (Invitrogen, Carlsbad, CA) at 1:400 or mouse monoclonal antibody raised against AAV2 (A20) at 1:400. The sections were then incubated with Alexa 488– conjugated secondary anti-rabbit or anti-mouse antibody (Molecular Probes, Grand Island, NY) at 1:1000 in blocking solution for 2 hours at room temperature. The results were analyzed by fluorescence microscopy using an Axiophot microscope (Zeiss, Thornwood, NY) equipped with X-Cite PC200 light source and QCapture Pro camera, or by confocal microscopy (LSM5; Carl Zeiss Microimaging, Thornwood, NY).

In Vitro Transduction Analysis

Transduction studies using rAAV-CAG-GFP were performed with $5x10^4$cells (CHO, pgsA, Pro5, and Lec1) in 6-well plates. Cells were transduced with rAAV-GFP vectors at a gMOI of 10^3–10^5 (n = 3), and the percentage of GFP-expressing cells was determined by flow cytometry 4 days post-infection.

Electroretinograms

Mice were dark-adapted for 2 hours and then anesthetized, followed by pupil dilation. Mice were placed on a 37°C heated pad and contact lenses were positioned on the cornea of both eyes. A reference electrode connected to a splitter was inserted into the forehead and a ground electrode was inserted in the tail. For scotopic conditions electroretinograms were recorded (Espion E2 ERG system; Diagnosys LLC, Littleton, MA) in response to six light flash intensities ranging from −3 to 1 log cd × s/m^2 on a dark background. Each stimulus was presented in series of three. For photopic ERGs the animal was first exposed to a rod saturating background for 5 minutes. Stimuli ranging from -0.9 to 1.4 log cd × s/m^2 were presented 20 times on a lighted

background. Stimulus intensity and timing were computer controlled. Data were analyzed with MatLab (v7.7; Mathworks, Natick, MA). ERG amplitudes were compared using a student's t-test.

High-resolution spectral domain optical coherence tomography

Histological imaging was performed using an 840nm SDOIS OCT system (Bioptigen, Durham, North Carolina) including an 840nm SDOIS Engine with 93nm bandwidth internal source providing < 3.0 μm resolution in tissue. Mice were anesthetized and the pupils dilated with atropine before imaging. Images of retinal cross sections were averaged from 8 contiguous slices. Fundus images were taken from en face views through the INL.

Acknowledgements

The authors would like to thank Dr Kathy Durkin of the Berkeley Molecular Graphics Facility for her help in generating the visual representations of the 7m8 capsid. We are thankful to Dr Alberto Auricchio for sharing the AAV-rho-GFP plasmid. This work was supported by grants from the National Institutes of Health Nanomedicine Development Center for the Optical Control of Biological Function (PN2EY018241), the Foundation Fighting Blindness USA.

Chapter 3

Engineered AAV-Mediated Delivery of Retinoschisin via Intravitreal Injection Rescues Retinal Structure and Function in the Rs1h-Deficient Mouse[2]

[2]This work was done in collaboration with Deniz Dalkara, Trevor Lee, Meike Visel, David V. Schaffer, and John G. Flannery.

Abstract

X-linked retinoschisis (XLRS) is one of the most common forms of inherited retinal degeneration affecting juveniles, and is characterized by a splitting of the retina leading to a gradual loss of visual acuity. XLRS is caused by mutations in the gene encoding the putative cell-adhesion protein retinoschisin, which is secreted from photoreceptors. Currently, there is no effective treatment for XLRS, although recent studies have shown that viral vector-mediated gene replacement strategies hold promise. Previous studies have used subretinal injections of viral vectors to deliver the retinoschisin gene to the outer retina. However, subretinal injections cause a retinal detachment and lead to gene delivery in a limited area. A preferable approach would enable pan-retinal gene delivery to the outer retina while avoiding the damaging subretinal injection. Recently our group created a novel AAV variant called ShH10 that transduces Müller glia specifically from the vitreous, as well as a second vector, 7m8, which infects all retinal layers via intravitreal injection. A rhodopsin promoter restricts gene expression of 7m8 to photoreceptors. We used these three vectors (ShH10, 7m8, and 7m8-rho) to deliver a therapeutic copy of the human RS1 gene to the retina of mice lacking retinoschisin, and compared the rescue effects mediated by secretion from Müller glia, photoreceptors, or throughout the retina. Our results indicate that all three vectors deliver protein to the retina leading to structural and functional ameliorations in the XLRS phenotype. Müller glia are capable of delivering RS1 to its targets, however, a greater functional rescue is observed using 7m8, which transduces photoreceptors, the cell type normally producing retinoschisin. Similar rescue is observed if expression is limited to photoreceptors or the protein is expressed throughout the retina. These results indicate the importance of cell targeting and the surgical route of delivery in the success of retinal gene therapies.

Introduction

XLRS is an X-linked retinal degenerative disease affecting between 1/5,000 and 1/25,000 people worldwide [40-42], and is the result of a number of mutations in the gene encoding the secreted protein retinoschisin[43]. XLRS is a leading cause of juvenile macular degeneration in males, who are usually diagnosed in the first decade of life as a result of poor vision, squinting or nystagmus. The final visual outcome of the disease is highly variable, ranging from a minimal loss of visual acuity to blindness, with secondary complications including retinal detachment, vitreal hemorrhage and glaucoma with neovascularization. The defining characteristics of XLRS include the formation of cystic cavities in the inner and outer retina and a decrease in vision as a result of deterioration in the organization of the retina. One important functional assessment of the XLRS retina is the electroretinogram (ERG), where a flash of light is presented to the eye and the resulting change in the electrical potential of the retina is recorded. A loss of the amplitude of the ERG b-wave with relative preservation of the a-wave is thought to be indicative of the disorganization of the photoreceptor-bipolar cell synapse and a deficit in synaptic transmission. XLRS is an X-linked condition affecting only men; female carriers are generally asymptomatic.

The binding partners and the molecular mechanism of action of retinoschisin have not yet been definitively characterized[44,45], although it is generally thought to be a cell adhesion

protein involved in maintaining the structural integrity of the retina and the photoreceptor-bipolar cell synapse. Retinoschisin comprises a 23 amino acid leader sequence that is cleaved upon translocation of the polypeptide into the lumen of the ER, followed by a 39 amino acid retinoschisin domain, a 157 amino acid discoidin domain, and a 5 amino acid C-terminal region. The discoidin domain is a motif shared by a number of cell-adhesion molecules including blood coagulation factors, neuropilins 1 and 2 and neurexin IV [46]. Following cleavage of the leader sequence, retinoschisin is folded and assembled into an octomeric structure linked by disulfide bonds which is sorted and delivered to the plasma membrane for secretion from photoreceptors and bipolar cells[47-49]. Secreted retinoschisin is associated with the membranes of rod and cone inner segments, cell bodies and synaptic terminals, as well as the surface of bipolar cells in the inner nuclear layer and inner plexiform layer.

Over 180 XLRS-causing mutations have been identified (http://www.dmd.nl/rs/index) [50,51], including nonsense and missense mutations leading to retention of the protein in the lumen of the ER and rapid protein degradation, interference with secretion of the protein, oligomerization, or prevention of normal function of secreted RS1 [52]. The majority of mutations characterized so far are missense mutations in the discoidin domain, highlighting the importance of this region for the function of the protein.

The mouse model of XLRS has been created, lacking *Rs1h*, the mouse homolog of retinoschisin [32]. The retinas of mice deficient in the retinoschisin protein are highly disorganized, mimicking the human condition, and are characterized by the formation of cavities in the inner retina, the loss of the amplitude of the full-field ERG b-wave under both scotopic and photopic conditions, and a progressive loss of rod and cone photoreceptors as a result of apoptosis, peaking at postnatal day 18 [33].

As the underlying cause of this monogenic disease is well understood it is an excellent candidate for gene replacement therapy. Previous studies have shown the potential of this approach, by delivering a normal copy of the retinoschisin protein to the retinas of *Rs1h*-/- mice using a variety of AAV vectors transducing different subsets of retinal cell types and using different routes of vector administration. Intraocular injection of an AAV2 vector with a ubiquitous CMV promoter driving expression of the murine *Rs1h* gene in young or adult mice led to expression of the protein in multiple layers and partial rescue of the electronegative ERG response [53,54]. The set of injections at the earlier time point of postnatal day 14 led to improvement in preservation of photoreceptors 16 months post-injection and long-term functional rescue at 14 months of age.

In another study, subretinal injection of an AAV5 vector with the human RS1 cDNA under the control of a mouse opsin promoter drove expression in photoreceptors [55]. Here Min et al. showed that injections at P15 led to expression of therapeutic protein in photoreceptors and distribution of the protein into the inner retina like that of the wildtype mouse, leading to increasing functional and morphological improvement in treated retinas over time. The authors noticed significant improvement in the organization of the retina, the thickness of the outer nuclear layer, and a decrease in cavity formation. The time course of increasing functional rescue correlated with the level of RS1 protein expression and its distribution in the inner layers of the retina, as observed through immunohistochemistry. Interestingly, retinal imaging with scanning-laser opthalmoscopy revealed that areas away from the site of injection showed less rescue than areas near the bleb. Treatment under these conditions led to long-term rescue lasting more than a year.

A third approach using intravitreal delivery of AAV8 with a human retinoschisin promoter driving expression of retinoschisin also reported WT distribution of protein and improvement of retinal structure and function 11-15 weeks after injection, although this vector could not transduce cells in the outer retina in animals without severe structural damage [34]. This study reported a modest improvement in the b/a wave ratio, which is used in clinical assessment of XLRS, however, A and B-wave amplitudes were not reported.

Although recent clinical trials using subretinal injections for treatment of LCA have shown the potential for viral vector-mediated gene therapy in the retina, the most effective and safest gene replacement strategy would most likely make use of an intravitreal injection, since the subretinal approach requires the formation of a bleb and a retinal detachment. The structural abnormalities in XLRS retinas make this approach particularly risky, since they are already prone to retinal detachment and tearing. Recently, our lab has characterized two novel variants of AAV that are able to target specific cell types in the retina from the vitreous. The first, called ShH10, is a variant of AAV6 that is able to target Müller glia specifically and efficiently [22]. The second, named 7m8, is a variant most closely related to AAV2 that was identified on the basis of its ability to transduce the outer retina via intravitreal injection. 7m8 is able to infect cells throughout the retina, although expression can be limited to photoreceptors using a rhodopsin promoter.

Here, we evaluate the efficacy of structural and functional rescue using intravitreal injections of three different viral vectors targeting different subsets of retinal neurons, and compare the rescue observed after transduction of specific cell types in the retina. A self-complementary ShH10 vector with one tyrosine mutation and a ubiquitous promoter efficiently targets Müller glia, which span the retina from the inner limiting membrane to the outer limiting membrane and are closely apposed to photoreceptors (Figure 1). Müller glia normally play a role in maintaining the retinal milieu and providing structural support for retinal neurons. In addition, they have been suggested to play a role in the trafficking of retinoschisin to the inner retina [56]. Müller cell endfeet are easily accessible from the vitreous, but reach to the outer retina, and therefore may be ideal candidates to channel therapeutic protein to its targets throughout the retina. 7m8 with a rhodopsin promoter limits expression of the protein to photoreceptors in the outer retina. Retinoschisin is mainly expressed by photoreceptors and may therefore be the most natural candidate cell type for delivering the protein. And lastly, 7m8 with a ubiquitous promoter transduces cells throughout the retina including ganglion cells, amacrine cells, Müller glia, rods and cones.

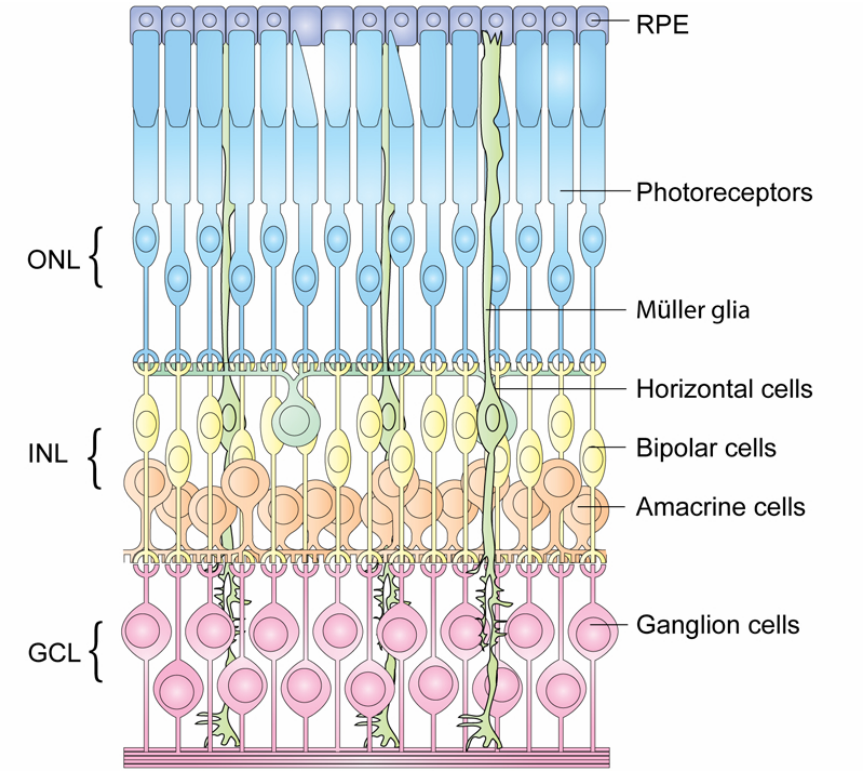

Figure 1. Anatomy of the retina.

Retinal cell types of the retina including Müller glia, which span the retina from the inner limiting membrane to the photoreceptors and the outer limiting membrane. Photoreceptor cell bodies lie in the outer nuclear layer. Ganglion cells lie in the innermost retina in the ganglion cell layer. Cell bodies of Müller glia lie in the inner nuclear layer along with horizontal, bipolar and amacrine cells.

We show here that all three vectors are able to successfully deliver a normal copy of the gene to the retina, leading to high levels of expression of the protein with a nearly wild-type distribution, following intravitreal injection. While all three delivery strategies lead to amelioration of the symptoms of retinoschisis in the mouse knockout model, 7m8, which transduces photoreceptors, was the most efficient and led to a greater rescue of the amplitude of the ERG B-wave as well as a reduction in the characteristic cavities seen in the *Rs1h*-/- mouse. This structural and functional rescue was similar with rhodopsin promoter-restricted expression or a ubiquitous CAG promoter, suggesting the benefit of production of the protein in photoreceptors. Overall these results indicate the potential of engineered AAV for delivering therapeutic genes to the outer retina without subretinal injections, and highlight the need for a rational design of therapies, including the choice of vector and the delivery route.

Results

Expression of retinoschisin protein in Rs1h-/- retinas with engineered viral vectors ShH10 and 7m8

The expression profiles of the three viral vectors used in the study were characterized using GFP as a reporter and by immunolabeling of RS1 in *Rs1h*-/- retinas (Figure 2A-I). 7m8 with a photoreceptor-specific rhodopsin promoter led to expression of GFP that was limited to photoreceptors in the ONL. Labeling of the RS1 protein in eyes injected with 7m8.rho.RS1 indicated high levels of RS1 protein were produced in the retina, and that the protein was transported to its targets throughout the retina, as indicated by a pattern of RS1 localization identical to a WT retina (Figure 2L). Intense staining of photoreceptor inner segments was apparent with anti-RS1 antibody, although staining was also apparent in the outer nuclear layer, outer plexiform layer, inner plexiform layer and inner nuclear layer.

7m8 with a ubiquitous promoter transduced cells throughout the retina, including photoreceptors, horizontal cells, ganglion cells and Müller glia, as seen through GFP expression. Similar patterns of RS1 protein localization compared to the 7m8.rho.RS1 vector were noted, with heavy labeling in photoreceptors.

Self-complimentary ShH10 with one tyrosine mutation (Y445F) and a CAG promoter efficiently and specifically transduced Müller glia in the *Rs1h* knockout mouse, leading to significant production of the protein that was transported from the inner to outer retina. Photoreceptor inner segments were also labeled with anti-RS1 antibody after injection with ShH10, although the labeling was not as intense as seen with 7m8. Colabeling with an anti-glutamine synthetase (GS) antibody showed RS1 protein on the surface of Müller cell processes indicating Müller-cell expression of RS1 in both 7m8.scCAG.RS1 and ShH10sCAG.RS1 vectors. In eyes injected with all three vectors, strong retinoschisin expression was noted pan-retinally.

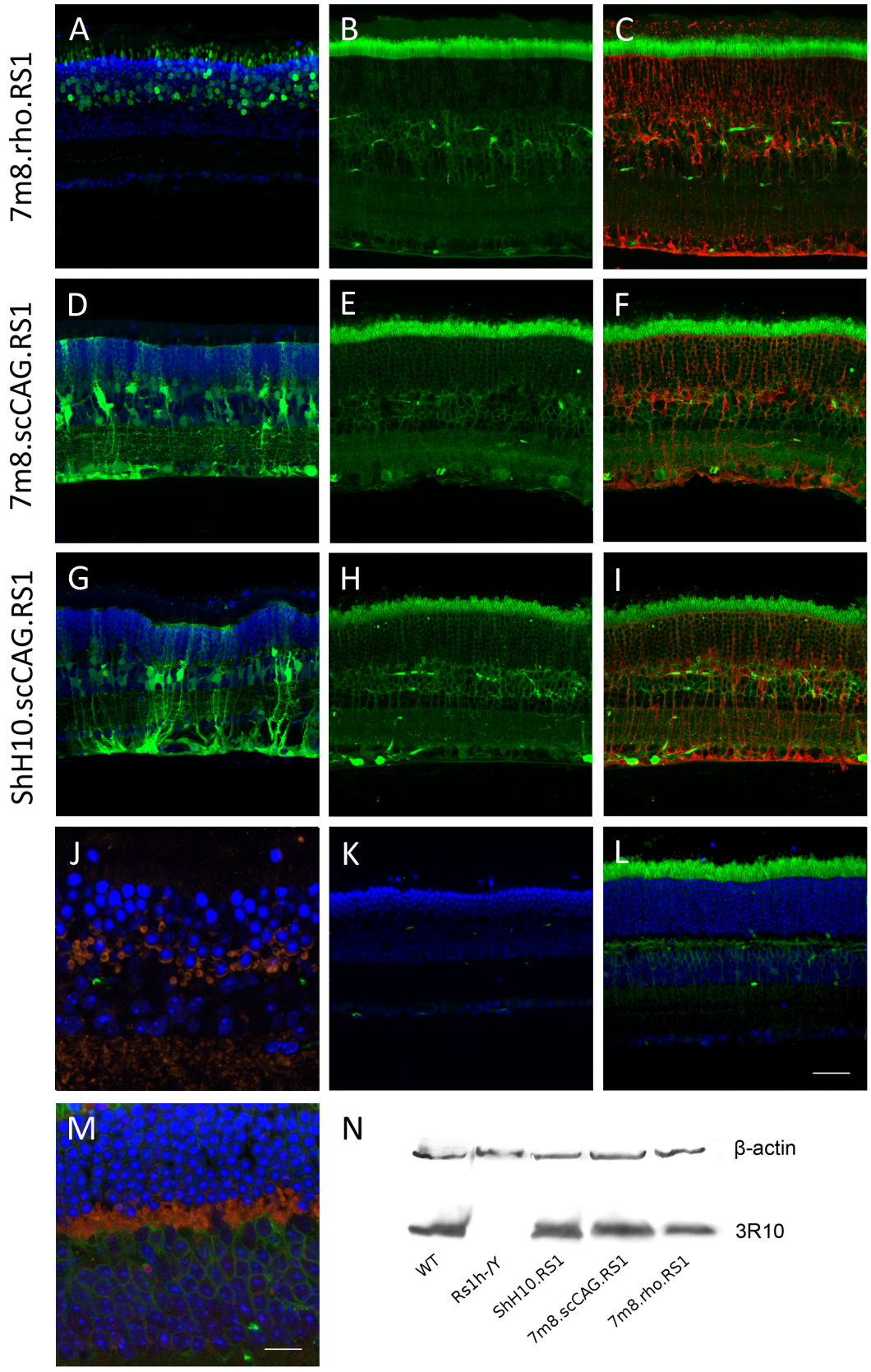
7m8.rho.RS1
7m8.scCAG.RS1
ShH10.scCAG.RS1
A
B
C
D
E
F
G
H
I
J
K
L
M
N
β-actin
3R10
WT
Rs1h-/Y
ShH10.RS1
7m8.scCAG.RS1
7m8.rho.RS1

Figure 2. Expression of GFP and RS1 following intravitreal injection of ShH10Y445F.scCAG, 7m8.scCAG or 7m8.rho AAV vectors.

Figure 2A-C: 7m8.rho, Figure 2D-F: 7m8.scCAG, Figure 2G-I: ShH10Y445F.scCAG. A,C,G: GFP expression. B,E,H,K, and L: anti-RS1 staining (green). F,I,L: anti-RS1 staining (green) with anti-GS colabeling (red). K: negative *Rs1h*-/- control retina. L: positive WT control. J,M: 40X images of photoreceptor-bipolar cell synapses showing colabeling of RS1 (green), mGluR6 (red) and synaptophysin (yellow). J: untreated retina. M:7m8.scCAG.RS1-injected retina. N: western blot of RS1 expression in 3 pooled retinas for each condition. Scale bar in A-I, K-L is 40μ. Scale bar in J and M is 20μ.

A western blot of retinas injected with these vectors (3 retinas pooled for each condition) indicate similarly high levels of protein were produced using all three vectors, comparable to the levels produced in a WT retina (Figure 2N). No retinoschisin protein was apparent in untreated eyes.

A higher resolution image of the photoreceptor-bipolar cell synapse in a retina transduced by 7m8.scCAG.RS1 and colabeled with anti-RS1, mGluR6, and synaptophysin antibodies show localization of RS1 near the synapse and indicates improved synaptic organization (Figure 2M) compared to an untreated retina (Figure 2J).

Time course of rescue of the electroretinogram

As a measure of retinal function, the amplitude of the full-field scotopic ERG B-wave was measured on a monthly basis after injection with the three vectors (Figure 3). ShH10.scCAG.RS1 n=5, 7m8.rho.RS1 n=8, 7m8.scCAG.RS1 n=5. AAV.GFP n=8. All three vectors led to an improvement in B-wave amplitude 1 month after injection. Both 7m8 with a ubiquitous promoter and 7m8 with the photoreceptor-specific promoter led to significant and stable improvement in the amplitude of the B-wave for 4 months post-injection. ShH10-mediated expression of RS1 from Müller glia led to a long-lasting improvement that decreased over time, although 4 months post-injection a significant rescue effect was still apparent.

A more detailed examination of ERGs recorded from mice injected with 7m8.rho.RS1 and 7m8.scCAG.RS1 reveals significant improvement of the B-wave over a range of stimulus intensities and under photopic (rod-saturating) and scotopic (dark-adapted) conditions (Figure 4). Representative traces from ERG recordings resulting from 7m8.rho.RS1 and 7m8.rho.GFP treated eyes 4 months post-injection (Figure 4 lower panel) at the highest stimulus intensity demonstrate rescue of the A-wave and B-wave and a more normal waveform compared to 7m8.rho.GFP-injected eyes.

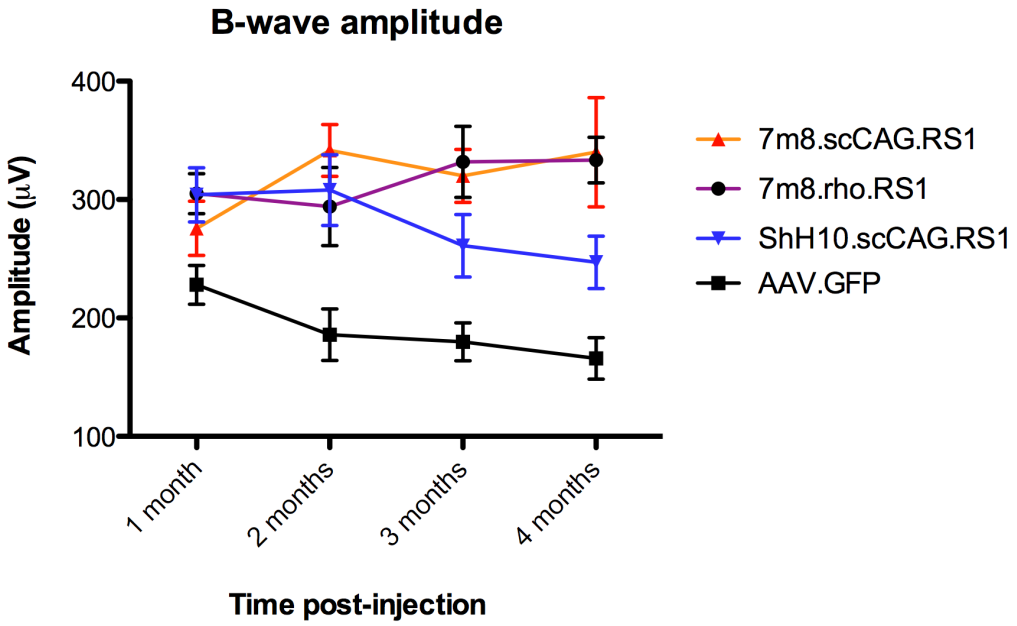

Figure 3. Time course of amplitude of the scotopic ERG B-wave in treated and control retinas.

The amplitude of the B-wave resulting from a high intensity (1 log cd x s/m^2) stimulus was recorded on a monthly basis beginning one month after injection at PN15 for each condition. Recordings were made from eyes injected with ShH10.scCAG.RS1, 7m8.rho.RS1, 7m8.scCAG.RS1 or AAV.GFP control-injected eyes. Mean ERG amplitudes are plotted as a function of time post-injection.

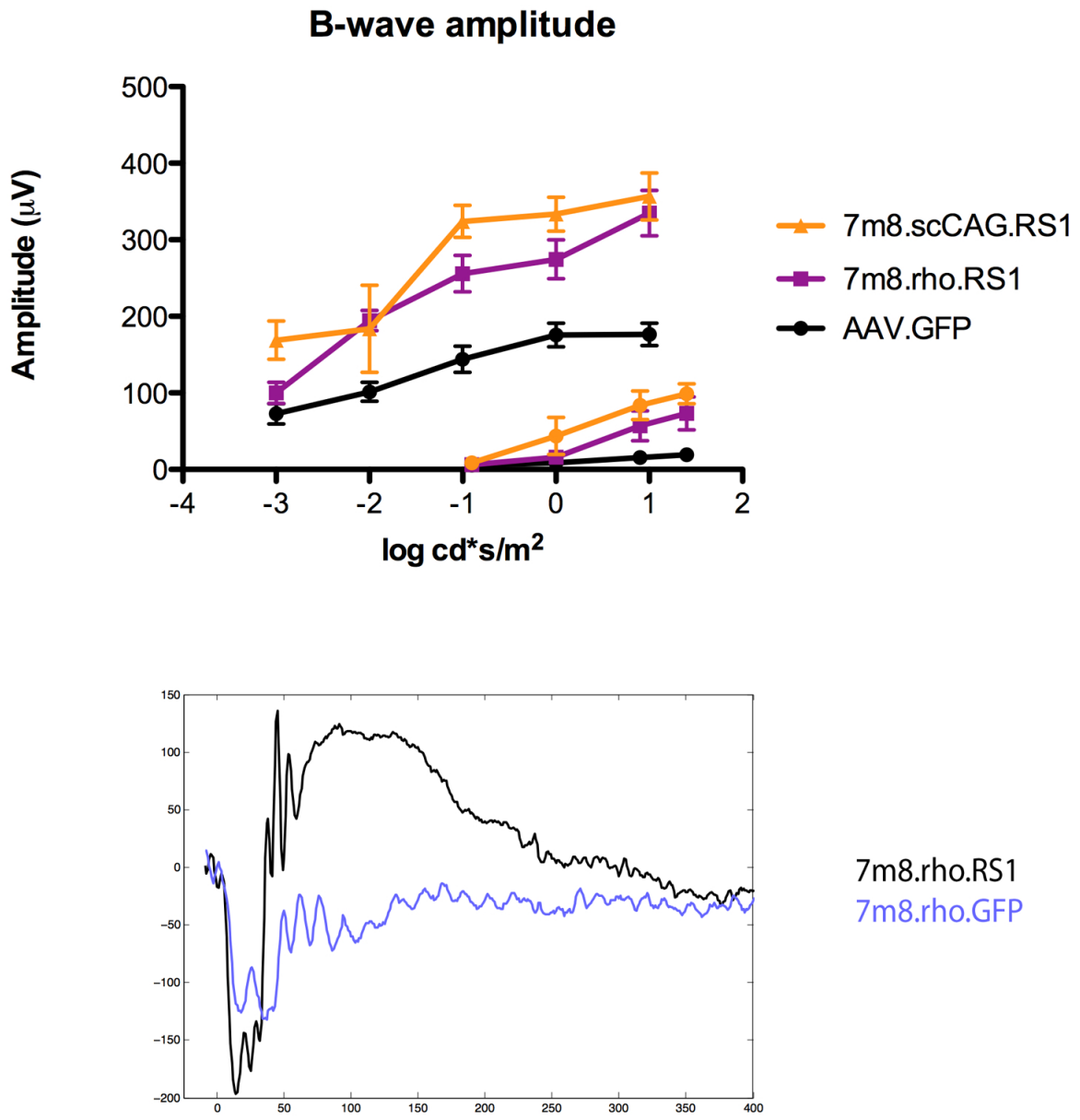

Figure 4. Scotopic (dark adapted) and photopic (light adapted) ERG B-wave amplitudes from 7m8-injected eyes

Top panel: detailed analysis of B-wave amplitudes under scotopic (top traces) or photopic (bottom traces) conditions for 7m8.scCAG.RS1 and 7m8.rho.RS1. Scotopic measurements were recorded over a range of stimulus intensities from -3 to 1 cd x s/m^2. Photopic cone-mediated ERGs were measured over a range of -0.9 to 1.4 log cd × s/m^2. Bottom panel: representative ERG traces from 7m8.rho.RS1 injected (black trace) and 7m8.rho.GFP injected (blue trace) eyes under scotopic conditions after presentation of a 1 log cd × s/m^2 stimulus.

Later injections at 30 days after birth also led to significant, but less dramatic, improvement of the amplitude of the scotopic B-wave when measured 4 months post-injection. Injection with 7m8.scCAG.RS1 and 7m8.rho.RS1 led to greater rescue than ShH10. Rescue with all three vectors was reduced with injection at this later time point (Figure 5).

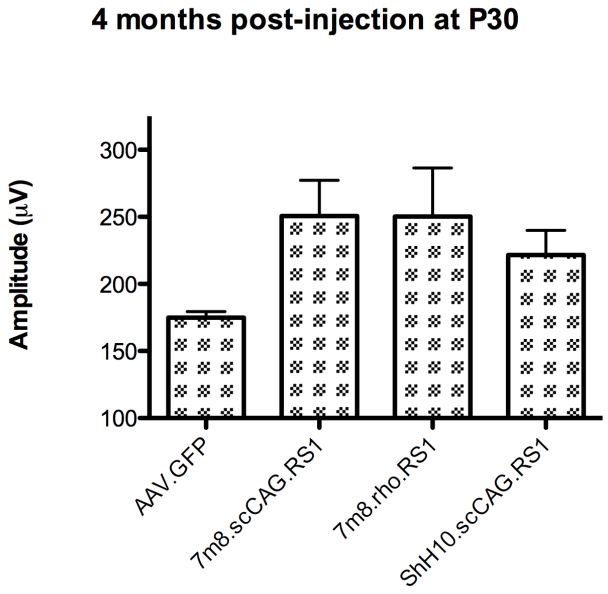

Figure 5. ERG B-wave amplitudes 4 month post-injection at PN30.

ERGs were recorded from AAV.GFP (n=11) 7m8.scCAG.RS1 (n=5) 7m8.rho.RS1 (n=5) or ShH10scCAG.RS1 (n=6) injected eyes. Data represent mean ERG b-wave amplitudes 4 months post-injection at PN30.

Structural improvement resulting from injection with AAV.RS1

To confirm the structural improvement noted through immunohistochemistry, high-resolution SD-OCT images of retinas were gathered four months post-injection. Significant reduction in the number of cavities was noted in retinas treated with all three vectors, compared to GFP-treated eyes (Figure 6A). Eyes treated with AAV.GFP were marked by large cavities across the retina, which were obvious in retinal cross sections of the superior and inferior retina as well as fundus images taken through the inner nuclear layer (Figure 6B). Retinas treated with ShH10.scCAG.RS1, 7m8.rho.RS1, and 7m8.scCAG.RS1, in contrast, had far fewer cavities of smaller size, which were barely visible in fundus images and cross sections. Treated retinas were thinner than WT retinas of the same age, with decreased thickness of the outer nuclear layer indicative of loss of photoreceptors.

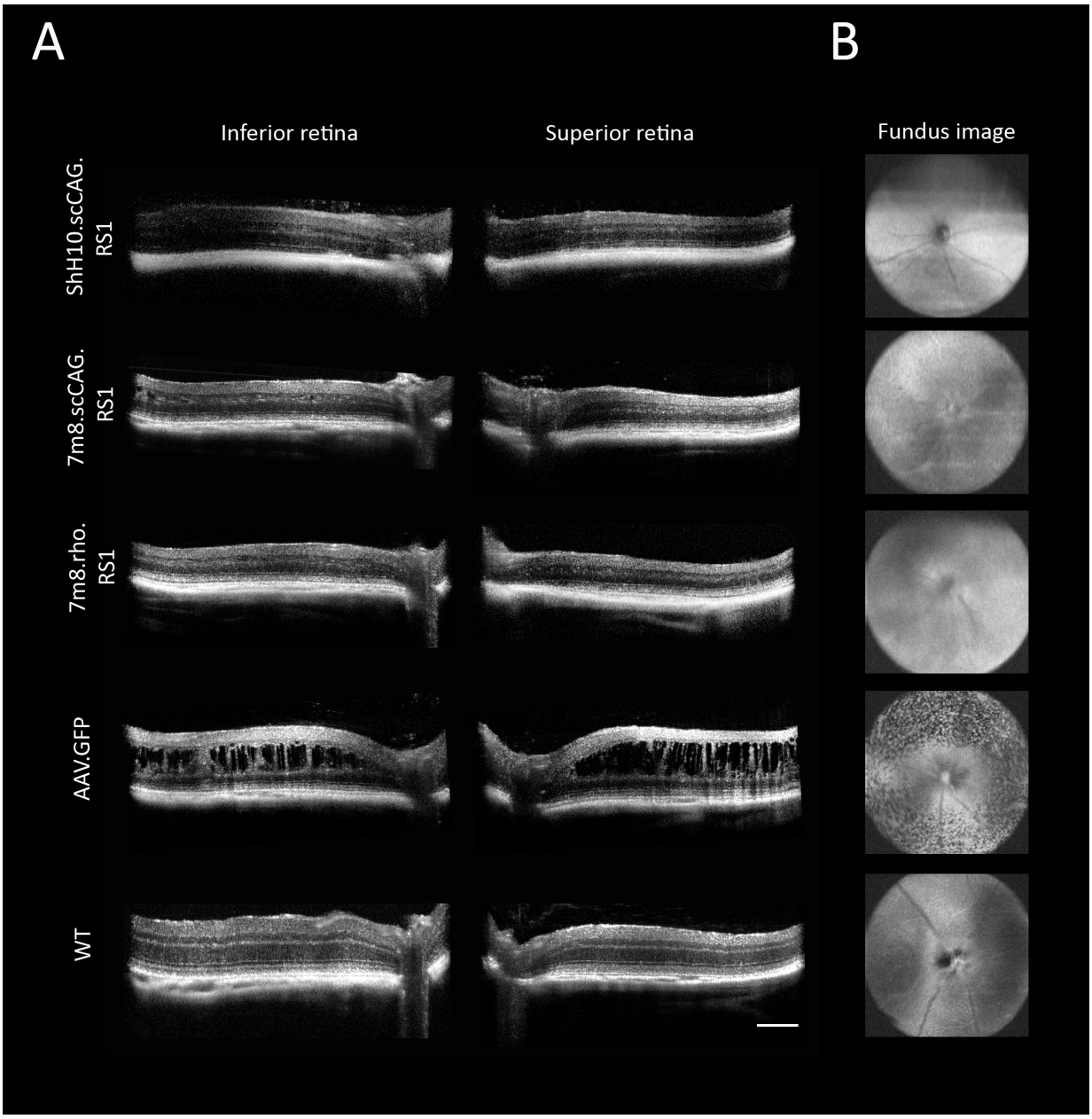

Figure 6. SD-OCT imaging of retinas

High-resolution SD-OCT images of cross sections through the inferior retina (left column) superior retina (middle column) or fundus images through the INL (right column) in treated (top three rows), control-injected (4th row) or WT (bottom row) eyes. Scale bar applies to retinal cross sections and indicates 0.2 mm.

Ten months post-injection with 7m8.rho.RS1, quantification of thickness of retinal layers in OCT images indicated improved thickness of the retina, the ONL and the inner and outer segments in inferior and superior quadrants of the retina (Figure 7B-D). Additionally, an improved organization of the retinal layers was observed (Figure 7A).

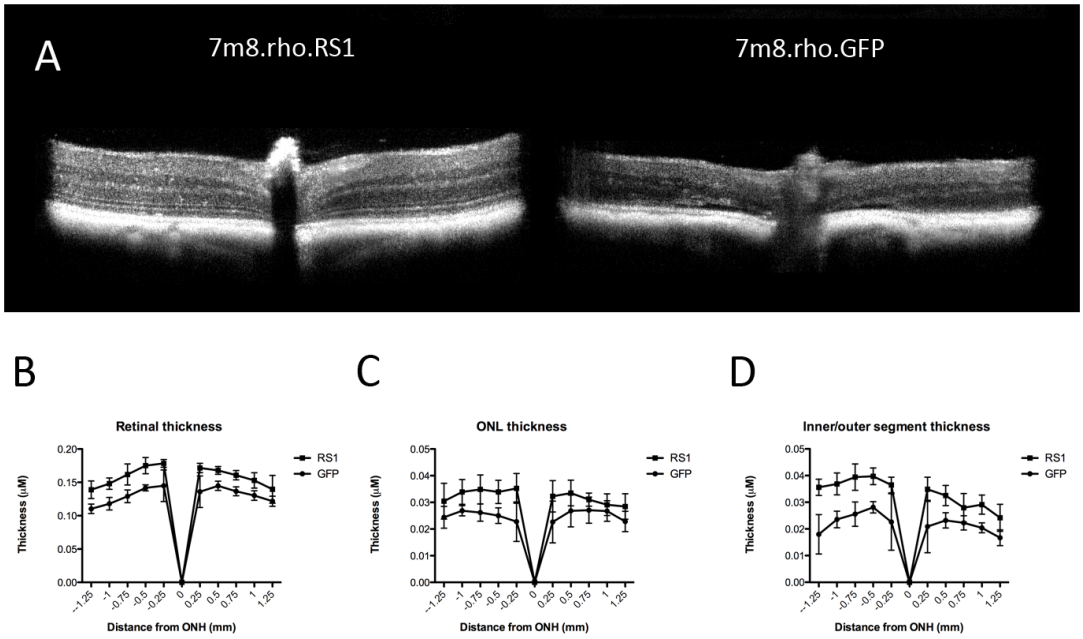

Figure 7. Retinal thickness measurements

SD-OCT images of 7m8.rho.RS1 (n=5) or 7m8.rho.GFP (n=5) treated retinas 10 months post-injection at PN15 (A). Measurements of retinal thickness (B), ONL thickness (C) and inner and outer segment thickness (C) plotted as a function of distance from the optic nerve head (ONH).

Discussion

XLRS is a well-characterized monogenic inherited retinal degenerative disease, and represents a promising candidate for a gene replacement treatment. Recent clinical trials for treatment of LCA have proven the safety of AAV viral vector administration in the pseudo-immune privileged and compartmentalized space of the eye, although the subretinal injections used in these trials may not be suitable for the structurally compromised retinoschisis retina. While previous studies in the mouse model of XLRS have shown proof-of-concept that the disease is amenable to gene therapy, significant hurdles exist in translating these studies to patients. Before moving into the clinic it will be important to use a rational approach to determine the best approach for gene delivery, including the route of vector administration, promoter selection and viral vector serotype, which will also determine the cell type targeted for gene delivery.

XLRS is characterized by the formation of cystic cavities in the inner and outer layers of the retina and the increased potential for retinal detachment. Subretinal injections represent a less than ideal approach in these fragile retinas. In addition, subretinal injections typically transduce no more than a quarter of the retina, and although a secreted protein like retinoschisin may be able to diffuse to a certain degree laterally across the retina, in a larger human eye the extent of this diffusion is uncertain. The ideal vector, therefore, would be able to transduce the optimal cell type pan-retinally via a less intrusive intravitreal injection.

Here we evaluated 3 vectors for delivery of the retinoschisin protein using an intravitreal injection. First, we evaluated the use of ShH10, a virus that specifically and efficiently infects Müller glia, which have a unique morphology spanning the retina from the nerve fiber layer to the outer limiting membrane, and come into close contact with all neuronal cell types in the retina. Müller glia endfeet are easily accessible from the vitreous, and these cells have been shown to be able to mediate expression of trophic factors leading to amelioration of the symptoms of murine retinal degeneration [57]. Müller cells are preserved even in late stages of XLRS, and therefore are candidates to deliver the protein to compromised areas of the retina under conditions of more advanced degeneration. In addition, Müller glia have been suggested to be involved in retinoschisin trafficking and localization to the inner retina [56]. Our vector was optimized using a tyrosine mutation, which has been shown to increase retinal transduction of AAV vectors through increased nuclear trafficking [20], and through the use of a double stranded AAV genome, speeding onset of expression [58]. We show here that Müller glia are capable of delivering retinoschisin to the retina and that Müller glia-mediated delivery of the protein improves the symptoms of XLRS as evaluated by ERG recording and histological assessment with OCT. Müller glia-mediated gene replacement led to an almost WT distribution of RS1 in the mouse retina, however, the functional benefit conferred by Müller-cell expression of the therapeutic protein decreased over the course of our experiment.

In a second approach we used a novel engineered AAV vector called 7m8 that was originally identified through a directed evolution approach for its ability to transduce photoreceptors via intravitreal injection. 7m8 is also able to infect many other cell types in the retina, including high numbers of ganglion cells, amacrine cells, horizontal cells, and Müller glia. Expression can also be restricted to photoreceptors using a rhodopsin promoter to drive expression. Photoreceptors are the cell type that normally produce the retinoschisin protein in the retina, and may therefore be most suited to processing the protein and trafficking it to its binding partners. Using the 7m8.rho vector we observed long lasting and stable rescue as measured by functional and structural tests, including normal distribution of the protein, rescue of the amplitude and waveform of the scotopic and photopic ERG, as well as reduction of cavities and relative preservation of retinal thickness and organization.

A third vector was also tested, consisting of the 7m8 vector packaged with a ubiquitous CAG promoter. Transgenic expression with this vector is widespread amongst many cell types in the retina and leads to rapid expression from inner to outer retina. This vector also carried a double-stranded genome for more efficient expression. Interestingly, although similarly high titers of virus were injected in all eyes and levels of RS1 were similar among all three vectors as assessed by semi-quantitative western blotting, gene delivery with 7m8.scCAG was only insignificantly improved over 7m8 with a photoreceptor-specific promoter, suggesting that photoreceptors are important for the rescue effect noted with 7m8-mediated expression, and that this cell type is a promising target for gene replacement therapy.

All three vectors were unable to reverse the loss of photoreceptors that peaks soon after the injection at P18, and it is likely that the onset of gene expression after injection at PN15 is not rapid enough to prevent this early wave of apoptosis. In an ongoing study we are assessing whether earlier administration of AAV vectors can reduce or eliminate even this most aggressive period of cell death. However, it is important to note that in humans the rate of degeneration in XLRS is much slower than in the murine model, and therefore the window of opportunity for gene replacement treatments may be longer.

These results do not support the theory that Müller glia are involved in trafficking of RS1 in the normal retina, as functional benefit was not maintained four months after injection with ShH10 vector, although Müller cells may remain a potential candidate for RS1 gene replacement strategies because of their morphology, strategic location and relative preservation in later stages of retinal degeneration.

In summary, this work indicates the importance of a rational approach in designing gene replacement therapies and evaluating the strategy used for viral vector-mediated delivery, including the cell type targeted, the promoter chosen, the selection of viral vector and the delivery method. These results confirm those of earlier studies indicating the potential for gene therapy in XLRS, and emphasize a rational approach to designing an optimized, minimally invasive method of gene delivery.

Materials and Methods

Production of viral vectors

AAV vectors carrying human RS1 cDNA or GFP were produced by the plasmid co-transfection method [59]. Recombinant AAV was purified by iodixanol gradient ultracentrifugation and heparin column chromatography (GE Healthcare, Chalfont St Giles, UK). The viral eluent was buffer exchanged and concentrated with Amicon Ultra-15 Centrifugal Filter Units in PBS and titered by quantitative PCR relative to a standard curve.

Immunohistochemistry

Retinas were freshly dissected and immediately placed in 10% formalin overnight. Relief cuts were made and the retinas were embedded in 5% agarose. Using a microtome, 200 μm transverse sections were cut and the sections were floated in PBS. After blocking in 1% bovine serum albumin, 0.5% Triton X-100, and 2% normal donkey serum for 2–3 hours, sections were incubated in primary antibody overnight at 4° C. After washing in PBS, secondary antibodies were applied at room temperature for 1 hour. Sections were again washed and then mounted for confocal microscopy (LSM710, Carl Zeiss). Antibodies were as follows: 3R10 mouse anti-RS1 [32] (generous gift of Professor Robert Molday) (1:5); rabbit anti-GS (1:1000); guinea pig anti-mGluR6 (Abcam, 1:1000); rabbit anti-synaptophysin (1:1000).

Intravitreal injections

C57Bl6 or *Rs1h-/-* mice were used for all experiments, which were conducted according to the ARVO Statement for the Use of Animals and the guidelines of the Office of Laboratory Animal Care at the University of California, Berkeley, CA. Mice were anesthetized with ketamine (72 mg/kg) and xylazine (64 mg/kg) by intraperitoneal injection. An ultrafine 30 1/2-gauge disposable needle was then passed through the sclera, at the equator and posterior to the limbus, into the vitreous cavity. One μL of AAV with a titer of 1-10 vg/mL was injected into the vitreous cavity with direct observation of the needle directly above the optic nerve head. Contralateral control eyes received vectors carrying the gene encoding GFP.

Western blot

Three retinas for each condition were pooled. Retinas were removed from the eyecup in cold PBS and sonicated in buffer with proteinase inhibitor cocktail. Protein concentration was measured using a BCA kit and normalized. Protein was run on a 4-20% Tris-HCL gradient gel. Protein was transferred to a PVDF membrane, and blocked in 5% milk for 2 hours. The membrane was then washed 2X 5 minutes in PBST, and incubated in primary antibodies overnight at RT: 3R10 mouse anti-RS1 (1:50); anti-B-actin (Abcam, 1:2000). Secondary antibodies conjugated to alkaline phosphatase were applied for 2 hours at RT before washing and visualization using NBT/BCIP (Roche).

Electroretinograms

Mice were dark-adapted for 2 hours and then anesthetized, followed by pupil dilation. Mice were placed on a 37°C heated pad and contact lenses were positioned on the cornea of both eyes. A reference electrode connected to a splitter was inserted into the forehead and a ground electrode was inserted in the tail. For scotopic conditions ERGs were recorded (Espion E2 ERG system; Diagnosys LLC, Littleton, MA) in response to six light flash intensities ranging from −3 to 1 log cd × s/m^2 on a dark background. Each stimulus was presented in series of three. For photopic ERGs the animal was exposed to a rod saturating background for 5 minutes. Stimuli ranging from -0.9 to 1.4 log cd × s/m^2 were presented 20 times on a lighted background. Stimulus intensity and timing were computer controlled. Data were analyzed with MatLab (v7.7; Mathworks, Natick, MA). ERG amplitudes were compared using a student's t-test.

High-resolution spectral domain optical coherence tomography

Histological imaging was performed using an 840nm SDOIS OCT system (Bioptigen, Durham, North Carolina) including an 840nm SDOIS Engine with 93nm bandwidth internal source providing < 3.0um resolution in tissue. Retinal thickness, ONL and inner and outer segment thickness measurements were gathered and analysis done using InVivoVue software. Mice were anesthetized and the pupils dilated with atropine before imaging. Images of retinal cross sections were averaged from 8 contiguous slices. Fundus images were taken from en face views through the INL.

Acknowledgements

The authors thank Robert Molday for providing the 3R10 anti-RS1 mouse monoclonal antibody. We thank Bernhardt Weber and Bill Hauswirth for supplying the mouse model of XLRS. Our thanks to Günter Niemeyer, Greg Nielsen, and Matt LaVail for valuable advice on ERG recordings.

Chapter 4

Enhanced gene delivery to the retina through systemic administration of tyrosine mutated AAV9[3]

[3]This work was done in collaboration with Deniz Dalkara, Trevor Lee, Natalie V. Hoffmann, David V. Schaffer and John G. Flannery.

Abstract

Non-invasive and widespread retinal gene delivery has been a long-sought goal of gene therapy for inherited retinal degenerations. Recently, studies have shown that AAV9 can reach the CNS and part of the retina when administered systemically and therefore has promise to meet this goal. We investigated whether the retinal transduction efficiency of systemically delivered AAV9 could be improved by mutating capsid surface tyrosines, previously shown to increase the infectivity of several AAV vectors. Specifically, we evaluated retinal transduction following neonatal intravascular administration by AAV9 vectors containing tyrosine to phenylalanine mutations at two highly conserved sites. Our results show that the novel double tyrosine mutant AAV9 leads to significantly enhanced CNS and retinal gene delivery, providing an efficient platform for the development of retinal gene therapy strategies or the generation of animal models of neurodegenerative diseases.

Introduction

Numerous retinal degenerative diseases are caused by single gene mutations that lead to either loss of protein function or gain of deleterious properties. Recently, adeno-associated viral vector-mediated gene therapy has enjoyed success in over 40 LCA2 patients within three separate clinical trials for treating the monogenic retinal dystrophy LCA2 caused by null mutations in the retinoid isomerase RPE-65 [11,59,60]. These clinical trials clearly demonstrate that AAV-mediated gene replacement therapies are an effective strategy for treating inherited retinal degeneration. In addition, they raise hope that this mode of gene therapy can be extended to treat dominant disease involving gain of function mutations via the delivery of gene constructs that induce RNA interference.

Reviewing the positive LCA2 results underscores the importance of the surgical route of delivery to successful treatment outcome. The vast majority of retinal disease mutations affect photoreceptors and pigment epithelium [61], and vector administration into the subretinal space and thus into close proximity with these cells has been preferable for gene replacement strategies targeting the outer retina. This approach is highly effective at generating localized expression of the transgene at levels sufficient to correct the retinal degeneration phenotype in LCA2 [62] or where a diffusible factor is secreted from a group of infected cells in sufficient quantities to benefit the whole tissue [28]. However, subretinal injections are highly invasive and induce a transient retinal detachment where the bleb of vector solution is introduced, and this risky procedure may not be applicable in degenerations where the retina has already undergone significant degeneration and retains only islands of surviving neural tissue. In addition, the subretinal injections can only deliver transgenes to a limited number of cells directly adjacent to the bleb.

A preferable approach to address retinal dystrophies that affect large areas of the retina would be to deliver the viral vector into the vitreous cavity. Intravitreal injections are routinely used in the clinic, introduce considerably less trauma to the retinal tissue, and importantly have the potential to yield pan-retinal gene expression. Unfortunately, there are a number of formidable barriers to gene delivery to the retina from the vitreous. Vector delivered to this region becomes diluted in the large volume of vitreal fluid, diminishing the local concentrations of the vector in close proximity of the retina. Furthermore, the inner limiting membrane (ILM) poses a physical barrier to the vector and sequesters significant number of viral particles. Much

progress has been made in uncovering barriers to retinal transduction from the vitreous for AAV [29,30] as well as improving the limited transduction of the naturally occurring serotypes by rational [20] and directed evolution [21,22] approaches in the past 5 years. While AAV-mediated gene delivery to the retina has thus made significant progress, major obstacles remain in reaching therapeutically effective levels of gene expression, especially in larger animals where the inner limiting membrane is significantly thicker than in rodents and thus significantly limits access of the viral vector into the retina [63]. Moreover, efficiently transducing the outer retina, which lies furthest away from the vitreous cavity, currently represents a challenge in small and especially in large animals.

An alternative approach for transducing large areas of retina is to administer vectors through the vasculature. The retina is a highly vascularized structure with the highest oxygen consumption per weight of any human tissue [64]. Vectors that can permeate the blood-retina barrier thus have the potential to gain access to multiple layers of the retina. In particular, the retina is nourished by a dual blood supply from the choroidal capillaries (covering the outer retina) and by branches of the central retinal artery (supplying the inner two thirds of the sensory retina) (Figure 1). In the pig retina, similar to its human counterpart in overall structure and blood supply, the choriocapillaris flow is estimated at about 27 times the retinal flow [65]. Although administration of gene delivery vehicles from the vasculature entails greater risks from an immunological standpoint [66], it may be particularly promising in neonates where the immaturity of the newborn immune system leads to a 'physiological immunodeficiency' that encompasses all arms of the host response.

It was recently demonstrated that the retina can be can be transduced via systemic administration of AAV [67], though the implications of this pioneering study have been somewhat limited to date by the relatively low levels of gene expression observed in limited retinal cell types, potentially due to the relatively low dosages employed. Importantly, recent reports have shown that the CNS can be very effectively transduced via systemic administration [68-70] and higher doses of the self-complimentary vector genomes utilized in these studies [71] may have contributed to this capability. These results thus indicate that improving the vector delivery system may hold promise for enhancing retinal transduction.

The AAV capsid mediates vector binding to cell surface receptors, internalization, cytoplasmic trafficking to the nuclear membrane, and vector genome release [17] and is thus a critical determinant of vector transduction efficiency. It has been shown that tyrosines exposed on the AAV capsid surface can undergo tyrosine kinase-mediated phosphorylation, leading to ubiquitination and degradation of viral particles. Site-directed tyrosine to phenylalanine (Y-F) mutagenesis of one or more of the seven capsid surface-

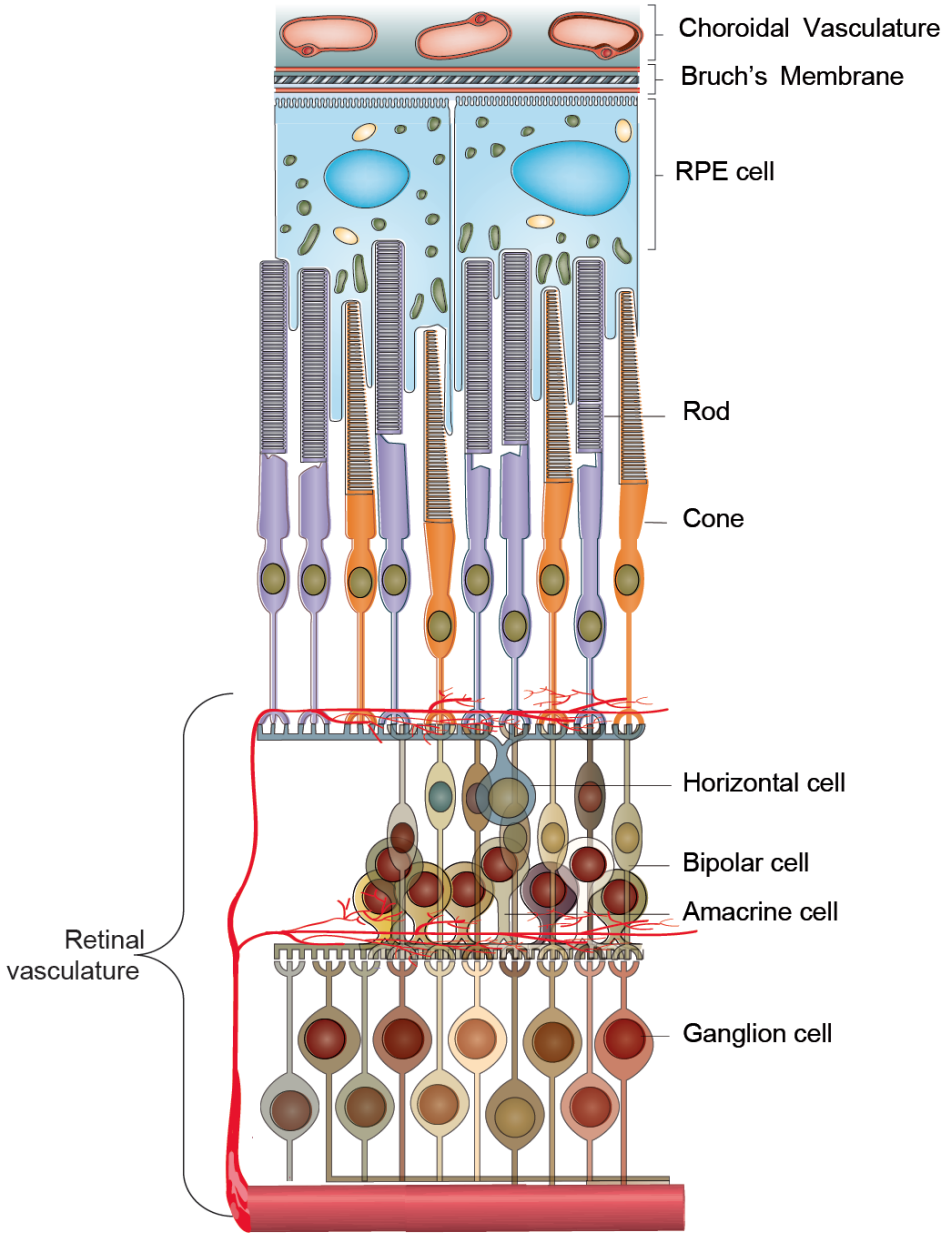

Figure 1. Illustration depicting the dual blood supply of the retina.

The inner two thirds of the retina is perfused by capillary networks of the central retinal artery, while the outer third receives its blood supply from the choroidal vasculature. The choroidal circulation has a higher flow rate and a fenestrated (leaky) capillary bed.

exposed AAV tyrosine residues in the VP3 common region has been reported to protect vector particles from proteasome degradation and yield significant increases in the transduction efficiency of mutant vectors relative to their wild-type counterparts both in cell culture [19] and *in vivo*. For example, AAV2, AAV8, or AAV9 vectors containing single Y-F point mutations on two of the seven surface-exposed capsid tyrosine residues mediate significantly increased transduction efficiencies in the retina when injected subretinally or intravitreally.

Here, we investigate whether intravenous delivery to neonatal mice can be improved using AAV9 vector variants containing single or double Y-F mutations. We report that the double tyrosine mutant exhibits enhanced *in vivo* transduction properties and the ability to express the transgene in all retinal layers following a single injection. The potential to transduce photoreceptors and RPE cells (the targets of most inherited retinal degenerations) – as well as ganglion cells, amacrine cells and Müller glia – following systemic vector delivery represents a promising alternative to surgically traumatic subretinal injections that are currently necessary to transduce these cell types and open new avenues in experimental gene therapy. Furthermore, the ability to efficiently target the photoreceptor and RPE cells of the retina bilaterally suggests this technology can be used to generate large animal models of retinal degeneration [72]. For example, a novel transgenesis approach based not on germ line transgenesis, but instead harnessing AAV vectors to overexpress causative, mutant RP genes in the photoreceptors of models such as the macaque would offer an attractive strategy to fill the gap of a primate animal model in the field of retinal degeneration [73].

Results

Quantitative and histological comparison of AAV9, AAV9-1YF vs. AAV9-2YF mediated GFP expression

Single phenylalanine (F) to tyrosine (Y) substitutions at positions 446 and 731 have been shown to increase retinal transduction by AAV9 following intraocular administration. Based on these findings, we introduced a single tyrosine mutation at position 446 of AAV9 (AAV9-1YF) and an additional mutation at position 731 (AAV9-2YF), then analyzed green fluorescent protein (GFP) expression from these mutants relative to wild-type AAV9 after intravascular delivery. Each vector contained a self-complimentary genome encoding GFP under the control of a ubiquitous CAG promoter or a single stranded genome with GFP under the control of mouse rhodopsin promoter. For all experiments C57BL/6 mice were injected intravascularly with $4x10^{11}$ genome copies of AAV9 one day after their birth (P1).

Histology, fundus imaging, and RT-PCR were used to quantify levels of GFP expression resulting from AAV9 and its tyrosine mutated variants. Retinal flat-mounts from pups one week post-injection exhibited strong GFP expression in retinal ganglion cells (data not shown), indicating a very early onset of gene expression. Two weeks after injection, at eyelid opening in pups, fundus imaging was performed, and the highest levels of GFP fluorescence were detected with AAV9-2YF. AAV9-1YF showed lower levels of GFP expression compared to AAV9-2YF but higher than AAV9 (Figures 2a-c). To evaluate the amounts of GFP expression in a more quantitative fashion, we performed RT-PCR on pooled RNA extracted from retinal lysates obtained from pups injected with each of the viruses (n=5 for AAV9, n=4 AAV9-1YF and n=5 for AAV9-2YF), and AAV9-2YF showed a 6-fold improvement over AAV9 (Figure 2d).

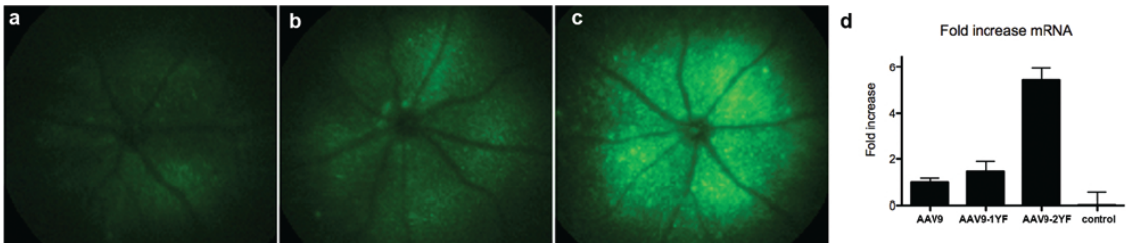

Figure 2. Quantitative comparison of AAV9, AAV9-1YF and AAV9-2YF.

Representative fundus photographs showing GFP expression in live mice that received tail vein injections of (a) AAV9, (b) AAV9-1YF, or (c) AAV9-2YF one month after injection. Visible fluorescence using fundus imaging was detectable in eyes two weeks post-injection and stayed constant after that time point. d) RNA extracted from retinas of AAV9 (n=5), AAV9-1YF (n=4), or AAV9-2YF (n=5) injected mice retinas were pooled, and RT-PCR was performed in triplicate. The ddCT method was used to calculate fold difference of GFP expression normalized to AAV9. Error bars depict the standard deviations of dCT values. An uninjected mouse retina was included as a negative control.

Following these observed enhancements in GFP expression using the mutant AAV9 capsids, we evaluated histological expression patterns of GFP in retinal layers via confocal microscopy 8 weeks after injection (Figure 3). In agreement with fundus images, retinas that received AAV9-2YF exhibited the most GFP. The microscope was adjusted to the fluorescence intensity from the AAV9-2YF retina, and the same settings were retained for all subsequent acquisitions. For each image, a 10x objective was used to image approximately 212 x 212 µm fields next to the optic nerve head (ONH). Confocal z-stacks spanning 5-15 µm of the RGC layer, inner nuclear layer, photoreceptor layer, and RPE cells were acquired and merged (Figure 3a-l). Our results consistently show that GFP expression is stronger with AAV9-2YF in each layer. The most striking differences between the WT AAV9 and AAV9-2YF are observed in the number of transduced inner nuclear layer (amacrine cells) and photoreceptor cells (Figure 3d-i). Also, both vectors lead to significant levels of expression in RPE and RGCs. Interestingly, however, only an insignificant number of bipolar cells were infected even with AAV9-2YF. Higher magnification images of the AAV-2YF treated retinas further reveal transgene expression in the RGC layer (Figure 4j, with NeuN staining in red), the INL layer (Figure 4k), and the ONL layer (Figure 4l).

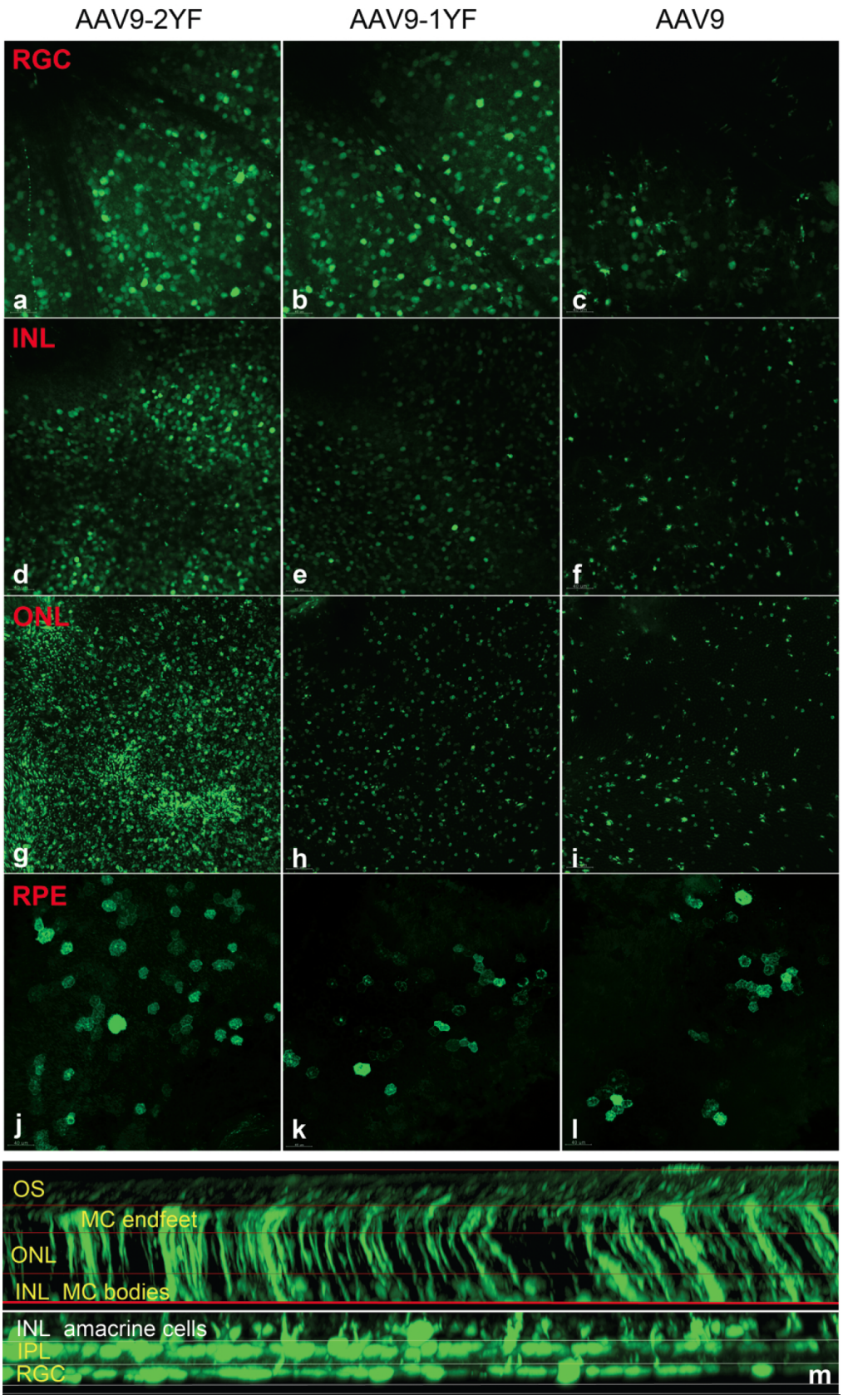
AAV9-2YF
AAV9-1YF
AAV9
RGC
INL
ONL
RPE
a
b
c
d
e
f
g
h
i
j
k
l
OS
MC endfeet
ONL
INL MC bodies
INL amacrine cells
IPL
RGC
m

Figure 3. Empirical comparison of AAV9, AAV9-1YF, and AAV9-2YF.

a-l) Z-projections of confocal stacks acquired from representative retinas transduced with AAV9, AAV9-1YF, or AAV9-2YF.

Representative retinas were harvested and dissected to separate the retinal tissue from its underlying choroid and RPE cells. The retinas were mounted flat on one side and the corresponding choroid with the detached RPE cells was mounted separately. The confocal stacks were taken close to the optic nerve head at different depths from the retinal surface, scanning one retinal cell layer at a time. Optic nerve appears on the upper left hand corner or each image. Expression at the RGC layer is shown for each virus, including (a) AAV9-2YF in the left column, (b) AAV9-1YF in the middle column and (c) AAV9 in the right column. The second row (d-f) shows expression at the inner nuclear layer cell bodies with the same viruses. (g-i) correspond to GFP fluorescence from cell bodies in the photoreceptor layer. The last row (j-l) shows a z-projection image collected from the RPE flat-mounts corresponding to the retinas. All stacks were acquired using identical acquisition parameters. The acquisition parameters were initially tuned for retinas transduced with AAV9-2YF, then used for all retinas.

m) 3D reconstruction of a representative retinal flat-mount showing transduction with AAV9-2YF.

Scanning confocal micrographs were acquired with 0.84 µm intervals through the inner and outer retinas transduced with AAV9-2YF using a 20x objective. The lower image was collected from a retinal flat-mount lying with the RGC side facing upwards. The upper image was collected from the contralateral retina mounted with the photoreceptor side facing up to avoid reduction of signal in the deeper layers of the tissue. Stacks were assembled to provide 3D reconstruction using IMARIS software.

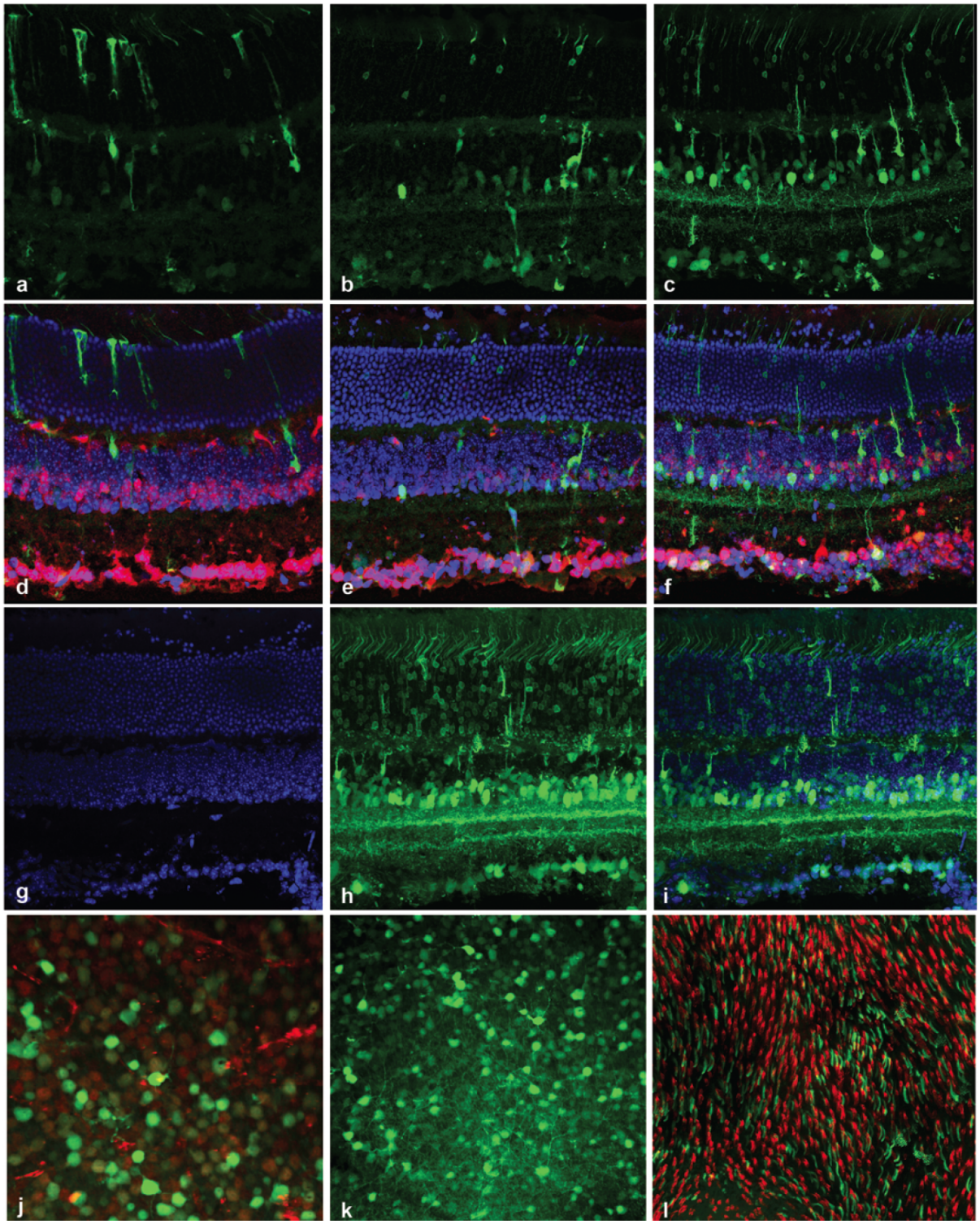
a
b
c
d
e
f
g
h
i
j
k
l

Figure 4. Detailed examination of retinal expression patterns using AAV9, AAV9-1YF and AAV9-2YF on transverse retinal sections.

GFP fluorescence is shown for transverse retinal sections from 15 µm thick cryosections of eyes injected with (a) AAV9, (b) AAV9-1YF, and (c) AAV9-2YF without anti-GFP immunostaining. The second row shows the same images as (a-c) overlaid with DAPI (blue) and NeuN (red) staining. The third row (g-i) shows a z-projection of a 15 µm thick retinal cryosection depicting expression with AAV9-2YF amplified by anti-GFP immunostaining. g) shows DAPI staining in blue, and h) depicts GFP fluorescence after immunostaining. The GFP and DAPI images are merged on i). j-l) shows a flat-mount of a retina treated with AAV9-2YF. j) neurons were stained with NeuN in red at the RGC layer, and k) inner nuclear layer. l) cone photoreceptor labeling with peanut agglutinin (PNA) Alexa-594 conjugate in red.

Expression in the mouse brain using AAV9 and its tyrosine mutated counterparts

The enhancements in retinal transduction by AAV9-2YF compared to wild-type AAV9 led us to also examine its transduction of various brain regions. Analogous increases in transduction levels were observed with AAV9-2YF (left column) compared to AAV9 (right column) in all brain regions examined (Figure 5a-h). Consistent with previous reports for AAV9, GFP-positive cells included both neurons and astrocytes throughout the brain [68], and the glial versus neuronal tropism of the vectors varied depending on the brain region. High levels of GFP expression in the pyramidal neurons and fimbria of the hippocampus was observed in AAV9-2YF brains as well as strong GFP signal in the cerebellum (Purkinje and granule cell layers) and hypothalamus (data not shown).

Strong and exclusive expression in the photoreceptors using AAV9-2YF with a rhodopsin promoter

In both clinical and experimental gene therapy applications using systemic delivery, it may be crucial to limit the expression of the transgene to a specific cell type in specific tissues such as the retina. To this end, we replaced the ubiquitous CAG promoter initially used with a mouse rhodopsin promoter and examined expression patterns 3 weeks post-injection. Our data show expression restricted to photoreceptor cells with no detectable expression in all other retinal cells or in the brain (data not shown). These results indicate that experimental gene therapies for photoreceptor diseases, as well as somatic transgenic RP models, may be developed using this approach.

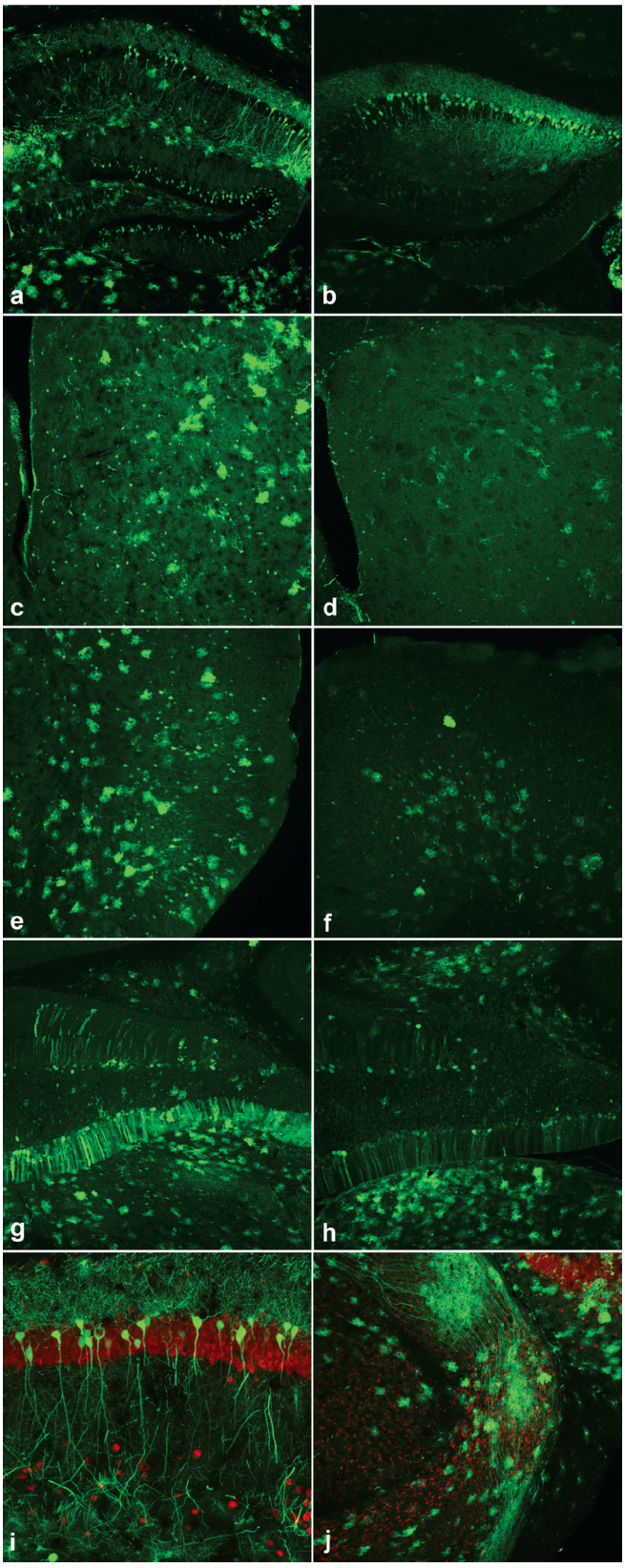

Figure 5. Brain sections illustrating GFP expression using AAV9-2YF vs. AAV9.

Representative fluorescence images of various brain regions showing GFP expression after transduction with AAV9-2YF (left column) versus AAV9 (right column). a,b) hippocampus, c,d) striatum, e,f) cortex, and g,h) cerebellum. The last row shows high magnification confocal images of AAV9-2YF mediated GFP expression in the pyramidal cells in the CA1 of the hippocampus (i) as well as in the fimbria (j). Both sections were stained for NeuN to mark neurons (red).

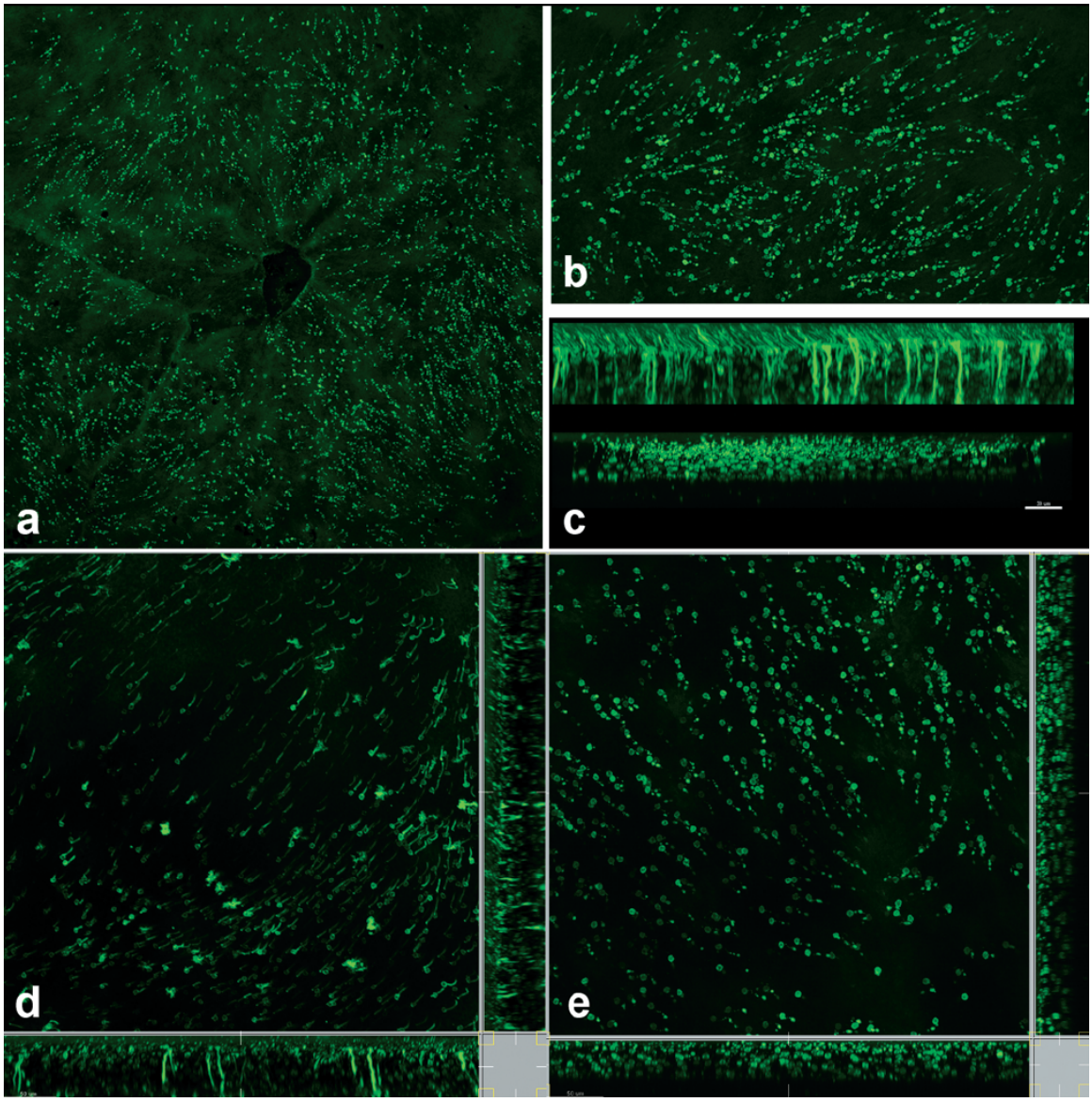

Figure 6. Expression patterns using AAV9-2YF-Rho-GFP.

a) Confocal images of a retinal flat-mount showing GFP expression after treatment with AAV9-2YF-Rho-GFP. Widespread expression can be observed around the optic nerve head (center), extending to the outer retina. b) A z-projection of a zoom on the photoreceptor layer is shown from the contralateral eye mounted with the photoreceptor cells facing up. c) Side views of 3D reconstructions from a retinal showing GFP expression following AAV9-2YF-CAG-GFP administration (upper image) versus expression patterns mediated by AAV9-2YF-Rho-GFP (lower image), with the latter exhibiting restricted expression in the rod photoreceptors of the retina. d,e) Oblique slice views of the 3D images in c.

Discussion

Our findings demonstrate the enhanced transduction properties of tyrosine mutated AAV9 variants for systemic gene delivery to the retina and the brain. In previous studies, mutation of Y446 or Y731 on the AAV9 capsid was shown to increase retinal transduction upon intraocular vector injection. We test a combination of the two mutations, which has not been previously tested intraocularly or via systemic administration. Our data show that the simultaneous mutation of these two residues yields a substantial improvement in the infectivity of the virus compared to Y446F and the Y731F mutations alone. First, RT-PCR reveals that gene delivery with this novel double mutant AAV9-2YF yields a 6-fold higher mRNA level compared to both wild-type AAV9 capsid and AAV9-Y446F. Moreover, histological examination of the infected retinas reveals striking differences, particularly in the transduction of inner nuclear layer and photoreceptor cells. These observations are in agreement with the described anatomic and physiologic features of the retinal blood supply (Figure 1). That is, choroidal vessels perfuse the outer retina and thereby likely offer the vector access to the basolateral RPE. Additionally, arteries and veins lying within the nerve fiber layer give rise to fine capillaries that perfuse the inner retina. Thus, a gradient of GFP expression could result from AAV transport into the retina from the inner and outer blood supplies, with the RPE and ganglion cells closest to the initial sources of vector. The time course of delivery of the AAV particles to the retinal vasculature likely has a direct parallel in the pattern observed in fluorescein angiography, with initial, rapid filling of the choroid followed by more gradual filling of the inner retinal vasculature. As predicted by the anatomy, we observe the strongest transduction in the inner and outermost layers of the retina with the wild-type AAV9 virus. Introduction of tyrosine mutations enables more efficient transduction of the middle retina, which previously had undetectable levels of expression with the wild-type AAV9.

This significant improvement to the expression pattern of AAV9 may enable gene therapies to target diseases that affect numerous, dispersed retinal cells including RGCs, PRs and RPE. Examples of such retinal dystrophies include glaucoma, RP, LCA, neovascularization, and X-linked retinoschisis. Furthermore, for anti-apoptotic or pro-survival therapies mediated by the secretion of neurotrophic factors [56,74], the secreted protein should ideally diffuse pan-retinally and into all retinal layers. For example, Müller glia, (which are efficiently transduced by AAV9-2YF), have been proposed as an ideal target for trophic factor secretion, due to their unique morphology and role in maintaining the retinal milieu [57].

The clinical relevance of systemic gene delivery for treating retinal degenerations will critically depend upon the ability to restrict gene expression to the cell type(s) of interest, and this specificity may be achieved through the use of cell specific promoters – as demonstrated here – or via miRNA strategies [75]. Therefore, the primary obstacle to the use of this technology in a clinical context is likely the risks of immune response to the capsid, which can cause significant safety concerns compared to local injections in the highly compartmentalized and immune privileged eye [66]. Regardless, the systemic injection of AAV is likely to be useful in the development of experimental gene therapies for inherited retinal degeneration, as retinal degeneration in animal models often follows a rapid progression compared to the human disease. We have observed significant levels of gene expression in retinal flat mounts from mice injected with AAV9-2YF one week post injection and steady levels of gene expression by the second week after the injection. This time course should enable gene replacement therapies before significant loss of photoreceptors and remodeling of the retina occurs in rodent models of

blindness, where the window of therapeutic intervention is narrower than the human disease [76].

The findings described here also have important implications for AAV9-mediated CNS gene delivery, particularly for diseases such as spinal muscular atrophy [69]. The use of the double tyrosine mutant AAV9 in future work may enable a reduction in the number of viral particles required to achieve similar rescue effects. This may be advantageous for reducing viral production costs and, more importantly, lowering the risks of immune response to the virus. In addition to these applications, this technology offers an alternative to traditional transgenesis for basic neuroscience research. This advance may be used to rapidly and economically generate somatic CNS transgenic animal models or gene knockdown animal models without costly and time intensive genetic manipulations. Furthermore, this technology offers the possibility of generating large animal models of diseases in which mutant proteins that induce neurodegeneration can be expressed in the afflicted regions of the brain [73] or retina with AAV9-2YF mediated transgenesis.

Materials and Methods

Generation of recombinant AAV vectors

AAV vectors were produced by the plasmid co-transfection method [59]. Recombinant AAV was purified via iodixanol gradient ultracentrifugation as described previously [29]. The viral eluent was buffer-exchanged against phosphate buffered saline (PBS) supplemented with 0.001% Tween and concentrated using Amicon Ultra-15 Centrifugal Filter Units to a final volume of 200 µl. The concentrated stock was then titered by quantitative PCR relative to standards.

Intravascular injections

C57/BL/6 littermates were used for all studies. The postnatal day-1 pups were immobilized, and an operating microscope was used to visualize the tail vain. 10 µl vector solution was drawn into a 3/10cc 30-gauge insulin syringe. The needle was inserted into the vein, and the plunger was manually depressed. A total of 4×10^{11} DNase resistant particles of AAV9-scCAG-GFP, AAV9-1YF-scCAG-GFP, AAV9-2YF-scCAG-GFP or AAV9-2YF-Rho-GFP were injected. A correct injection was verified by noting blanching of the vein. After the injection, pups were allowed to recover for several minutes on a 37ºC heating pad prior to being returned to their cages.

RT-PCR

Animals were humanely euthanized by CO_2 overdose and cervical dislocation. One retina was collected from n=5 (AAV9), n=4 (AAV9-1YF), or n=5 (AAV9-2YF) mice. RNA was extracted and subjected to DNase digestion, and the resulting RNA was used to create cDNA. RT-PCR for GFP, as well as the housekeeping gene GAPDH as an internal control, was performed on samples in triplicate using validated primers. The ddCT method was used to calculate fold difference of GFP expression normalized to AAV9. An uninjected wild-type mouse retina was used as a negative control.

Fundus photography

Fundus imaging was performed 2-8 weeks after injection with a fundus camera (Micron II; Phoenix Research Labs Inc., Pleasanton, CA) equipped with a filter to monitor GFP expression in live, anesthetized mice. Pupils were dilated for fundus imaging with phenylephrine (2.5%) and atropine sulfate (1%).

Flatmounts

Retinal flatmounts were prepared by gently detaching the retina from the RPE in PBS using a small brush. Once removed, radial cuts were introduced to flatten the retinal tissue. The tissue was positioned with either the RGC or the photoreceptor side up to allow confocal imaging from both directions. No immunostaining was performed on the intact retinal flat-mounts (Figure 3).

Peanut agglutinin (PNA) labeling

Whole retinas were dissected in PBS and transferred to 4% paraformaldehyde at 4°C overnight. Retinas were then rinsed 3X in PBS before blocking and labeling with PNA conjugated to Alexa-594 (1:40, Invitrogen - Molecular Probes) for 1 hr. After rinsing, relief cuts were made, and retinas were mounted and imaged.

Cryosections

Eyes were enucleated and immersion fixed in 10% formalin. The cornea and lens were removed, and the resulting eyecups were cryoprotected in 30% sucrose before embedding in OCT medium for cutting.

Immunolabeling

Where indicated, retinal cryosections were blocked in 1% bovine serum albumin, 0.5% Triton X-100, and 2% normal donkey serum for 2-3 hours and treated with a rabbit anti-GFP monoclonal antibody at 1:500 (Invitrogen, Carlsbad, CA, USA) and/or mouse anti-NeuN (MAB377, Chemicon, Billerica, MA, USA) in blocking solution overnight at 4 °C. After three PBS washes, Alexa-488-conjugated anti-rabbit secondary antibody (Invitrogen, Carlsbad, CA, USA) was applied at a 1:1,000 dilution in blocking solution for 2 hours at room temperature. The results were examined by confocal microscopy (LSM5; Carl Zeiss Microimaging, Peabody, MA).

Acknowledgements

The authors would like to thank Ryan Klimczak for performing the site directed mutagenesis to generate the AAV9 single and double tyrosine mutants. We are also thankful to Dr Alberto Auricchio for sharing the AAV-rho-GFP plasmid with us. This work was supported by grants from the National Institutes of Health Nanomedicine Development Center for the Optical Control of Biological Function (PN2EY018241), the Foundation Fighting Blindness USA and NIH grant RC2NS069476.

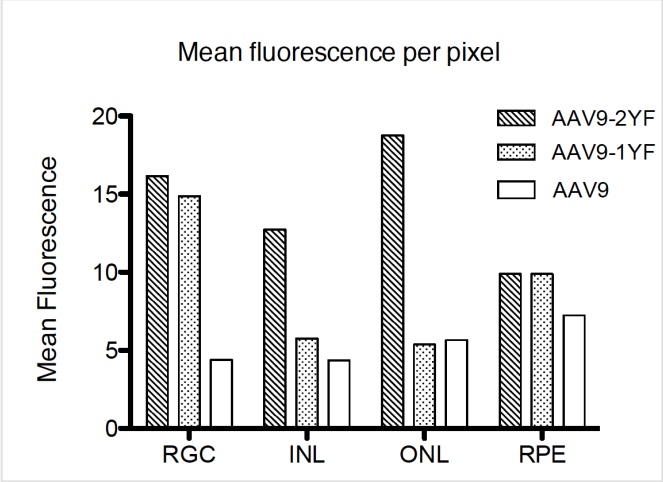

Supplemental Figure 1. Mean fluorescence per pixel calculated from confocal micrographs at each retinal layer

GFP intensity was evaluated with ImageJ and values indicate percentage of GFP intensity compared with wild-type AAV9 vector.

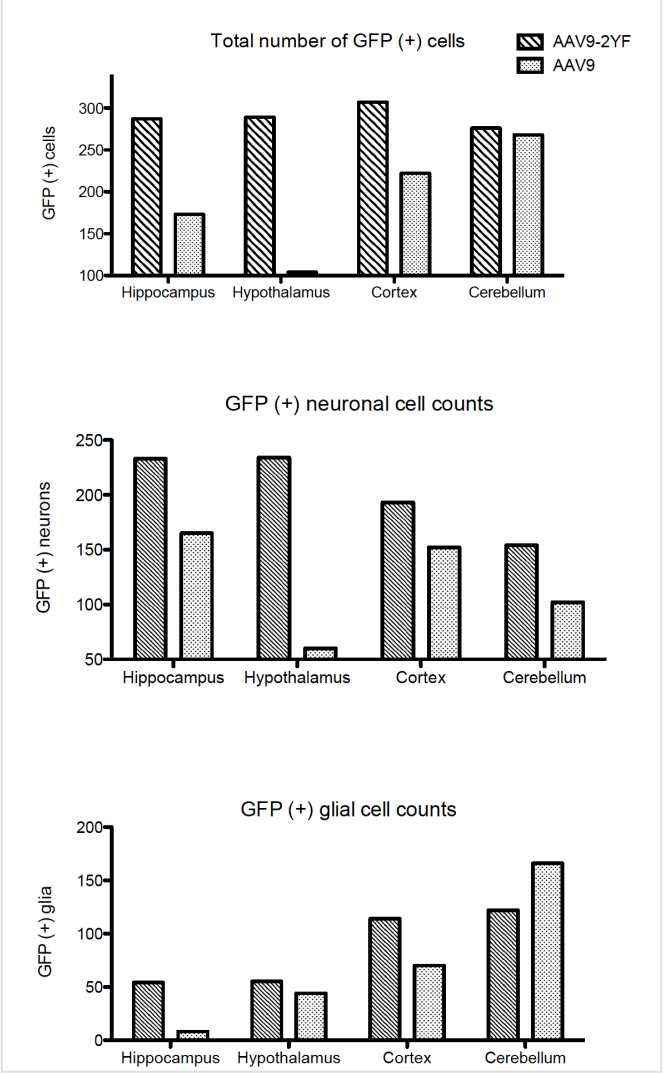

Supplemental Figure 2. Morphometric cell counts from confocal micrographs at each brain region

a) Total number of GFP positive cells obtained with each vector was counted using ImageJ b) and c) show GFP positive neurons and glia respectively in each brain region shown in Figure 5a-h.

Chapter 5

Engineered AAV-mediated expression of two isoforms of rod-derived cone viability factor delays retinal degeneration in the *rd10* mouse[4]

[4]This work was done in collaboration with Deniz Dalkara, Emmanuelle Clérin, Thierry Léveillard and John G. Flannery.

Abstract

The bifunctional gene *Nxnl1* encodes two products through alternative splicing. Rod-derived cone viability factor (RdCVF), a truncated thioredoxin-like protein, is secreted and has been shown to have a protective effect on the survival of cones in rodent models of retinitis pigmentosa (RP), while the full length protein, RdCVFL, contains a thioredoxin fold and may be involved in oxidative signaling and protection against hyperoxia. Here we use immunolabeling of cones in retinal flatmounts, optical coherence tomography and electroretinography to evaluate the effects of expression of these two isoforms in the *rd10* mouse model of recessive retinal degeneration. Expression of RdCVF and RdCVFL was accomplished via intravenous and intravitreal injection of engineered AAV vectors and evaluated by RTPCR and expression of GFP reporter genes. Our results indicate that systemic or intraocular expression of RdCVF leads to functional and structural rescue of cones, but does not affect rod degeneration. Early but not late expression of RdCVFL in dark-reared mice prolonged survival of rods and cones.

Introduction

Rod-cone dystrophies, such as retinitis pigmentosa (RP), are heterogeneous retinal degenerative diseases characterized by the death of rod photoreceptors, followed by the eventual loss of cones. RP is one of the most common forms of progressive inherited retinal degeneration, affecting around 1:3500 people worldwide [77]. Over 40 mutations causing RP have been identified to date (http://www.sph.uth.tmc.edu/retnet/sum-dis.htm) with the majority of these mutations in rod-specific transcripts. Patients diagnosed with RP lose peripheral and night vision as a result of rod dysfunction, with relative preservation of macular cone-mediated vision. As the disease progresses, however, the primary loss of rods frequently leads to cone degeneration, and it is this loss of high acuity and color vision that can be the most devastating to patients.

Although the mechanism of cone loss in RP is still poorly understood, several causes have been proposed. Cone death could be caused by the release of endotoxins from the massive degeneration of rods, or as a result of the loss of contact with rods, RPE or Müller glia. Alternatively, activation of Müller cells and the release of toxic molecules may play a role. Another hypothesis is that the high levels of oxygen supplied to the retina through the RPE from the choroidal blood circulation become toxic as rods die off and consume less oxygen. In agreement with this theory, high levels of oxidative stress have been shown to cause retinal degeneration, and treatment with antioxidants has been shown to prolong cone survival in animal models of rod-cone dystrophy [78]. Recently, Punzo et al. showed evidence that in murine models of retinal degeneration cones die in part as a result of starvation and nutritional imbalance, driven by the insulin/mammalian target of rapamycin pathway [79]. Finally, the loss of a survival factor secreted by rods and required for cone survival may contribute to cone loss [79,80].

In agreement with this hypothesis, transplantation of healthy retinal tissue has been shown to support cone survival in areas distant from the grafted tissue [81,82]. The rod-derived cone viability factor (RdCVF) was originally identified from a high-throughput method of screening cDNA libraries as a candidate for the secreted molecule responsible for this rescue effect [81]. This molecule has been shown to mediate cone survival in culture [83] and when injected subretinally in a rat model of dominant retinal degeneration [84]. The disruption of the gene encoding RdCVF renders mice susceptible to photoreceptor dysfunction over time [85].

The gene encoding RdCVF is *Nxnl1*, and it codes for two isoforms of the protein through alternative splicing. The isoform of RdCVF mediating cone survival is a truncated form of its longer counterpart, RdCVFL, which includes a C-terminal extension conferring a putative enzymatic function. RdCVFL is encoded by exons 1 and 2 of the *Nxnl1* gene, and contains a thioredoxin fold, suggesting that this protein is a member of the thioredoxin family. Thioredoxins have diverse functions, including maintaining proper reducing environment in the cell and participating in apoptotic pathways. These functions are accomplished via thioloxidoreductase reactions mediated by a conserved CXXC catalytic site within the thioredoxin fold [86]. RdCVFL has been shown to interact with the microtubule binding protein Tau, and in vitro protects against phosphorylation of Tau through oxidative stress. Mice lacking RdCVFL have disorganized rods which die over time and the retina is increasingly sensitive to hyperoxia. Together, this evidence supports the hypothesis that RdCVFL plays a role in protecting against oxidative stress through its activity as a thioredoxin-like enzyme.

The exact mechanisms by which these two isoforms act in the retina, or if they participate as part of the same signaling pathway, is still not well understood. Here, we describe experiments that seek to better understand the bifunctional nature of the *Nxnl1* gene by evaluating the effects of expression of the two RdCVF isoforms via engineered viral vectors in a mouse model of retinal degeneration, the *rd10* mouse. This mouse model is a well-characterized [86-88] model of rod-cone dystrophy resulting from a mutation in the ß-subunit of the rod-specific cyclic-GMP phosphodiesterase. The *rd10* mouse has been shown to be amenable to gene therapy [89,90] and antioxidant treatments have been shown to slow rod loss in this mouse model [78]. In addition, rearing in conditions of dim light has been shown to slow the rate of retinal degeneration, extending the window of opportunity for therapeutic treatment [62].

We show that the expression of the two isoforms of RdCVF has disparate effects on the survival of rods and cones, and that the time course of rescue mediated by these proteins is different. Expression of RdCVF, via intravitreal or intravenous injection of AAV vectors, leads to rescue of cone photoreceptors, but has little effect on rods. Early expression of RdCVFL, in comparison, prolongs survival of both rods and cones in dark-reared *rd10* mice.

Results

GFP reporter gene expression

Intravenous injection of AAV9 with two tyrosine mutations, driven by a ubiquitous CAG promoter in a self complementary vector in PN1 *rd10* pups resulted in early expression of GFP, which was visible in retcam images immediately after eye opening at PN15 (Figure 1A). By PN35 GFP expression was observed in all layers of the retina, in ganglion cells, Müller glia, amacrine cells, and photoreceptors. A similar pattern of expression was observed in WT (Figure 1B) and *rd10* (Figure 1C) retinas, in agreement with earlier results.

Intravitreal injections of the novel AAV variant 7m8 resulted in strong expression of GFP by PN35 in *rd10* mice (Figure 1D). Imaging of cross sections through cryostat sections of the retina revealed expression of the GFP reporter gene in all layers of the retina in WT and *rd10* mice.

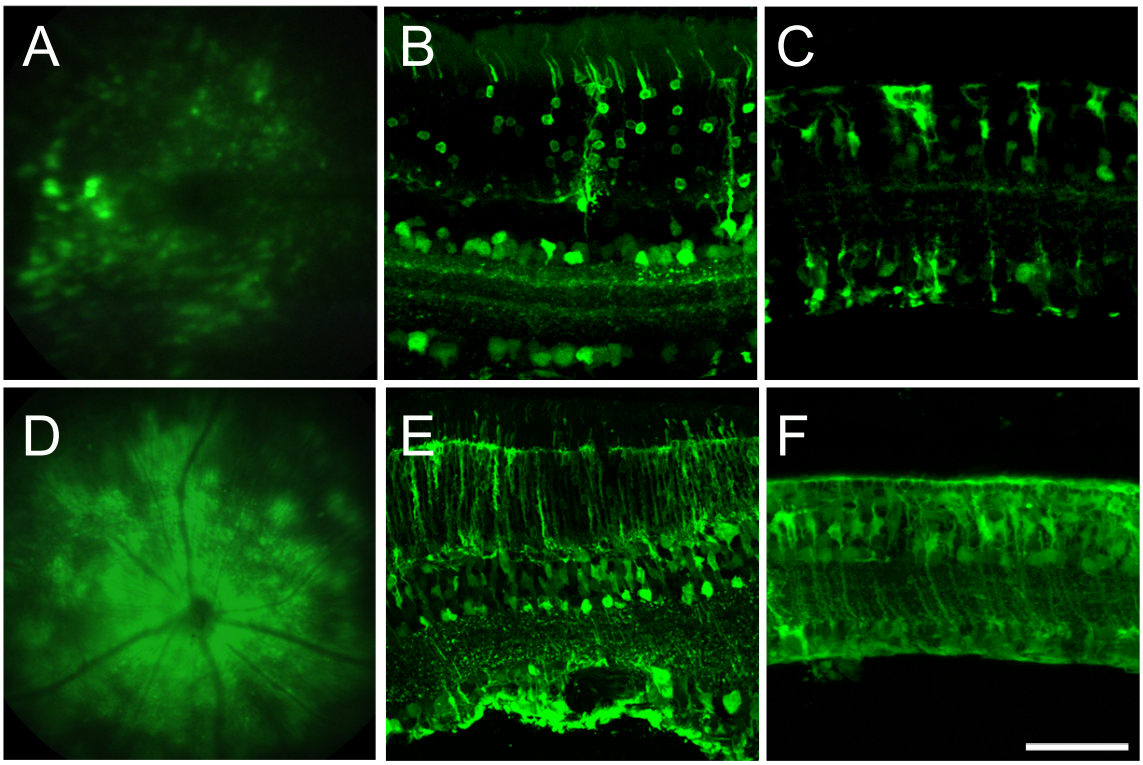

Figure 1. Viral vector expression.

Top row: AAV92YF.scCAG.GFP. Expression of reporter GFP gene is visible at PN15 after eyes open (A). GFP is expressed in all retinal layers in WT (B) and *rd10* mice (C). Bottom row: 7m8.scCAG.GFP. Expression of GFP is strong at PN35 (D). Virus transduces cells in all retinal layers in WT (E) and *rd10* mice (F). Scale bar applies to B,C,E,F and is 50 μm.

RT-PCR of RdCVF transcripts

RTPCR on mRNA samples taken from retinas injected with AAV92YF.scCAG.RdCVF, AAV92YF.scCAG.RdCVFL, or PBS in PN1 *rd10* mice revealed that intravenous injection of the virus results in high levels of expression of the transgene (Figure 2). Levels of expression are comparable to WT (RdCVF =79% ± 30%; RdCVFL = 59% ± 13%). Levels of expression of rhodopsin remain uniformly low across conditions, indicating similar rates of rod photoreceptor loss.

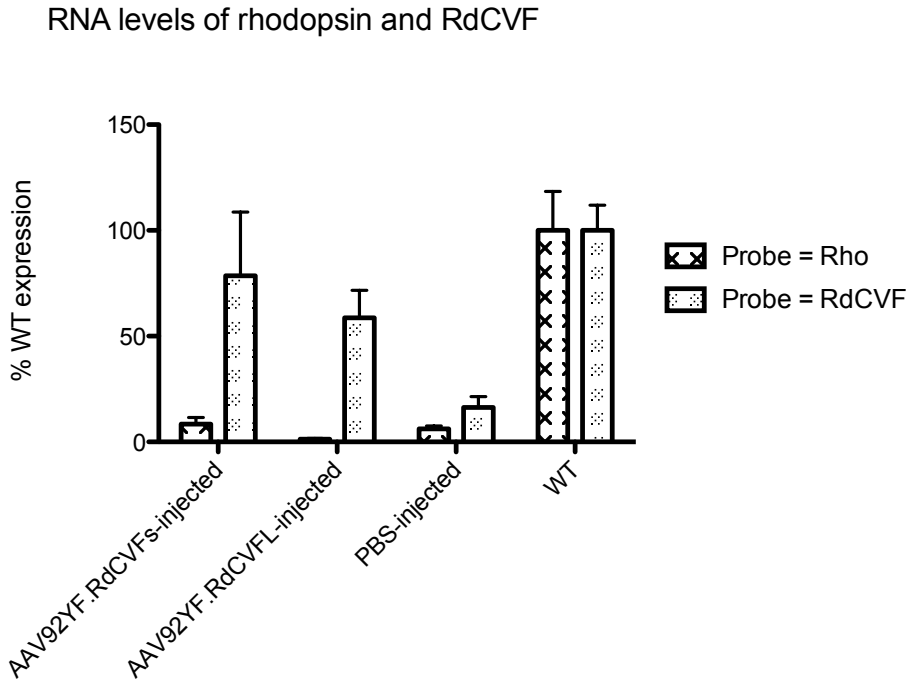

Figure 2. RTPCR from *rd10* mice injected with AAV92YF.scCAG.RdCVF/RdCVFL or PBS.

Graph depicts levels of mRNA collected from animals intravenously injected at PN1 with AAV92YF.scCAG.RdCVF/RdCVFL or PBS. Primers were used to amplify cDNA for RdCVF or rhodopsin, and expressed as percent WT levels.

Photopic electroretinogram recording in animals injected with AAV92YF.scCAG.RdCVF/RdCVFL/PBS

Tail vein injection of AAV92YF.scCAG.RdCVF resulted in significantly higher amplitude of the photopic ERG B-wave (97.1 ± 9.79 μV) compared to animals injected with AAV92YF.scCAG.RdCVFL (46.7 ± 96.35 μV) or PBS (56.5 ± 4.32 μV) (Figure 3A). Representative ERG traces illustrate the improved waveform and amplitude of ERGs from AAV92YF.scCAG.RdCVF-injected eyes compared to injections of vehicle (Figure 3B).

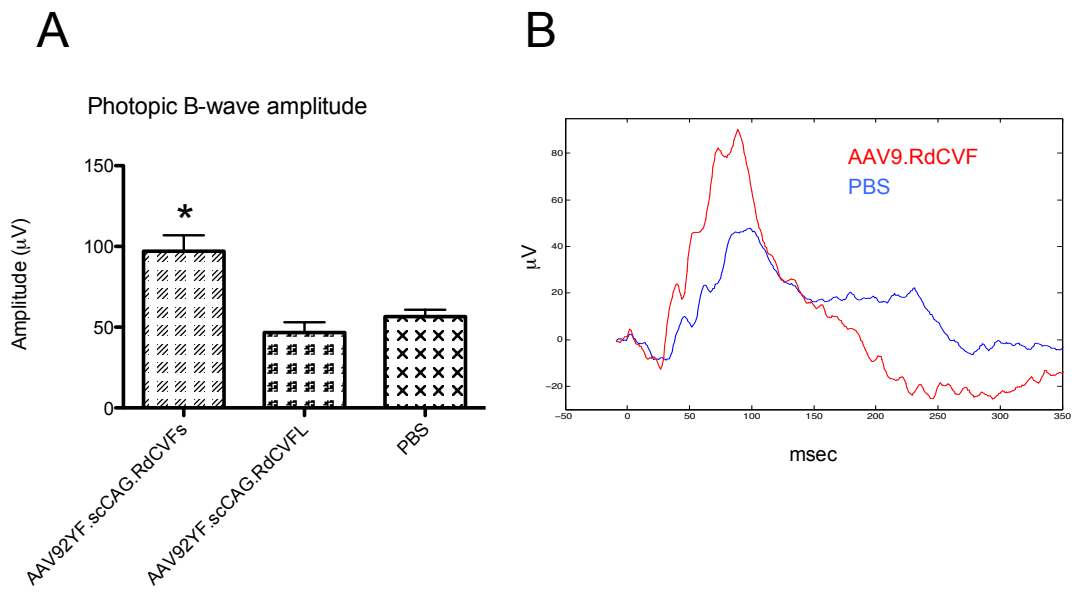

Figure 3. Injection of AAV9.RdCVF results in increased amplitude of the photopic ERG B-wave.

Cone-mediated ERGs were recorded with n=5 animals for each condition. Injection of AAV92YF.scCAG.RdCVF results in significantly higher amplitude of the photopic B-wave compared to both injection with AAV92YF.scCAG.RdCVFL or PBS (A). B: representative ERG traces from animals injected with AAV92YF.scCAG.RdCVF (blue) or PBS (red).

Cone counting in mice injected with AAV92YF.scCAG.RdCVF or PBS

Retinas from animals previously used for ERG recording were subsequently flatmounted and stained with antibodies against S-opsin (blue labeling) and L-opsin (red labeling). Flatmounts revealed improved labeling for both S- and L-opsin that was apparent in whole flatmounts from animals injected with AAV92YF.scCAG.RdCVF (Figure 4A). Higher numbers of surviving cones of both types are apparent in higher resolution images near the optic nerve head, the region of the retina with most severe degeneration (labeled with asterisk) (Figure 4B). Automated cone counting labeled cones in AAV92YF.scCAG.RdCVF- or PBS injected retinas resulted in significantly higher numbers of both S- and L-cones per retina (Figure 4C).

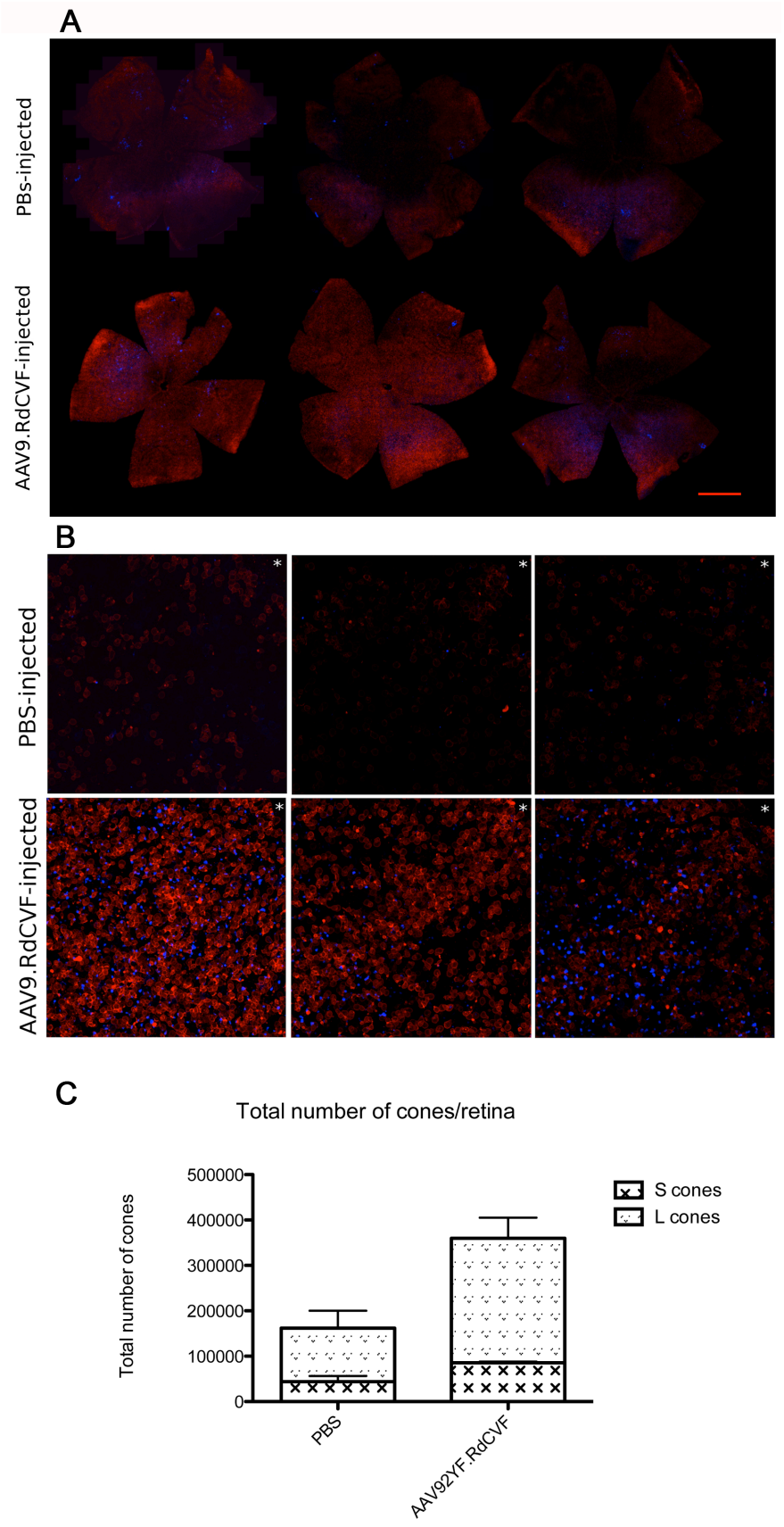
A
PBs-injected
AAV9.RdCVF-injected
B
PBS-injected
AAV9.RdCVF-injected
C
Total number of cones/retina
Total number of cones
500000
400000
300000
200000
100000
0
S cones
L cones
PBS
AAV92YF.RdCVF

Figure 4. Cone counting from animals injected with AAV92YF.scCAG.RdCVF or PBS.

Flatmounts of retinas from animals injected with AAV92YF.scCAG.RdCVF and labeled with antibodies against L-opsin (red) or S-opsin (blue) have more remaining cones than PBS injected mice (A). High-resolution images near the optic nerve (asterisk) show great number of L- and S-cones in the central retina (B). Quantification of the number of cones per retina reveals a significant increase in total numbers of L- and S-cones (C).

ERG recordings in dark-reared animals injected with AAV92YF.scCAG.RdCVFL, GFP or PBS

ERGs were recorded from dark-reared *rd10* animals injected at PN1 with AAV92YF.scCAG.RdCVFL, GFP or PBS (n=6 each group). Recordings were taken on a weekly basis for three weeks beginning 3 weeks after injection (Figure 5A). The amplitude of the scotopic A-wave revealed a delay in the decrease of the A-wave amplitude that was no longer apparent by 5 weeks after injection. The difference was statistically significant ($p=<0.05$, student's t-test) only at 4 weeks post-injection. No statistically significant difference in scotopic A-wave amplitude was noted between animals injected with AAV92YF.scCAG.RdCVF or PBS (data not shown). Representative ERG traces show increased amplitude of the A-wave as well as the B-wave in animals injected with AAV92YF.scCAG.RdCVFL compared to animals injected with GFP or PBS (Figure 5B). In contrast, ERG recordings of the photopic ERG revealed a delay in the decrease of the cone ERG that was significant only 5 weeks after injection (Figure 5C).

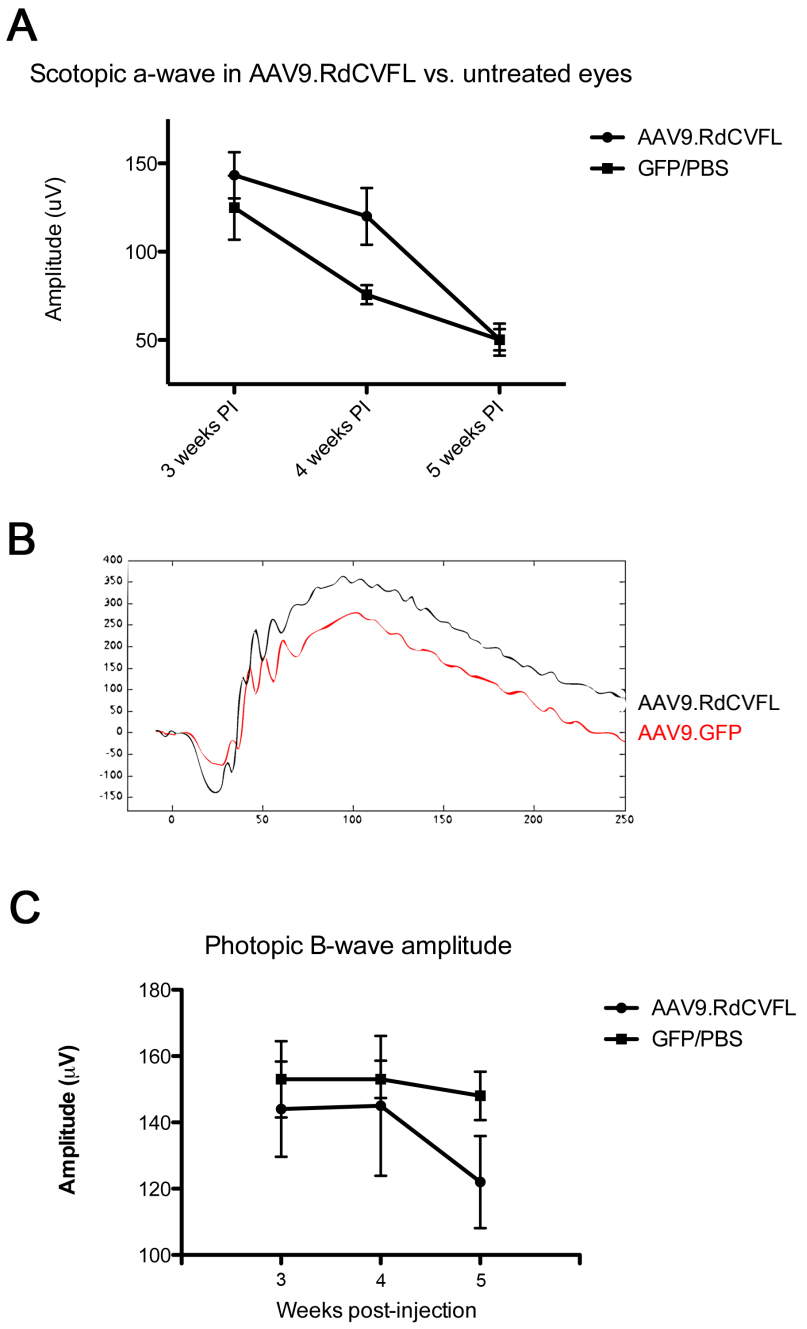

Figure 5. Injection of AAV92YF.scCAG.RdCVFL in dark-reared PN1 *rd10* mice results in rescue of the scotopic and photopic ERG.

Scotopic (A,B) and photopic (C) ERGs were recorded on a weekly basis 3-5 weeks post-injection in n=6 mice for each condition. Representative ERG traces from RdCVFL-treated (black trace) or GFP-injected (red trace) animals illustrating increased amplitude of the scotopic A-wave and B-wave 4 weeks post-injection in treated mice (B). Increased amplitude of the photopic ERG was noted only 5 weeks post-injection.

Intraocular injections of 7m8.scCAG.RdCVF, 7m8.scCAG.RdCVFL, or GFP in dark-reared rd10 mice

Intravitreal injections of 7m8.scCAG.RdCVF at PN15 resulted in an increase in the amplitude of the photopic B-wave at PN45, compared to contralateral GFP-injected eyes (Figure 6A-B). A slight increase in eyes injected with 7m8.scCAG.RdCVFL was not significant.

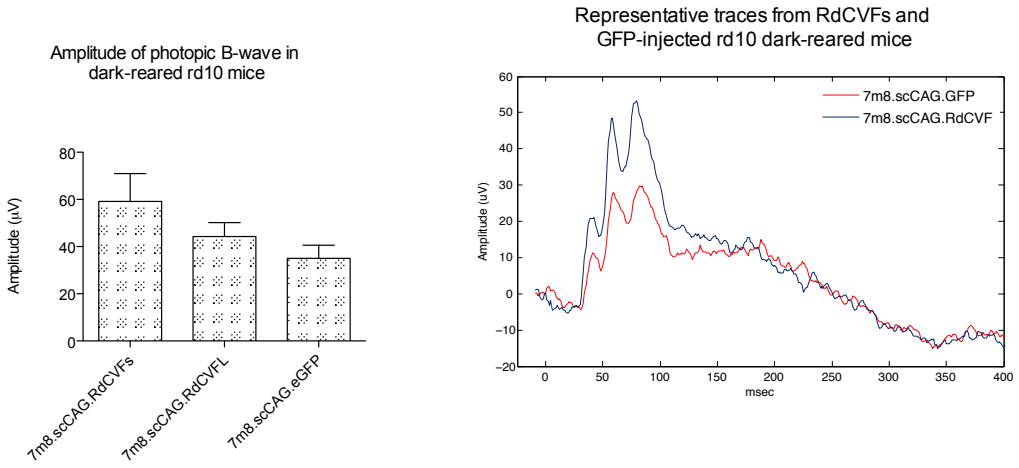

Figure 6. ERGs recorded from dark-reared *rd10* animals treated with intraocular injections of 7m8.scCAG.RdCVF/RdCVFL or GFP.

The amplitude of the photopic ERG was recorded 4 weeks post-injection at PN15. Injection with 7m8.scCAG.RdCVF results in increased amplitude of the photopic ERG, compared to animals injected with 7m8.scCAG.RdCVFL or GFP (A). B: representative ERG traces from eyes injected with 7m8.scCAG.RdCVF or 7m8.scCAG.GFP in the contralateral eye.

Discussion

For patients of rod-cone dystrophies like retinitis pigmentosa, the loss of cones is often the most debilitating phase of retinal degeneration. In modern industrialized societies, much of daily life requires high acuity color vision, which is mediated by cones. By contrast, the loss of rod-mediated vision is relatively easy to manage. Approximately 50% of disease causing genes have been identified for autosomal recessive forms of RP [4]. Of these, many have been identified in less than 200,000 people, relegating them to orphan status. Creating individualized treatments for all of these mutations may not be feasible. Therefore, a broadly applicable strategy aimed at supporting the survival of cones is an important area of research. Trophic factor treatments have been the subject of numerous preclinical studies of retinal degeneration and in clinical trials since their characterization [91,92]. Numerous studies have shown the functional

benefit of trophic factors for delaying apoptosis in both rod and cone photoreceptor cells in the retina.

RdCVF was originally identified as a diffusible factor capable of promoting cell survival, and was subsequently shown to be secreted by rods in healthy retina. The long isoform of RdCVF, also encoded by the *Nxnl1* gene, has been shown to contain a thioredoxin fold. Although the role of RdCVF in supporting survival of cones has been described in vitro and more recently explored in murine models of retinal degeneration, the function of RdCVFL is less well understood. Its similarity to thioredoxins and the presence of a C-terminal thioredoxin fold with putative enzymatic activity suggests that RdCVFL has a similar role to Thioredoxin 1 (TXR1). The role of TXR1 in scavenging free radicals, inhibiting apoptosis, regulating transcription factors, and regulating redox homeostasis has been described. TXR1 also plays a role in Alzheimer disease. Interestingly, RdCVFL has been shown to interact with Tau, a microtuble-associated protein that is phosphorylated in Alzheimer disease leading to aggregation of the protein, and reduced binding to microtubules that is associated with cell death.

Recently, the identification of RdCVF2 showed RdCVF to be one member of the RdCVF family. This family of proteins may represent a family of proteins with paracrine and antioxidant activity. Indeed, these proteins may interact as part of the same pathway to protect photoreceptors from apoptosis through cell signaling and maintaining proper redox status. These studies aimed to better understand the functionality of RdCVF and RdCVFL through investigating the effects of viral vector-mediated expression of these two proteins in a mouse model of recessive retinal degeneration. We show here that systemic injection of an AAV9 vector with two tyrosine-to-phenylalanine mutations led to high levels of expression of RdCVF in the retina. Expression of RdCVF led to greater numbers of surviving cones 35 days post-injection, as well as functional rescue of cones measured by photopic ERGs against a rod-saturating background. RdCVF expression had little effect on the survival or function of rods, however. Similar, but less dramatic results were obtained with intraocular injections of 7m8.

Intraocular and systemic expression of RdCVFL, in contrast, had little effect in mice reared in the light. In order to observe any possible effects of RdCVFL expression, therefore, *rd10* mice were reared in conditions of dim red light, which has been shown to slow retinal degeneration in this model. Using these methods, injections at PN1 with AAV92YF.scCAG.RdCVFL were followed by a modest delay in the degeneration of rods. This slower rate of rod degeneration was subsequently accompanied by a delay in the loss of cones, perhaps as a result of the prolonged survival of the source of RdCVF.

These experiments, in summary, support the role of *Nxnl1* as a bifunctional gene encoding two disparate isoforms of RdCVF. The expression of these two isoforms had different effects on the survival of rods and cones in the retina, indicating different functionalities. In addition, these experiments validate the use of AAV vectors as a delivery strategy for RdCVF. Ongoing experiments using these viral vectors are currently underway to further explore the role of these two proteins, including coexpression experiments. It will be interesting to investigate whether, acting simultaneously, these two proteins have synergistic effect on the survival of photoreceptors in the retina.

Materials and Methods

Production of viral vectors

AAV vectors carrying cDNA encoding mouse-RdCVF, RdCVFL or GFP were produced by the plasmid co-transfection method [59]. Recombinant AAV was purified by iodixanol gradient ultracentrifugation and heparin column chromatography (GE Healthcare, Chalfont St Giles, UK). The viral eluent was buffer exchanged and concentrated with Amicon Ultra-15 Centrifugal Filter Units in PBS and titered by quantitative PCR relative a standard curve.

Cryostat sectioning and confocal microscopy

Eyes were freshly dissected and immediately placed in 10% formalin for 1 hour. The lens was then removed and eyes were cryoprotected in 30% sucrose overnight. Eyecups were embedded in OCT. Using a cryostat, 20 μm transverse sections were cut and the sections were mounted onto slides. After rehydrating in PBS, sections were mounted for confocal microscopy (LSM710, Carl Zeiss).

Intravitreal injections

C57Bl6 or *rd10* mice were used for all experiments, which were conducted according to the ARVO Statement for the Use of Animals and the guidelines of the Office of Laboratory Animal Care at the University of California, Berkeley, CA. Mice were anesthetized with ketamine (72 mg/kg) and xylazine (64 mg/kg) by intraperitoneal injection. An ultrafine 30 1/2-gauge disposable needle was then passed through the sclera, at the equator and posterior to the limbus, into the vitreous cavity. One μL of AAV with a titer of 1-10 vg/mL was injected into the vitreous cavity with direct observation of the needle directly above the optic nerve head. Contralateral control eyes received vectors carrying the gene encoding GFP.

Intravascular injections.

The postnatal day-1 pups were immobilized, and an operating microscope was used to visualize the tail vain. 10 μl vector solution was drawn into a 3/10cc 30-gauge insulin syringe. The needle was inserted into the vein, and the plunger was manually depressed. A total of 5×10^{11} DNase resistant particles were injected. A correct injection was verified by noting blanching of the vein. After the injection, pups were allowed to recover for several minutes on a 37ºC heating pad prior to being returned to their cages.

Dark rearing

Mice were born and reared in light-safe boxes with under dim red light, which were only opened for brief periods for animal husbandry. Animals were transported to and from the box for experiments in covered cages.

RT-PCR

Animals were humanely euthanized by CO_2 overdose and cervical dislocation. One retina was collected from n=5 mice. RNA was extracted and subjected to DNase digestion, and the resulting RNA was used to create cDNA. RT-PCR for the housekeeping gene GAPDH was used as an internal control, and RTPCR was performed on samples in triplicate using validated primers for RdCVF or rhodopsin. mRNA levels were determined using a standard curve and are expressed as percent WT.

Fundus photography

Fundus imaging was performed with a fundus camera (Micron II; Phoenix Research Labs Inc., Pleasanton, CA) equipped with a filter to monitor GFP expression in live, anesthetized mice. Pupils were dilated for fundus imaging with phenylephrine (2.5%) and atropine sulfate (1%).

Electroretinograms

Mice were dark-adapted for 2 hours and then anesthetized, followed by pupil dilation. Mice were placed on a 37°C heated pad and contact lenses were positioned on the cornea of both eyes. A reference electrode connected to a splitter was inserted into the forehead and a ground electrode was inserted in the tail. For scotopic conditions electroretinograms were recorded (Espion E2 ERG system; Diagnosys LLC, Littleton, MA) in response to six light flash intensities ranging from −3 to 1 log cd × s/m^2 on a dark background. Each stimulus was presented in series of three. For photopic ERGs the animal was exposed to a rod saturating background for 5 minutes. Stimuli ranging from -0.9 to 1.4 log cd × s/m^2 were presented 20 times on a lighted background. Stimulus intensity and timing were computer controlled. Data were analyzed with MatLab (v7.7; Mathworks, Natick, MA). ERG amplitudes were compared using a student's t-test.

High-resolution spectral domain optical coherence tomography

Histological imaging was performed using an 840nm SDOIS OCT system (Bioptigen, Durham, North Carolina) including an 840nm SDOIS Engine with 93nm bandwidth internal source providing < 3.0um resolution in tissue. Retinal thickness, ONL and inner and outer segment thickness measurements were gathered and analysis done using InVivoVue software. Mice were anesthetized and the pupils dilated with atropine before imaging. Images of retinal cross sections were averaged from 8 contiguous slices. Fundus images were taken from en face views through the INL.

Cone counting

One retina from mice previously used for electroretinogram recording was freshly dissected from eyecups, and after blocking stained with anti-M or L-opsin antibodies. After incubation with secondary antibodies, retinas were washed and mounted for imaging. An automated microscope platform was used to visualize the entire retina. Images were compiled using Mayachitra imago imaging software (Santa Barbara, CA). Cone counting was subsequently performed using custom software written in Python.

Acknowledgements

Our thanks to Gabriel Luna and Steve Fisher for imaging retinal flatmounts. We thank Miguel Betegon for writing the cone counting software. We would like to thank Meike Visel for help with viral packaging, and Trevor Lee for his help with intraocular injections.

Chapter 6

Concluding Remarks

Inherited retinal degenerative diseases are a heterogeneous group of disorders that can be devastating, as the loss of sight can cause a drastic change in the quality of life for patients who depend on their sense of vision for most daily activities. To date, there are few effective treatments for most forms of inherited blindness, although recent advances have shown the potential for gene therapies. Viral vectors have evolved for millions of years to deliver genetic material to the nucleus of the cell, and recently we have been able to harness this ability to deliver therapeutic genes to the retina. AAV vectors are especially well suited to this task because they are small, nonpathogenic and have been shown to be amenable to modification, which will allow us to optimize expression in particular cell populations.

This dissertation presented work demonstrating the potential for the optimization of AAV through a directed evolution approach and through the use of tyrosine-to-phenylalanine mutations allowing the virion to avoid ubiquitination and degradation, and increasing nuclear trafficking and expression. Using directed evolution we show that screening of a highly diversified library of mutated viruses enabled the creation of a vector that bypassed the physical barriers of the inner retina to infect photoreceptors and other cells in the outer retina. In addition, two tyrosine-to-phenylalanine mutations on an AAV9 vector significantly improved expression, enabling early onset of intense expression throughout the retina. These modifications were used in combination with selection of delivery route, choice of promoter, and the use of self-complementary AAV genomes.

These optimized vectors were then used to deliver therapeutic genes to mouse models of retinal degeneration, demonstrating the importance of a rational approach to designing AAV-mediated gene therapy treatments. 7m8 and Müller glia-specific ShH10 were used to deliver a therapeutic copy of the human RS1 gene to the retinas of *Rs1h*-deficient mice. Delivery of the protein coding gene using 7m8, which targets photoreceptors, was more effective, although Müller cell delivery also conferred functional and structural benefit. These experiments emphasize the importance of targeting photoreceptors in this disease model. At the same time, both vectors were able to deliver the therapeutic gene panretinally, a dramatic improvement over subretinal injections, demonstrating the validity of the directed evolution approach for creating viral vectors able to infect the retina from the vitreous. For patients with retinoschisis, an intravitreal approach is highly preferable to subretinal injections, because of the low risk of retinal detachment and hemorrhage, two major concerns in this disease. In fact, the susceptibility of the structurally compromised retinoschisis retina makes the creation of a bleb highly dangerous as it may lead to permanent blindness. The extent of functional and structural recovery observed using 7m8 injected intravitreally demonstrates the promise of this approach and points a way forward for optimizing clinical trials in humans.

Using AAV92YF, RdCVFL was delivered to the *rd10* retina. Here, only early delivery in a dark-reared mouse made it possible to observe the delay of rod degeneration in this relatively rapid model of retinitis pigmentosa. It is important, then, that the vector used be able to deliver this therapeutic transgene during the appropriate window, as later intervention had little effect. Although in humans the time course of retinal degeneration is much slower, preclinical studies often use murine models, which have shorter lifespans and more rapid photoreceptor death. AAV vectors with improved efficiency are important for experiments demonstrating proof-of-concept

in these animal models.

We also show that delivery of RdCVF, the truncated isoform encoded by the *Nxnl1* gene, mediates survival of cone photoreceptors after rod loss in the *rd10* mouse. Together, these data indicate the bifunctionality of *Nxnl1* and raise interesting questions both about the potential of RdCVF for treating a wide spectrum of rod-cone dystrophies and the mechanism of RdCVF signaling. Successfully transitioning this type of treatment to the clinic could have a profound effect on the lives of millions of people affected by retinitis pigmentosa and other dystrophies marked by cone loss. One important aspect of these potential treatments is the delivery vector, and we demonstrate here that optimized vectors are able to mediate high levels of long-term transgene expression in the murine retina. Going forward it will be of great interest to implement these approaches in other animal models, including non-human primates, with the goal of creating vectors suitable for treating human disease.

In summary, this dissertation provides evidence that a rational approach to viral vector engineering and gene therapy is an important part of preclinical studies, and points a way forward for designing and testing novel viral vectors for delivery of gene replacement therapies, trophic factor therapies and other therapeutic genes for the treatment of progressive inherited retinal degeneration. These advancements will be an important part of gene therapy approaches that may soon be available in the clinic.

References

1. Hattar S, Liao HW, Takao M, Berson DM, Yau KW (2002) Melanopsin-containing retinal ganglion cells: architecture, projections, and intrinsic photosensitivity. Science 295: 1065–1070. doi:10.1126/science.1069609

2. Berson DM, Dunn FA, Takao M (2002) Phototransduction by retinal ganglion cells that set the circadian clock. Science 295: 1070–1073. doi:10.1126/science.1067262

3. Hollander den AI, Roepman R, Koenekoop RK, Cremers FPM (2008) Leber congenital amaurosis: genes, proteins and disease mechanisms. Progress in Retinal and Eye Research 27: 391–419. doi:10.1016/j.preteyeres.2008.05.003

4. Hollander den AI, Black A, Bennett J, Cremers FPM (2010) Lighting a candle in the dark: advances in genetics and gene therapy of recessive retinal dystrophies. J. Clin. Invest. 120: 3042–3053. doi:10.1172/JCI42258

5. Edwards AO, Ritter R, Abel KJ, Manning A, Panhuysen C, et al. (2005) Complement factor H polymorphism and age-related macular degeneration. Science 308: 421–424. doi:10.1126/science.1110189

6. Klein RJ, Zeiss C, Chew EY, Tsai J-Y, Sackler RS, et al. (2005) Complement factor H polymorphism in age-related macular degeneration. Science 308: 385–389. doi:10.1126/science.1109557

7. Haines JL, Hauser MA, Schmidt S, Scott WK, Olson LM, et al. (2005) Complement factor H variant increases the risk of age-related macular degeneration. Science 308: 419–421. doi:10.1126/science.1110359

8. Acland GM, Aguirre GD, Bennett J, Aleman TS, Cideciyan AV, et al. (2005) Long-term restoration of rod and cone vision by single dose rAAV-mediated gene transfer to the retina in a canine model of childhood blindness. Mol Ther 12: 1072–1082. doi:10.1016/j.ymthe.2005.08.008

9. Roy K, Stein L, Kaushal S (2010) Ocular Gene Therapy: An Evaluation of Recombinant Adeno-Associated Virus-Mediated Gene Therapy Interventions for the Treatment of Ocular Disease. Human Gene Therapy 21: 915–927. doi:10.1089/hum.2010.041

10. Bainbridge JWB, Smith AJ, Barker SS, Robbie S, Henderson R, et al. (2008) Effect of gene therapy on visual function in Leber's congenital amaurosis. N Engl J Med 358: 2231–2239. doi:10.1056/NEJMoa0802268

11. Cideciyan AV, Aleman TS, Boye SL, Schwartz SB, Kaushal S, et al. (2008) Human gene therapy for RPE65 isomerase deficiency activates the retinoid cycle of vision but with slow rod kinetics. Proc Natl Acad Sci U S A 105: 15112–15117.

12. Maguire AM, Simonelli F, Pierce EA, Pugh EN, Mingozzi F, et al. (2008) Safety and

efficacy of gene transfer for Leber's congenital amaurosis. N Engl J Med 358: 2240–2248. doi:10.1056/NEJMoa0802315

13. Ashtari M, Cyckowski LL, Monroe JF, Marshall KA, Chung DC, et al. (2011) The human visual cortex responds to gene therapy-mediated recovery of retinal function. J. Clin. Invest. 121: 2160–2168. doi:10.1172/JCI57377

14. Boutin S, Monteilhet V, Veron P, Leborgne C, Benveniste O, et al. (2010) Prevalence of serum IgG and neutralizing factors against adeno-associated virus (AAV) types 1, 2, 5, 6, 8, and 9 in the healthy population: implications for gene therapy using AAV vectors. Human Gene Therapy 21: 704–712. doi:10.1089/hum.2009.182

15. Kotin RM, Menninger JC, Ward DC, Berns KI (1991) Mapping and direct visualization of a region-specific viral DNA integration site on chromosome 19q13-qter. Genomics 10: 831–834.

16. Smith RH (2008) Adeno-associated virus integration: virus versus vector. Gene Ther 15: 817–822. doi:10.1038/gt.2008.55

17. Wu Z, Asokan A, Samulski RJ (2006) Adeno-associated virus serotypes: vector toolkit for human gene therapy. Mol Ther 14: 316–327.

18. Sweigard JH, Cashman SM, Kumar-Singh R (2010) Adenovirus vectors targeting distinct cell types in the retina. Investigative Ophthalmology & Visual Science 51: 2219–2228. doi:10.1167/iovs.09-4367

19. Zhong L, Li B, Mah CS, Govindasamy L, Agbandje-McKenna M, et al. (2008) Next generation of adeno-associated virus 2 vectors: point mutations in tyrosines lead to high-efficiency transduction at lower doses. Proc Natl Acad Sci U S A 105: 7827–7832.

20. Petrs-Silva H, Dinculescu A, Li Q, Min S-H, Chiodo V, et al. (2009) High-efficiency transduction of the mouse retina by tyrosine-mutant AAV serotype vectors. Mol Ther 17: 463–471. doi:10.1038/mt.2008.269

21. Koerber JT, Klimczak R, Jang J-H, Dalkara D, Flannery JG, et al. (2009) Molecular evolution of adeno-associated virus for enhanced glial gene delivery. Mol Ther 17: 2088–2095. doi:10.1038/mt.2009.184

22. Klimczak RR, Koerber JT, Dalkara D, Flannery JG, Schaffer DV (2009) A Novel Adeno-Associated Viral Variant for Efficient and Selective Intravitreal Transduction of Rat Müller Cells. PLoS ONE 4: e7467. doi:10.1371/journal.pone.0007467.g007

23. Daiger SP, Bowne SJ, Sullivan LS (2007) Perspective on genes and mutations causing retinitis pigmentosa. Arch. Ophthalmol. 125: 151–158. doi:10.1001/archopht.125.2.151

24. Remé CE, Grimm C, Hafezi F, Wenzel A, Williams TP (2000) Apoptosis in the Retina: The Silent Death of Vision. News Physiol. Sci. 15: 120–124.

25. Rolling F (2004) Recombinant AAV-mediated gene transfer to the retina: gene therapy perspectives. Gene Ther 11: S26–S32. doi:10.1038/sj.gt.3302366

26. Grüter O, Kostic C, Crippa SV, Perez M-TR, Zografos L, et al. (2005) Lentiviral vector-mediated gene transfer in adult mouse photoreceptors is impaired by the presence of a physical barrier. Gene Ther 12: 942–947. doi:10.1038/sj.gt.3302485

27. Harvey AR, Kamphuis W, Eggers R, Symons NA, Blits B, et al. (2002) Intravitreal injection of adeno-associated viral vectors results in the transduction of different types of retinal neurons in neonatal and adult rats: a comparison with lentiviral vectors. Mol Cell Neurosci 21: 141–157.

28. Sanftner L (2001) Glial Cell Line Derived Neurotrophic Factor Delays Photoreceptor Degeneration in a Transgenic Rat Model of Retinitis Pigmentosa. Molecular Therapy 4: 622–629. doi:10.1006/mthe.2001.0498

29. Dalkara D, Kolstad KD, Caporale N, Visel M, Klimczak RR, et al. (2009) Inner limiting membrane barriers to AAV-mediated retinal transduction from the vitreous. Mol Ther 17: 2096–2102. doi:10.1038/mt.2009.181

30. Kolstad KD, Dalkara D, Guerin K, Visel M, Hoffmann N, et al. (2010) Changes in adeno-associated virus-mediated gene delivery in retinal degeneration. Human Gene Therapy 21: 571–578. doi:10.1089/hum.2009.194

31. Chan F, Bradley A, Wensel TG, Wilson JH (2004) Knock-in human rhodopsin-GFP fusions as mouse models for human disease and targets for gene therapy. Proc Natl Acad Sci U S A 101: 9109–9114. doi:10.1073/pnas.0403149101

32. Weber BHF, Schrewe H, Molday LL, Gehrig A, White KL, et al. (2002) Inactivation of the murine X-linked juvenile retinoschisis gene, Rs1h, suggests a role of retinoschisin in retinal cell layer organization and synaptic structure. Proc Natl Acad Sci U S A 99: 6222–6227. doi:10.1073/pnas.092528599

33. Gehrig A, Janssen A, Horling F, Grimm C, Weber BHF (2006) The role of caspases in photoreceptor cell death of the retinoschisin-deficient mouse. Cytogenet Genome Res 115: 35–44. doi:10.1159/000094799

34. Park TK, Wu Z, Kjellstrom S, Zeng Y, Bush RA, et al. (2009) Intravitreal delivery of AAV8 retinoschisin results in cell type-specific gene expression and retinal rescue in the Rs1-KO mouse.: 1–11. doi:10.1038/gt.2009.61

35. Li Q, Miller R, Han P, Pang J (2008) Intraocular route of AAV2 vector administration defines humoral immune response and therapeutic potential. Molecular ….

36. Maheshri N, Koerber JT, Kaspar BK, Schaffer DV (2006) Directed evolution of adeno-associated virus yields enhanced gene delivery vectors. Nat Biotechnol 24: 198–204. doi:10.1038/nbt1182

37. Perabo L, Büning H, Kofler DM, Ried MU, Girod A, et al. (2003) In vitro selection of viral vectors with modified tropism: the adeno-associated virus display. Mol Ther 8: 151–157.

38. Müller OJ, Kaul F, Weitzman MD, Pasqualini R, Arap W, et al. (2003) Random peptide libraries displayed on adeno-associated virus to select for targeted gene therapy vectors. Nat Biotechnol 21: 1040–1046. doi:10.1038/nbt856

39. Koerber JT, Jang J-H, Schaffer DV (2008) DNA shuffling of adeno-associated virus yields functionally diverse viral progeny. Mol Ther 16: 1703–1709. doi:10.1038/mt.2008.167

40. George ND, Yates JR, Moore AT (1995) X linked retinoschisis. British Journal of Ophthalmology 79: 697–702.

41. Sikkink SK, Biswas S, Parry NRA, Stanga PE, Trump D (2007) X-linked retinoschisis: an update. Journal of Medical Genetics 44: 225–232. doi:10.1136/jmg.2006.047340

42. Forsius H, Krause U, Helve J, Vuopala V, Mustonen E, et al. (1973) Visual acuity in 183 cases of X-chromosomal retinoschisis. Can. J. Ophthalmol. 8: 385–393.

43. Sauer CG, Gehrig A, Warneke-Wittstock R, Marquardt A, Ewing CC, et al. (1997) Positional cloning of the gene associated with X-linked juvenile retinoschisis. Nat Genet 17: 164–170. doi:10.1038/ng1097-164

44. Vijayasarathy C, Takada Y, Zeng Y, Bush RA, Sieving PA (2007) Retinoschisin is a peripheral membrane protein with affinity for anionic phospholipids and affected by divalent cations. Investigative Ophthalmology & Visual Science 48: 991–1000. doi:10.1167/iovs.06-0915

45. Molday LL, Wu WWH, Molday RS (2007) Retinoschisin (RS1), the Protein Encoded by the X-linked Retinoschisis Gene, Is Anchored to the Surface of Retinal Photoreceptor and Bipolar Cells through Its Interactions with a Na/K ATPase-SARM1 Complex. Journal of Biological Chemistry 282: 32792–32801. doi:10.1074/jbc.M706321200

46. Kiedzierska A, Smietana K, Czepczynska H, Otlewski J (2007) Structural similarities and functional diversity of eukaryotic discoidin-like domains. Biochim. Biophys. Acta 1774: 1069–1078. doi:10.1016/j.bbapap.2007.07.007

47. Reid SN, Akhmedov NB, Piriev NI, Kozak CA, Danciger M, et al. (1999) The mouse X-linked juvenile retinoschisis cDNA: expression in photoreceptors. Gene 227: 257–266.

48. Molday LL, Hicks D, Sauer CG, Weber BH, Molday RS (2001) Expression of X-linked retinoschisis protein RS1 in photoreceptor and bipolar cells. Investigative Ophthalmology & Visual Science 42: 816–825.

49. Wu WWH, Wong J, Kast J, Molday R (2005) RS1, a Discoidin Domain-containing Retinal Cell Adhesion Protein Associated with X-linked Retinoschisis, Exists as a Novel

Disulfide-linked Octamer. Journal of Biological Chemistry 280: 10721–10730. doi:10.1074/jbc.M413117200

50. Wang T, Zhou A, Waters CT, O'Connor E, Read RJ, et al. (2006) Molecular pathology of X linked retinoschisis: mutations interfere with retinoschisin secretion and oligomerisation. British Journal of Ophthalmology 90: 81–86. doi:10.1136/bjo.2005.078048

51. Consortium (1998) Functional implications of the spectrum of mutations found in 234 cases with X-linked juvenile retinoschisis. The Retinoschisis Consortium. Human Molecular Genetics 7: 1185–1192.

52. Wu WWH, Molday RS (2003) Defective discoidin domain structure, subunit assembly, and endoplasmic reticulum processing of retinoschisin are primary mechanisms responsible for X-linked retinoschisis. J. Biol. Chem. 278: 28139–28146. doi:10.1074/jbc.M302464200

53. Zeng Y (2004) RS-1 Gene Delivery to an Adult Rs1h Knockout Mouse Model Restores ERG b-Wave with Reversal of the Electronegative Waveform of X-Linked Retinoschisis. Investigative Ophthalmology & Visual Science 45: 3279–3285. doi:10.1167/iovs.04-0576

54. Kjellstrom S, Bush RA, Zeng Y, Takada Y, Sieving PA (2007) Retinoschisin Gene Therapy and Natural History in the Rs1h-KO Mouse: Long-term Rescue from Retinal Degeneration. Investigative Ophthalmology & Visual Science 48: 3837–3845. doi:10.1167/iovs.07-0203

55. MIN S, MOLDAY L, SEELIGER M, Dinculescu A, TIMMERS A, et al. (2005) Prolonged Recovery of Retinal Structure/Function after Gene Therapy in an -Deficient Mouse Model of X-Linked Juvenile Retinoschisis. Molecular Therapy 12: 644–651. doi:10.1016/j.ymthe.2005.06.002

56. Reid SNM, Yamashita C, Farber DB (2003) Retinoschisin, a photoreceptor-secreted protein, and its interaction with bipolar and Müller cells. Journal of Neuroscience 23: 6030–6040.

57. Dalkara D, Kolstad KD, Guerin KI, Hoffmann NV, Visel M, et al. (2011) AAV Mediated GDNF Secretion From Retinal Glia Slows Down Retinal Degeneration in a Rat Model of Retinitis Pigmentosa. Mol Ther. doi:10.1038/mt.2011.62

58. McCarty DM (2008) Self-complementary AAV vectors; advances and applications. Mol Ther 16: 1648–1656.

59. Grieger JC, Choi VW, Samulski RJ (2006) Production and characterization of adeno-associated viral vectors. Nat Protoc 1: 1412–1428. doi:10.1038/nprot.2006.207

60. Bainbridge JW, Ali RR (2008) Success in sight: The eyes have it! Ocular gene therapy trials for LCA look promising. Gene Ther 15: 1191–1192. doi:10.1038/gt.2008.117

61. Leveillard T, Sahel J-A (2010) Rod-Derived Cone Viability Factor for Treating Blinding Diseases: From Clinic to Redox Signaling. Science Translational Medicine 2: 26ps16–26ps16. doi:10.1126/scitranslmed.3000866

62. Pang S, Dai X, Boye S, Barone I, Boye S, et al. (2011) Long-term retinal function and structure rescue using capsid mutant AAV8 vector in the rd10 mouse, a model of recessive retinitis pigmentosa. Mol Ther 19: 234–242. doi:10.1038/mt.2010.273

63. Yin L, Greenberg K, Hunter JJ, Dalkara D, Kolstad KD, et al. (2011) Intravitreal injection of AAV2 transduces macaque inner retina. Invest. Ophthalmol. Vis. Sci. 52: 2775–2783. doi:10.1167/iovs.10-6250

64. Masland RH (2001) The fundamental plan of the retina. Nat Neurosci 4: 877–886. doi:10.1038/nn0901-877

65. Törnquist P, Alm A (1979) Retinal and choroidal contribution to retinal metabolism in vivo. A study in pigs. Acta Physiol. Scand. 106: 351–357.

66. Mingozzi F, High KA (2011) Immune Responses to AAV in Clinical Trials. Curr Gene Ther 11: 321–330.

67. Bostick B, Ghosh A, Yue Y, Long C, Duan D (2007) Systemic AAV-9 transduction in mice is influenced by animal age but not by the route of administration. Gene Ther 14: 1605–1609. doi:10.1038/sj.gt.3303029

68. Foust KD, Nurre E, Montgomery CL, Hernandez A, Chan CM, et al. (2008) Intravascular AAV9 preferentially targets neonatal neurons and adult astrocytes. Nat Biotechnol 27: 59–65. doi:10.1038/nbt.1515

69. Foust KD, Wang X, McGovern VL, Braun L, Bevan AK, et al. (2010) Rescue of the spinal muscular atrophy phenotype in a mouse model by early postnatal delivery of SMN. Nat Biotechnol 28: 271–274. doi:10.1038/nbt.1610

70. Zhang H, Bin Yang, Mu X, Ahmed SS, Su Q, et al. (2009) Several rAAV Vectors Efficiently Cross the Blood–brain Barrier and Transduce Neurons and Astrocytes in the Neonatal Mouse Central Nervous System. Molecular Therapy: 1–9. doi:10.1038/mt.2011.98

71. Rahim AA, Wong AMS, Hoefer K, Buckley SMK, Mattar CN, et al. (2011) Intravenous administration of AAV2/9 to the fetal and neonatal mouse leads to differential targeting of CNS cell types and extensive transduction of the nervous system. FASEB J. doi:10.1096/fj.11-182311

72. Maingay M, Romero-Ramos M, Kirik D (2005) Viral vector mediated overexpression of human alpha-synuclein in the nigrostriatal dopaminergic neurons: a new model for Parkinson's disease. CNS Spectr 10: 235–244.

73. Ulusoy A, Decressac M, Kirik D, Björklund A (2010) Viral vector-mediated

overexpression of α-synuclein as a progressive model of Parkinson's disease. Prog. Brain Res. 184: 89–111. doi:10.1016/S0079-6123(10)84005-1

74. Dorrell MI, Aguilar E, Jacobson R, Yanes O, Gariano R, et al. (2009) Antioxidant or neurotrophic factor treatment preserves function in a mouse model of neovascularization-associated oxidative stress. J. Clin. Invest. 119: 611–623. doi:10.1172/JCI35977

75. Ma C, Liu Y, He L (2009) MicroRNAs - powerful repression comes from small RNAs. Sci. China, C, Life Sci. 52: 323–330. doi:10.1007/s11427-009-0056-x

76. Chang B, Hawes NL, Hurd RE, Davisson MT, Nusinowitz S, et al. (2002) Retinal degeneration mutants in the mouse. Vision Research 42: 517–525.

77. Buch H, Vinding T, La Cour M, Appleyard M, Jensen GB, et al. (2004) Prevalence and causes of visual impairment and blindness among 9980 Scandinavian adults: the Copenhagen City Eye Study. Ophthalmology 111: 53–61.

78. Komeima K, Rogers BS, Campochiaro PA (2007) Antioxidants slow photoreceptor cell death in mouse models of retinitis pigmentosa. J. Cell. Physiol. 213: 809–815. doi:10.1002/jcp.21152

79. Punzo C, Kornacker K, Cepko CL (2008) Stimulation of the insulin/mTOR pathway delays cone death in a mouse model of retinitis pigmentosa. Nat Neurosci 12: 44–52. doi:10.1038/nn.2234

80. Mohand-Said S, Deudon-Combe A, Hicks D, Simonutti M, Forster V, et al. (1998) Normal retina releases a diffusible factor stimulating cone survival in the retinal degeneration mouse. Proc Natl Acad Sci U S A 95: 8357–8362.

81. Léveillard T, Mohand-Saïd S, Lorentz O, Hicks D, Fintz A-C, et al. (2004) Identification and characterization of rod-derived cone viability factor. Nat Genet 36: 755–759. doi:10.1038/ng1386

82. Mohand-Said S, Hicks D, Simonutti M, Tran-Minh D, Deudon-Combe A, et al. (1997) Photoreceptor transplants increase host cone survival in the retinal degeneration (rd) mouse. Ophthalmic Res. 29: 290–297.

83. Wang XW, Tan BZ, Sun M, Ho B, Ding JL (2008) Thioredoxin-like 6 protects retinal cell line from photooxidative damage by upregulating NF-κB activity. Free Radical Biology and Medicine 45: 336–344. doi:10.1016/j.freeradbiomed.2008.04.028

84. Yang Y, Mohand-Saïd S, Danan A, Simonutti M, Fontaine V, et al. (2009) Functional Cone Rescue by RdCVF Protein in a Dominant Model of Retinitis Pigmentosa. Molecular Therapy 17: 787–795. doi:10.1038/mt.2009.28

85. Cronin T, Raffelsberger W, Lee-Rivera I, Jaillard C, Niepon M-L, et al. (2010) The disruption of the rod-derived cone viability gene leads to photoreceptor dysfunction and susceptibility to oxidative stress. Cell Death and Differentiation 17: 1199–1210.

doi:10.1038/cdd.2010.2

86. Lillig CH, Holmgren A (2007) Thioredoxin and related molecules--from biology to health and disease. Antioxid. Redox Signal. 9: 25–47. doi:10.1089/ars.2007.9.25

87. Barhoum R, Martínez-Navarrete G, Corrochano S, Germain F, Fernandez-Sanchez L, et al. (2008) Functional and structural modifications during retinal degeneration in the rd10 mouse. Neuroscience 155: 698–713. doi:10.1016/j.neuroscience.2008.06.042

88. Phillips MJ, Otteson DC, Sherry DM (2010) Progression of neuronal and synaptic remodeling in the rd10mouse model of retinitis pigmentosa. J. Comp. Neurol. 518: 2071–2089. doi:10.1002/cne.22322

89. Gargini C, Terzibasi E, Mazzoni F, Strettoi E (2006) Retinal organization in the retinal degeneration 10 (rd10) mutant mouse: A morphological and ERG study. J. Comp. Neurol. 500: 222–238. doi:10.1002/cne.21144

90. Pang JJ, Boye SL, Kumar A, Dinculescu A, Deng W, et al. (2008) AAV-Mediated Gene Therapy for Retinal Degeneration in the rd10 Mouse Containing a Recessive PDE Mutation. Investigative Ophthalmology & Visual Science 49: 4278–4283. doi:10.1167/iovs.07-1622

91. Thanos C, Emerich D (2005) Delivery of neurotrophic factors and therapeutic proteins for retinal diseases. Expert Opin Biol Ther 5: 1443–1452. doi:10.1517/14712598.5.11.1443

92. Cao W, Wen R, Li F, Lavail MM, Steinberg RH (1997) Mechanical injury increases bFGF and CNTF mRNA expression in the mouse retina. Exp Eye Res 65: 241–248. doi:10.1006/exer.1997.0328